FACULTEIT INGENIEURSWETENSCHAPPEN

ESCUELA TÉCNICA SUPERIOR DE INGENIEROS INDUSTRIALES Y DE TELECOMUNICACIÓN

Design and manufacture of a low cost wind turbine for developing countries

Arraiza Clemente, Nerea

Íñiguez Chácharo, Paula

Thesis submitted under the supervision of
Prof. dr. Mark Runacres

Academic year
2014-2015

In order to be awarded the Degree in
Industrial Engineering

"There is a driving force more powerful than steam, electricity and atomic energy: the will."

- Albert Einstein -

Acknowledgments

First and foremost, we wish to acknowledge our promoter, Prof. Dr. Mark Runacres, for giving us this golden opportunity to develop this such fascinating thesis, and help us with his expertise, support and advice. Bringing out always the best of us.

We would like to say a special thanks to both universities, Universidad Pública de Navarra and Vrije Universiteit Brussel, for making possible to participate in this exchange students programme, Erasmus. Particularly, to our promoter, Prof. Dr. Pablo Sanchís Gúrpide, for his support and attention when we have needed it.

In addition, we are especially grateful to our colleague Arno Motte, for all his continuous useful comments and support.

We, also, would like to name all the people who have been our family in Brussels, for making us feel at home, their support, advice and for all the memories we will always remember.

Finally, our best sincere thank you to our family. Without them, we could never have achieved our life goals and they are our strongest support to follow our dreams. Thank for your unconditional faith in us, support and patience, without which, this day could not be possible.

Abstract

English Abstract

The challenge of the project presented below is the generation of an electricity access to all points where it is not accessible, because there is no grid or because of the high cost of the electricity.

The main idea is to design a low power wind turbine from recycled elements or easily accessible and cost ones, which provides enough energy for daily consumption of the inhabitants of these places. As key design features are highlighted the simplicity of the manufacturing and the easy assembling. Thanks of that, the users will be able to manufacture, to install, to start up and to perform maintenance for the machine. Thereby, we the provide technology needed for energy self-sufficiency.

The thesis is developed on different phases. Firstly, analyse the feasibility of materials and tools as well as environmental and sociocultural characteristics of the countries under study. Secondly, the study, design and analysis of the different elements of the machine, taking into account the aspects previously evaluated. Finally, the third phase, manufacture and assemble the different components of the machine.

As a final result, a completely equipped wind turbine is obtained. It can be split up in three main elements, the first one a rotor with two different configurations depending on the material to be used, wood or PVC pipes, the second one an electrical permanent magnet synchronous generator (PMSG), whose output is 24 V nominal in sinusoidal current, and the third one an electronic conversion system to control and adjust the voltage in order to charge batteries.

This project is carried out in the Belgian university, Vrije Universiteit Brussel, with a bilateral collaboration with the Universidad Pública de Navarra located in Pamplona, thanks to the exchange students program, Erasmus.

Spanish Abstract

El objetivo del proyecto presentado a continuación es la generación de un acceso a la energía eléctrica para todos aquellos puntos en la que no está accesible, ya bien por no existir red eléctrica o por el alto coste del consumo de la misma.

La idea fundamental es diseñar un aerogenerador de baja potencia a partir de elementos reciclados o elementos de fácil acceso y coste, que proporcione energía suficiente para el consumo diario de los habitantes de dichos emplazamientos. Como características principales del diseño, se destacan su simplicidad en la fabricación y fácil montaje a fin de que sean los propios usuarios finales capaces de la construcción, montaje, puesta a punto y mantenimiento del mismo. Proporcionndoles de este modo la tecnología necesaria para la autosuficiencia energética.

La tesis se ha realizado en diferentes fases. La primera, se trata del análisis de la viabilidad de materiales y herramientas así como de las características medioambientales y socioculturales de los países bajo estudio. La segunda, el estudio, diseño y análisis de los diferentes elementos de la máquina teniendo en cuenta los aspectos evaluados anteriormente. La tercera, la fabricación y ensamblaje de los componentes de la máquina.

Como resultado final se obtiene un aerogenerador con dos configuraciones diferentes de rotor dependiendo del material a emplear, madera o tubos de PVC, un generador eléctrico síncrono de imanes permanentes (PMSG) cuya salida es de 24 V nominales en corriente senoidal y un sistema electrónico de conversión, control y adecuación de voltaje para la carga de baterías.

Este proyecto se lleva a cabo en la universidad belga, Vrije Universiteit Brussel, con una colaboracin bilateral con la Universidad Pública de Navarra situada en Pamplona, gracias al programa de intercambio de estudiantes Erasmus.

Dutch Abstract

Het brede doel van deze masterproef is om elektriciteit op te wekken in gebieden waar er op dit moment weinig of geen elektriciteit beschikbaar is, door de hoge elektriciteitsprijs en/of de afwezigheid van een stroomnet.

De centrale onderzoeksvraag van deze thesis is om een windturbine te ontwerpen die gemaakt kan worden uit goedkope, bij voorkeur gerecycleerde, onderdelen, en of een dergelijke windturbine voldoende elektriciteit kan opwekken om bij te dragen tot het verbeteren van de levenskwaliteit van een gemeenschap die over weinig of geen elektriciteit beschikt. Het beoogde ontwerp moet gemakkelijk te maken, te monteren en te onderhouden zijn, zonder interventies buiten de lokale gemeenschap.

In het eerste deel van de masterproef wordt de keuze van materiaal en gereedschap besproken, samen met een bondige sociale en ecologische analyse van een aantal gebieden in Afrika die in aanmerking komen als toepassingsgebied van het ontwerp. In het tweede deel worden de verschillende componenten van de windturbine ontworpen (rotor, generator, mast, vermogenselektronica en energie-opslag). Er wordt geopteerd voor een rotor uit hout of PVC, een synchrone generator die gebruik maakt van permanente magneten, met een spanning van 24 V, energie-opslag via batterijen en een eenvoudig controlesysteem om de spanning te regelen. In het derde deel wordt een prototype gerealiseerd dat de praktische haalbaarheid van het ontwerp aantoont.

Dit onderzoek werd uitgevoerd aan de Vrije Universiteit Brussel, binnen het kader van een Erasmusuitwisseling met de Universidad Pblica de Navarra Pamplona (Spanje).

Contents

Nomenclature list

Chapter 2

P	Power	W
ρ	Air density	kg/m^3
A	Area where the flow of the air goes through	m^2
V_∞	Undisturbed wind speed	m/s
Cp	Power factor	-
η	Wind turbine efficiency	-
$\bar{U}$	Average speed	m/s
Γ	Gamma function	-
TSR	Tip speed ratio	-

Chapter 5

	Section 5.1 Rotor	
P	Power	W
ρ	Air density	kg/m^3
A	Area where the flow of the air goes through	m^2
U_x	Wind speed in the location x	m/s
Cp	Power factor	-
TSR	Tip speed ratio	-
λ	Tip speed ratio	-
ω	Rotor rotational speed	rad/s
R	Rotor radius	m
V_∞	Undisturbed wind speed	m/s
W	Apparent wind speed	m/s
α	Angle of attack	rad
θ	Pitch angle	rad
φ	Angle of relative wind	rad
γ	Complementary angle of φ	rad
c	Chord length of the blade	m
B	Number of blades in the rotor	-
r	Radius coordinate	m
x	Relative radius coordinate	-
F	Tip loos correction	-
a	Axial induction factor	-
a'	Tangential induction factor	-
Cl	Lift coefficient	-
Cd	Drag coefficient	-
k	Lift drag ratio	-
σ	Solidity	-

	Section 5.2 Generator	
H	Magnetic field intensity	A/m
i_{enc}	Free and bound current	A
$i_{f,enc}$	Free current	A
dl	Path differential	-
ϕ	Magnetic flux	Wb
B	Flux density or magnetic induction	T
S	Surface traversed by the flux density	m^2
B_{mc}	Flux density with the magnetization curve	T
H_{mc}	Magnetic field intensity with the magnetization curve	A/m
B_m	Flux density in the magnet	T
H_m	Magnetic field intensity in the magnet	A/m
S_m	Surface in the magnet traversed by the flux density	m^2
a_m	Length of the magnet	m
b_m	Width of the magnet	m
l_m	Thickness of the magnet	m
B_g	Flux density in the gap	T
H_g	Magnetic field intensity in the gap	A/m
S_g	Surface in the gap traversed by the flux density	m^2
l_g	Thickness of the gap	m
μ	Magnetic permeability of the material	N/A^2
B_r	Flux density in the rotor	T
S_r	Surface in the rotor traversed by the flux density	m^2
l_r	Thickness of the brake disc (rotor)	m
S_{tm}	Sum of the surfaces in the magnets traversed by the flux density	m^2
Ns	Total number of wire turns per phase of the stator	-
Ω	Rotor rotational speed = Mechanical speed	Rps
N_{cp}	Number of coils per phase	-
$E_{A_1A_1'}$	Voltage generated in the coil A_1A_1'	V
p	Number of pole pairs	-
θ	Mechanical angle	rad
V_{batt}	Batteries voltage	V
V_{rect}	Voltage drop in the rectifier	V
R_{coil}	Coil resistance	Ω
σ	Conductivity of copper	S/m
R_s	Stator resistance	Ω

	Section 5.4 Electronics and conversion system	
P_{nom}	Nominal power	W
V_{batt}	Voltage in the batteries	V
$I_{battmax}$	Maximum intensity in the batteries	A
E_{batt}	Stored energy in the batteries	Ah
E_v	Vacuum tension	V
R_s	Resistance of the stator	Ω
X_s	Inductance of the stator	H
I_s	Intensity in the stator	A
V_s	Voltage in the stator	V
Z_s	Impedance in the stator	Ω
I_r	Intensity in the rotor	A
V_{rect}	Tension in the rectifier	V

Chapter 1

Introduction

1.1 Context and background

The availability of energy is essential for the good mankind. In developed countries this issue is not given much attention due to its easy accessibility. However, in countries in development it is a scarce commodity. In the most of these cases the energy is limited to primary energy i.e. coal, firewood, solar energy or wind energy. In some cases, apart from giving rise to environmental problems, this issue limits the potential for both individual and country development and for the quality of life. A clear example of this situation is the use of some systems that in developing countries are indispensable such as fridge or electric light, since in most circumstances these systems are supplied by electrical energy.

The objective of this project is to generate electrical energy in these communities where it is not an easily accessible good. The main purpose is to write a project with the ideas, designs, materials and steps to follow, not only to manufacture independently an electricity generation system, but also to use, maintain and repair it if it is necessary.

Therefore, the design presented in this thesis tries to combine pure technical and theoretical analysis with traditions, customs and way of life of these communities, as well as the appropriate choice of materials, tools and equipments, in general. Thus with the goal of integrating, as far as possible, the result in the society.

1.2 The role of the energy in human development

Energy is the capacity to do work. It is known that historically the use of energy has been a key factor in human development. There is a very strong link between per capita energy consumption and the Human Development Index. And this link is ever stronger for the poorer developing countries. Figure 1.1 is clear: a higher HDI goes hand in hand with increased per capita energy use.

The HDI sets a maximum and minimum for each dimension, called goalposts, and then shows where each country stands in relation to these goalposts, expressed as a value between 0 and 1 [3]. The HDI has three dimensions, measured by one or two indicators each:

- Leading a long and healthy life
  - Life expectancy and birth
- Education
  - Adult literacy rate

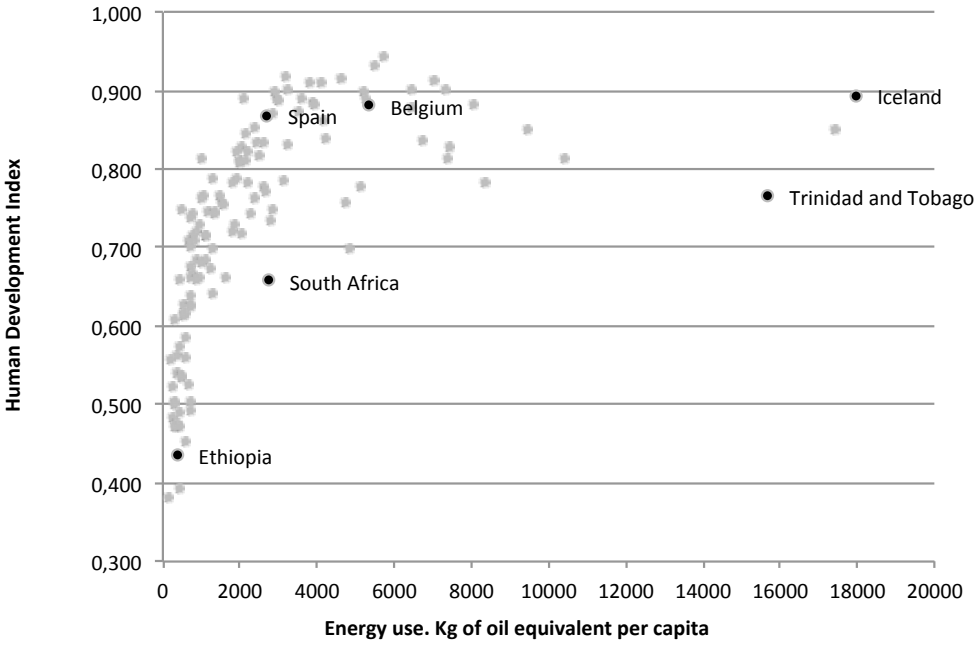

Figure 1.1: Relationship between Human Development Index and Energy consumption. Adapted data from [1] for the Human Development Index and from [2] for the Energy consumption.

  - Gross primary, secondary and tertiary enrollment

- A decent standard of living

  - GDP per capita (PPPUS$)

As fig. 1.1 shows, the curve is logarithmic. Therefore, on the one hand, the poorest countries could significantly increase HDI when a modest increase of energy consumption, but normally, that energy is not available. On the other hand, it is difficult for developed countries to raise the HDI increasing energy consumption in a small space of time. There is also a strong link between the energy and the 8 development goals, which were established following the Millennium Submit. In each goal we can see how important the energy is to achieve them.

Goal 1. Eradicate extreme poverty and hunger

The easiest way to eradicate poverty is by generating employment. Energy is essential to this achievement because with more readily available electricity enterprises would develop faster, and therefore would generate more employments.

This holds for large companies but also for the SMEs or small workplaces. With lighting the workshops could work also during the evening hours and become more competitive.

Also energy can be use for cooking aliments. Most of the staple aliments (95%) have to be cooked before eating them.

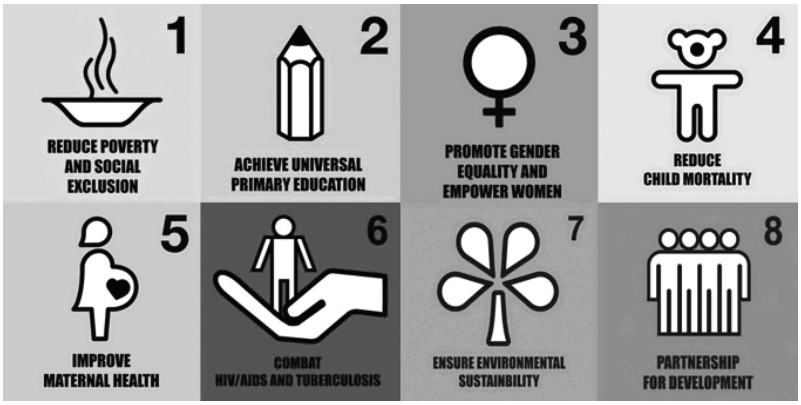

Figure 1.2: 8 Millennium Development Goals. Data from [4].

Goal 2. Achieve universal primary education

Electricity may help encouraging children to study and go to school. With hot water, heating or lighting schools can offer a more pleasant environment. In addition, having electricity gives the possibility of using PCs, projectors, printers and, above all, the possibility of studying at home during the night.

Goal 3. Promote gender equality and empower women

The availability of energy resources releases young girls and women from part of the households, gives the chance of cooking efficiently... In this way they do not waste a lot of time doing the housework and they can spend time studying once they have finished all those works even in night hours.

Goal 4. Reduce child mortality

Pollution in houses increases child mortality because of respiratory illness. The pollution of houses would decrease if stores were no longer fueled by charcoal but by using electricity. In addition, energy allows refrigeration, which means, fresh food and easier cook, obtaining health benefits through the population. Other possibility to improve this situation could be solar cookers, that are cheap and also work well in this situation.

Goal 5. Improve maternal health

Energy is essential to improve medical facilities, for example cooling medicine or the sterilisation of equipments.

Goal 6. Combat HIV/AIDS, malaria and other diseases

It is easy to see the importance of energy in this subject. With cooling systems medicines could be preserved in good condition. Furthermore, it is important to take into account that the patients could be treated not only during the day, but also after sunset.

Goal 7. Ensure environmental sustainability

As we know, traditional biomass pollutes a lot. So the availability of new resources of energy and above all, the electricity would ensure environmental sustainability.

Goal 8. Develop a global partnership for development

Although energy is not directly involved in this goal, access to electricity facilities access to a computer, even if it is one for each village, and in this way help in the introduction of a global partnership for development.

To conclude, it is known that the energy and the use of it is essential for the human development. Because of this situation, we have to keep in mind that technical aspects are as important as the social traditions of those countries and their resources. Therefore, this project tries to reflect a balance between all of them, using their own materials, tools and resources and making them self-sufficient in the use and maintenance of the system that is going to be implanted.

1.3 Situation of the electricity in Africa

According to The World Bank database [2], nowadays, around the 21,8% of the population in the world is living without electricity access, which is more than 1500 million of people. This situation is particularly stark if we focus on developing countries where the most of the rural population do not have electrification.

As we can see in fig. 1.3, countries such as United States of America, Belgium or Spain, the electrification reaches the 100% of the population, but in developing countries this effect does not occur. This factor is profoundly relevant in Sub-Saharan Africa, where there are the lowest ratios in the world.

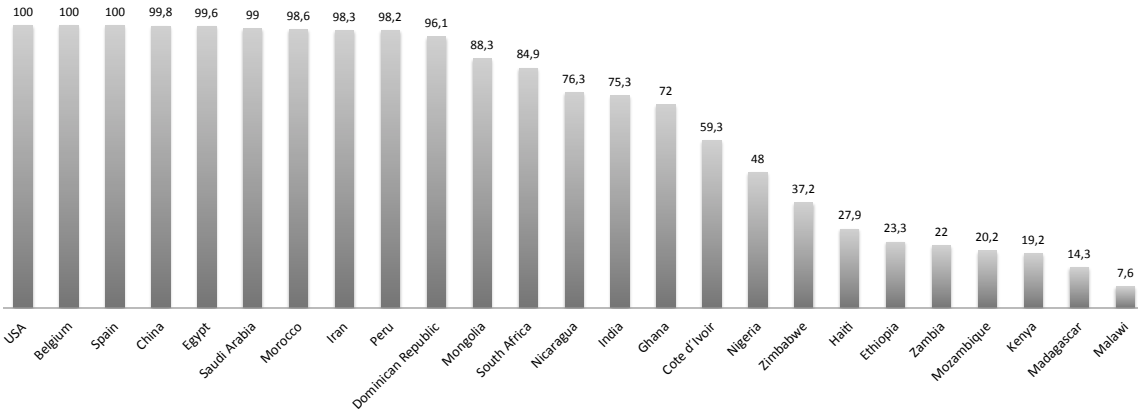

Figure 1.3: Electrification ratio per countries. Adapted data from [2].

Around the world, the energy production and distribution is managed by public agencies. For that reason in developed countries exist enough governmental power and financing to guarantee the electric supply. However, in other regions where they are not so developed we can identify 5 factors, which limit the access of electric power system. These factors are:

Dispersion of the population:

The rural areas of inhabitants sometimes represent a small average of the total population. Also, they usually are distributed throughout a vast region with a changeable orography. In addition, the production is centralized. Because of all this situation, it is needed a big and strong electrification grid to transport the electricity, which is too expensive and too

difficult to maintain. Emphasize also, that copper wires are more likely to be stolen, and damages less probably to be repaired.

Limited public funding:

If we continue thinking about the rural areas, the electrical companies have to spend a lot of money in electrify them and they are not the most of the population, so it is not profitable for those enterprises. Because of that, companies refuse to make those types of projects. In other framework, the government would be the responsible to undertake those plans but the economy in developing countries is weak, so they cannot afford to finance it.

Rural population indifference:

Also, the rural population are used to have a traditional way of life, and are sometimes reluctant to change. Often, they do not trust the new technology and prefer to continue living in their own way.

Under organizational power in rural communities:

The dispersion and the shortage of training and capital in those communities makes their organizations be unprotected, so that, they have not enough power to pressure on institutions to obtain improvements in their lifestyle.

Political indifference:

Due to the fact that the rural population represents a small average, and what is more a small market size, the government does not pay attention to the people who live there, and their life conditions.

Furthermore, it is known not only the energy transmission connectors with neighbours are weak but also that countries have political and technical barriers to trade.

During the last 10 years, the non-electrified population has been decreasing even thought the world population has become bigger than bigger. This decrease has not been homogeneous worldwide, on the one hand Latin America and Asia have accelerated their electrification, but on the other hand, Sub Saharan Africa has seen no improvement. The continent is sometimes referred to *"The blackout continent"*.

The strong population growth and the lack of economic and political resources in this area has originated substantial support from the international communities around the world have had to help and support this regions but the situation is still devastating. According to WEO 2011 (World Economic Outlook 2011), only 41.8% of the population has access to electricity in Africa. The situation is more extreme if we consider two regions of this continent, North Africa and Sub Saharan Africa.

In countries such as Morocco, Egypt or Tunisia, the electrification rates are over 98.9% of the population, with rural and urban levels close to full electrification. But in others like Tanzania or Zambia it does not exceed 22%. Observing the data, we can conclude that there are very big disparities between these two continental regions, which are unacceptable.

In the future this situation cannot keep on and the developing countries could be which are going to improve it in a reasonable period of time. ARE(Alliance for Rural Electrification) has recommended in the World Bank Energy Strategy Approach that the

national electrification ought to increase 2.5% above the population growth. With this goal, in 2025, 67.3% of the population in Sub-Saharan Africa would have access to modern energy. This would require the electrification of at least 350 million people in the next 10 years.

1.3.1 Situation of the rural electrification

The electrification situation is critical in Sub-Saharan Africa regions, and even more in rural areas. Table 1.1 below shows those contrasts supported by numbers and averages around the world.

Table 1.1: Electricity access in 2009 - Regional aggregates

Region	**Non electrified population (Million)**	**Electrification rate (%)**	**Urban electrification rate (%)**	**Rural electrification rate (%)**
Africa	587	41.8	68.8	25.0
North Africa	2	99.0	99.6	98.4
Sub-Saharan Africa	585	30.5	59.9	14.2
Developing Asia	675	81.0	94.0	73.2
China and East Asia	182	90.8	96.4	86.4
South Asia	493	68.5	89.5	59.9
Latin America	31	93.2	98.8	73.6
Middle East	21	89.0	98.5	71.8
Developing countries	1,314	74.7	90.6	63.2
World*	1,317	80.5	93.7	68.0

* World total includes OECD (Organization for Economic Cooperation and Development) and Eastern Europe/Eurasia. Data from [5].

According with the data, almost the entire African population without electrification is living in the Sub-Saharan area, with an electrification rate slightly higher than 30%, which is the lowest rural electrification ratio in the world. There, only 14% people have access to the grid.

The energy in Sub-Saharan Africa is a scarcer commodity; the annual energy consumption is about 518 kWh, which is more or less the same amount used by a person living in a OECD's country in 25 days.

Energy sources

The energy supply in rural areas is covered by mini-grid and off-grid systems fed by generators running on diesel or gasoline, but most of the population uses fuelwood, charcoal or solid biomass as the main energy. Because of that fact bioenergy is considered the heart of the energy mix in this area.[2]. Furthermore, almost all agriculture relies on power of animals and humans and it is thought that around Africa there are more than 200 millions of kerosene lamps for lighting the population. [6].

Considering Sub-Saharan countries such as Congo, Nigeria and Angola and observing their primary energy consumption indicators, we can conclude that the most important energy source is the traditional biomass and waste, being its average more than half of the total. Also, there are other sources such as oil, petroleum or natural gas that are predominantly used in the cities.

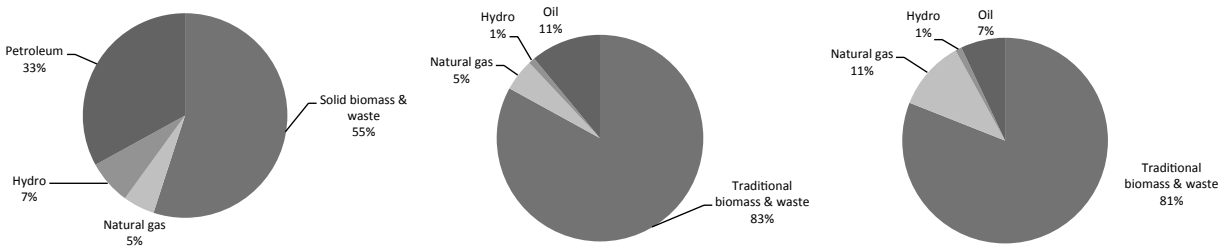

(a) Angola 2011 (b) Nigeria 2011 (c) Congo (Brazzaville)2011

Figure 1.4: Primary energy consumption per countries. Adapted data from [2].

Renewable sources

As the average in fig. 1.4 shows, there is renewable energy in the energy mixes. In all of these cases, is hydro electrical power. But also there are others like solar, geothermal or wind power:

Hydropower It is known that this source supplied in 2014 the 20% of the power. In spite of that, only the 10% of its technical potential is being utilized. Mozambique, Guinea, Democratic Republic of Congo or Ethiopia, are some examples of countries where this energy could play a major role.

Photovoltaic and solar technologies: These technologies can be used not only on-grid but also off-grid or mini-grid. That means, it is possible to use in situation where the electric supply exists, where there is no supply and where exist a small community grid. Because of that and because of the appropriate weather conditions in some African areas, this technology is being used more and more to supply rural population on electricity, [7].

Geothermal power: In some countries in East Africa such as Kenya and Ethiopia, this source has become the second largest of power supply. To get an idea, according to Kenya's state-owned Geothermal Development Company, the country has the potential to produce 14,000 megawatts of geothermal-powered electricity of which only 60 MW has been exploited, [8].

Wind power: This type of energy is researched in the following section.

In 35 years, it is thought that two-thirds of the isolated systems and the mini-grids in rural areas will be powered by these renewable energy sources, highlighting small hydropower, photovoltaic panels and small wind power, [7]. To achieve this scenario, numerous efforts by governments and international assistance have to be done during the following years, in order to finance and lead the projects.

1.3.2 Situation of wind energy in Africa

As we have seen Africa is facing an energy crisis. The existing production capacity cannot meet the electricity demand. But Africa has lots of opportunities, including large renewable potential which is the highest in the world. The continent has enough renewable energy potential to meet its future energy need, so to take advantage of this situation and

to cope with the problem of the lack of energy in the moment, lots of enterprises have invested in this kind of generation systems, above all in wind and photovoltaic power [9].

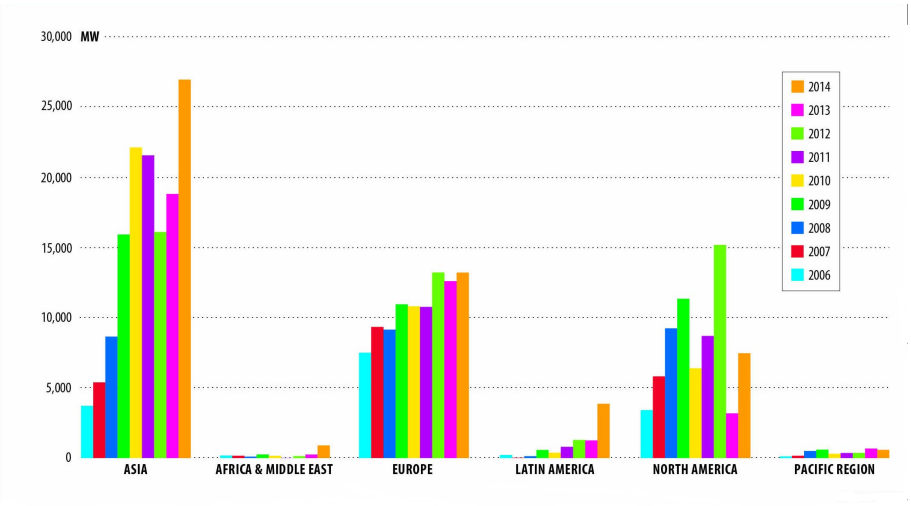

Figure 1.5: Annual installed capacity of wind power by region. Data from [10].

We can see in fig. 1.5 that the installed capacity of wind energy in the African continent is very small compared to the other regions. This is, among other reasons, because it is a new technology which requires a big initial investment

It is known that there is a lack of space in the developed continents for installing big wind turbines. That is one more reason to understand why the big enterprises have decided to take into account this continent [11]. And as fig. 1.6 shows the installing capacity has grown a lot and still keeps on increasing.

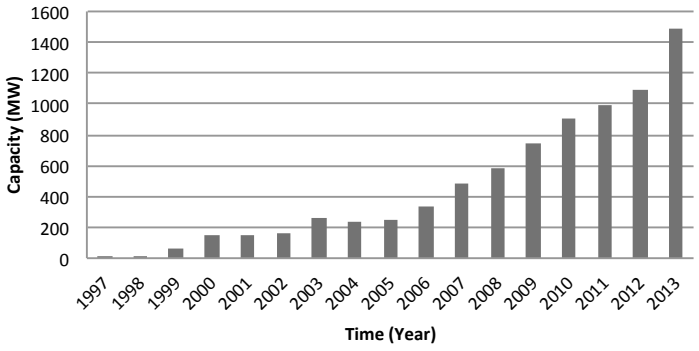

Figure 1.6: Installed wind power capacity in Africa. Adapted data from [12].

In any case, the growth is modest. According to the International Energy Agency projections (2010) [11] wind energy is expected to contribute only 2% of generated electricity in Africa by 2030. Wind energy capacity in the continent is dismissed.

Chapter 2

Choice of the location and diagnosis

In the present chapter we analyse the location, where our turbine may be delayed considering aspects such as weather, orography (the study of the topographic relief of mountains), number of inhabitants... Furthermore, we study the potential energy sources, comparing the advantages and disadvantages and choosing one of them.

As it is said, this project has been created in order to contribute to rural development in areas of the third world. Because of different reasons, like wind source, which we will discuss during this chapter, we have decided to concentrate on three Africans countries: Kenya, Ethiopia, and Somalia.

The final location diagnosis, researched in the first and second sections, will be studied following the methodology developed by Bruno Domenech Lèga in his PhD: *Metodología para el diseño de sistemas de electrificación autónomos para comunidades rurales* [13].

2.1 Socioeconomic evaluation

We cannot forget the technology we are designing is going to be used by a group of people who have their own culture, economy and social life. Therefore, researching the characteristics of the population and community are critical to the final design model, which not only has to suit the power demand but also be tailored to the culture and social context.

Because of the countries' choice and because there are so many differences between them, only the most relevant factors will be studied. Also, it would be possible that some villages did not fit perfectly with the characteristics described below since the regions are very heterogeneous.

2.1.1 Characteristics of the community:

Access roads and paved

The World Bank Data, about this issue because of the development of the countries, can only provide this information on Kenya, which the 7% of the roads are paved. Due to the development of other countries, we can consider the same rate or less for the other regions.

Transportation

Because of the paved road rate and because the project is focused on recycling the material of the community, will be little or no transportation.

Neighbour communities with renewable electrification

The rural population rate is in Ethiopia 81%, in Kenya 75%, and in Somalia 61%, so that it is expected the surroundings of the final location have nearby villages. Otherwise, it is difficult to find, in a general way, villages with renewable technology developed in this area.

Geography and Wildlife

Kenya has a large geological variety: the coastline along the Indian Ocean, a huge zone of arid or semi-arid desert in the north, a central fertile plateau, dense forest areas, some mountains like Aberdares or the mounts Elgon and Kenya, the Victoria Lake, areas of savannah and scrubland, and Rift Valley, that crosses the country from north to south.

This geography allows having a very extended wildlife, highlighting some flora such as: African Olive, Podo, Pencil cedar, Coconut tree, Mangrove swamps or Bamboo. The fauna is outsize; it is found giraffes, elephants, ostriches, rhinos, buffaloes, warty boar, Nile crocodile hippos and others.

With regard to Ethiopia, located in the "Horn of Africa", it has no outlet to the sea, its geography is characterized by having a very large plateau divided by two mountain ranges crossed by the Rift Valley. Also, the Tana Lake and the Blue Nile River have strongly influence on the climate, which it is also strongly influenced by the topography. The flora in this country is represented by: Yeheb (or Cordeauxia edulis, native tree to the Horn of Africa), Shiny-leaf Buckthorn (Rhamnus prinioides), savannah and in the valleys almost all forms of African vegetation. On the other hand, the species of wild animals are giraffes, leopards, hippos, elephants, several species of monkeys and most of the common species found in East Africa.

The third country, Somalia, is located in an arid area without any marked geographic features, the most part of the area is desert which is expanding gradually. So that, there is lack of water, grazing, wood and arable land. In the South, there are three important rivers: Tana, Juba and Shabelle, this last one forms a fertile inland marshes in its end. The flora of this country is mainly bushes: Acacia, Eucalyptus tree, Euphorbia, Boswellia, Commiphora and Yeheb. The fauna is similar to the other two countries: crocodiles, elephants, giraffes, leopards, lions, zebras, ostriches, pelicans and many other types of birds, and a wide variety of poisonous snakes.

Number of houses or other buildings

In this case, it is not necessary to know exactly the number of houses the wind turbine has to supply, due to the fact that the design idea is to create the machine as bigger as possible, taking into account that the wind turbine has to be manufactured and installed in a village and always thinking that at least two people can handle it. Once, we have in mind this limitations we will be able to determine how many households the turbine can power.

Although for ease of reference, it is estimated that for those who do have electricity access in sub-Saharan Africa, average residential electricity consumption per capita is

equivalent to around half the average level of China or one-fifth of Europe. Around 124 W/person. [14].

2.1.2 Characteristics of the population

The wealth of the community and their income sources

Due to the fact that this project is focused on poor communities of the third world, the budge is very low or nonexistent. The main pillars of their economy are cattle ranching and agriculture for survival.

The acceptance of new technologies

The groups targeted by this project are off grid, resulting in a precarious state of knowledge of new technologies. Sometimes it could be possible for the group to be reluctant to change habits and customs. Therefore, the insertion of the technology should be progressive, working with people of that society to create awareness and trust of the technology.

2.1.3 Current energy supply

The most commonly used energy sources are:

- Biomass and wood fuel
- Candles and kerosene lamps
- Diesel generators

Furthermore, in all the three countries not only the population growth rate is positive and more than 2,5% (Kenya 2.7%, Ethiopia 2.6% and Somalia 2.9% in 2013) but also the gross domestic product (GDP) has been growing exponentially in the last years.

These parameters suggest that there will be further development of productive activities, purchase of appliances and increased quality of life, which imply the electrical demand will grow in the coming years.

It is important to know this information to determine the demand of energy to adjust the design to the requirements. Furthermore, all characteristics have to be taken into account in order to tailor the machine design to the population expectation, using all their natural resources and respecting their culture, traditions, environment and way of life.

2.2 Energetic evaluation

The two most common renewable generation sources are wind and solar energy [11]. During this section, we are going to evaluate both of them and determinate why the choice is the wind energy, as we have known during the previous pages.

2.2.1 Solar resource

The solar resource is determined by the irradiation or insolation that affects at a point on the surface in a given period of time.The variability of it depends on:

- The area we are focused on

- The seasons
- The time of day
- The weather
- The altitude or elevation

The irradiation can be converted into energy thanks to the photovoltaic panels or the solar thermoelectric power plants. Because of the project aim, we only consider the first ones.

The global equation to estimate the energy generated in output of a photovoltaic system is:

$$E = ArH\,\mathrm{PR} \tag{2.1}$$

where: E = Energy (kWh), A = Total solar panel Area (m^2), r = Solar panel yield (%), H = Annual average solar radiation on tilted panels (kWh/m^2), PR = Performance ratio, coefficient for losses (range between 0.5 and 0.9 default value = 0.75) where the orientation and inclination of the panel is included.

Examples of losses details that give the PR value (depend on the site, the technology, and sizing of the system) according to [15].

- Inverter losses (4% to 15%)
- Temperature losses (5% to 18%)
- DC cables losses (1 to 3%)
- AC cables losses (1 to 3%)
- Shadings (0% to 80%) (Specific to each site)
- Losses due to diffuse radiation (3% to 7%)
- Losses due to dust, snow... (2%)

As well is know, the annual average solar radiation on tilted panels differs according to the location. In the images showed below, we can see different maps with the radiations, one of them shows the African continent, and the other that emphasize the research area. Thanks to that, it can be concluded that the radiation in Africa and in that concrete regions is very closed and near the 2050 kWh/m^2 in the most part of the area.

To give a closer idea of that...

Using equation (2.1) and the data of fig. 2.1 and 2.2, we can calculate the energy that could be extracted, in a general and quick way.

We assume:
A = 10 m^2, more or less the common home-format
r = 15%, because this yield is typically between 10% and 20%
H = 2050 kWh/m^2, according to the figs.
PR = 73% because:

- Inverter losses= 8%, assuming the medium rate
- Temperature losses= 8%, assuming the medium rate

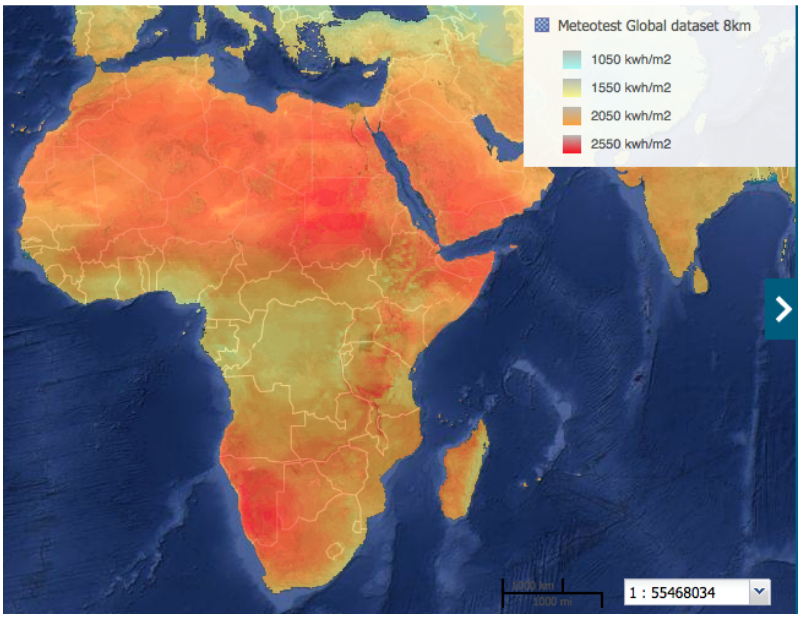

Figure 2.1: Solar radiation in Africa. Data from [16], Meteotest Global dataset 8km.

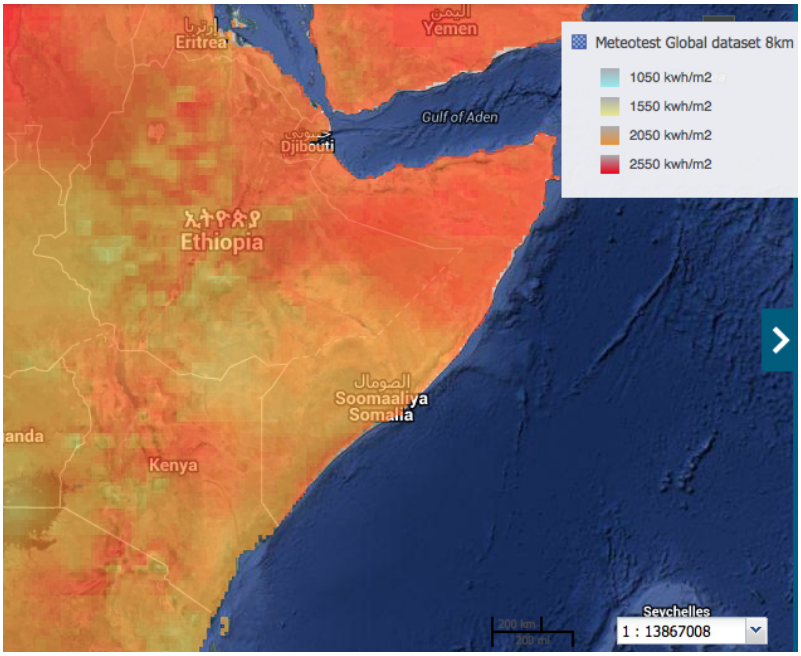

Figure 2.2: Solar radiation in Africa, focused on Somalia, Kenya and Ethiopia. Data from [16], Meteotest Global dataset 8km.

- DC cables losses= 2%, assuming the medium rate
- AC cables losses= 2%, assuming the medium rate
- Shadings= 3%, because it is consider that in that area the panels do not have a lot of shades

- Losses weak radiation= 5%, assuming the medium rate
- Losses due to dust, snow... = 2% It is not possible to have snow, but it is probably to have powder

We then have:
$E = 2244.75$ kWh

2.2.2 Wind resource

Just as the sun, also the wind is an unlimited source of energy. The wind resource is strongly variable.

Wind variation in space:

- The area we are focused on
- Wind direction changes continually
- Effects of orography and obstacles
- The height of the machine or above the ground, wind shear

Wind variation in time:

- Long term (>year)
- Annual
- Seasonal
- Diurnal
- Short time, gusts and turbulence.

Also, it is necessary to know that local winds are studied in various scales:

- Global: Great hemispheric movements
- Synoptic: Anticyclones, depressions
- Mesoscale: Local Winds, local storms, sea and land breezes, mountain wind
- Micro-scale: Effect of obstacles, vegetation and terrain roughness

Wind turbines convert the wind resource into energy. There are many configurations of wind turbines but the main concept is the same. Therefore, there is a equation, which can help us to calculate the extractable energy:

$$P = \frac{1}{2}\rho A V_{\infty}^{3} \eta Cp \tag{2.2}$$

where P = Power (W), ρ = Air density (kg/m^3), A = Area where the flow of the air goes through (m^2), V_{∞} = Undisturbed wind speed (m/s), Cp = Power factor (maximum range 0,6 because of the Betz Law) and η = Electricity and mechanics losses (%).

Note that this power equation is a strong function of undisturbed wind speed due to the fact that their relation is cubic, and linearly dependent on the area, as in the case of the solar resource.

As it is said, the wind can be studied with different scales, fig. 2.3 and fig. 2.4 are 2 wind maps of Africa, where it is observed the wind resources in a global scale, the first one, and in mesoscale the second one.

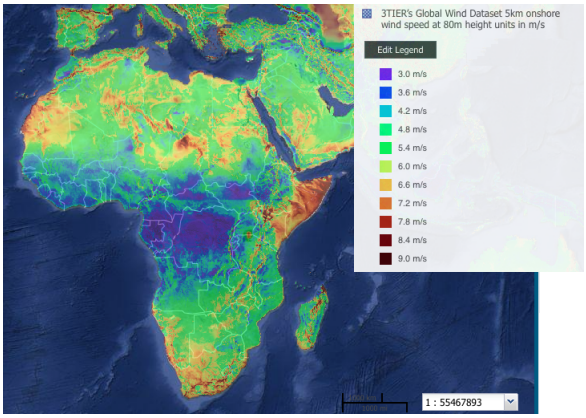

Figure 2.3: Wind resource in Africa. Data from [16], 3TIERs Global Wind Dataset 5km onshore wind speed at 80m height units in m/s.

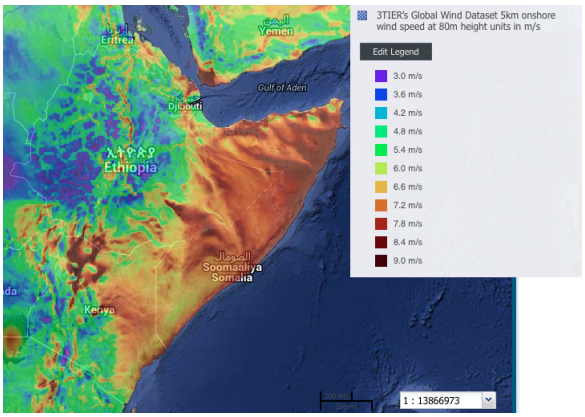

Figure 2.4: Wind resource in Africa, focused on Somalia, Kenya and Ethiopia Data from [16], 3TIERs Global Wind Dataset 5km onshore wind speed at 80m height units in m/s.

It is interesting to observe that in the wind source case, the resource is less homogenous than the solar. Therefore, the final location will have to be studied taking in account all the scales. It is necessary to choose a windy zone, thanks to the orography, local winds... and also know how the environment, the terrain complexity and roughness affect the wind profile, and its speed. All this parameters are going to be studied in the next section.

To give a closer idea of that...
Using the equation 2.3 and supposing that the undisturbed wind speed is 6 m/s, we calculate the energy could be extracted with this resource, in a general and quick way:

assuming:
$\rho = 1.126$ kg/m^3, Air density in Africa with conditions: Relative humidity: 45%, Temperature: 30°C and Air pressure: 1010 hPa.
$A = 7.06$ m^2, Area with a rotor diameter 3 m.
$U = 6$ m/s, as we have supposed.
$Cp = 0.45$ common coefficient for three-bladed rotor.
$r = 0.95$

we then have:
$P = 367.477$ W
Which in kWh is:
$E = 3219.09$ kWh

2.2.3 Comparison and election

To conclude this chapter, it is interesting to determine the advantages and the disadvantages of using these resources in the area where we are focused on:

Firstly, say that there are some advantages linked to be natural resources such as: These resources are free and unlimited; energy extraction does not cause pollution and allow us having electricity out of grid. Also, there are some disadvantages like: These resources are strongly dependent on the sunny or windy weather, they have a reduced efficiency and it is necessary a large initial investment.

In the second place, thinking about solar resource, in one hand, this system follows perfectly the daily industrial consumption curve, which it means; the energy is produced exactly when it is going to be used. That it is interesting for the batteries measurement, because it could allow use smaller ones. But in the other hand, if we talk about home lighting, it changes. As the energy is needed during the night, where it is not sun, so that the batteries should be oversized. Also, the main advantage of the solar resource in this area is that the radiation is much bigger than in the most of the regions in the world, as is clear from the Solar radiation maps fig. 2.1 and fig. 2.2.

Conversely, the solar panels cannot be homemade, and their purchase cost is relatively expensive because of their manufacture. Furthermore, owing to the high prizes, there is a high risk of theft.

With regards to the wind resource, the area chosen is one of the windiest in Africa, so that the wind resource is high and it supposed to provide us enough force to make work the machine. Furthermore, a wind turbine is easy to make from scratch using material such as copper, timber, resin and steel.

Finally, it has been decided that the generation resource we implement in that area is the wind. The main reason is that it is worth building a wind turbine not only because in that regions there are good wind conditions but also because the manufacturing can be cheap and handcrafted.

2.3 Wind resource evaluation

The assessment of the on-site wind potential is an essential phase of any wind project. The electrical machine can extract energy from the wind in determined by two facts: the wind turbine parameters and the wind characteristics in the site like velocity or density. In the present section we discuss the wind characteristics.

The wind power passing through the rotor is given by:

$$P = \frac{1}{2}\rho A V_\infty^3 \tag{2.3}$$

As we can see in equation (2.3)apart from the wind speed U, the wind power also depends on the air density ρ. The weather conditions in this African zone are far from the standard conditions, which are: 1013.25 hPa and 0°C. So that, the air density will be different from the standard: 1.293 kg/m^3. If we suppose a 45% of relative humidity, 30°C and 1010 hPa, we will have 1.126 kg/m^3 of air density. In these conditions, the air density is smaller than the standard value, implying that the power extractable will be lower, how the following fig. shows:

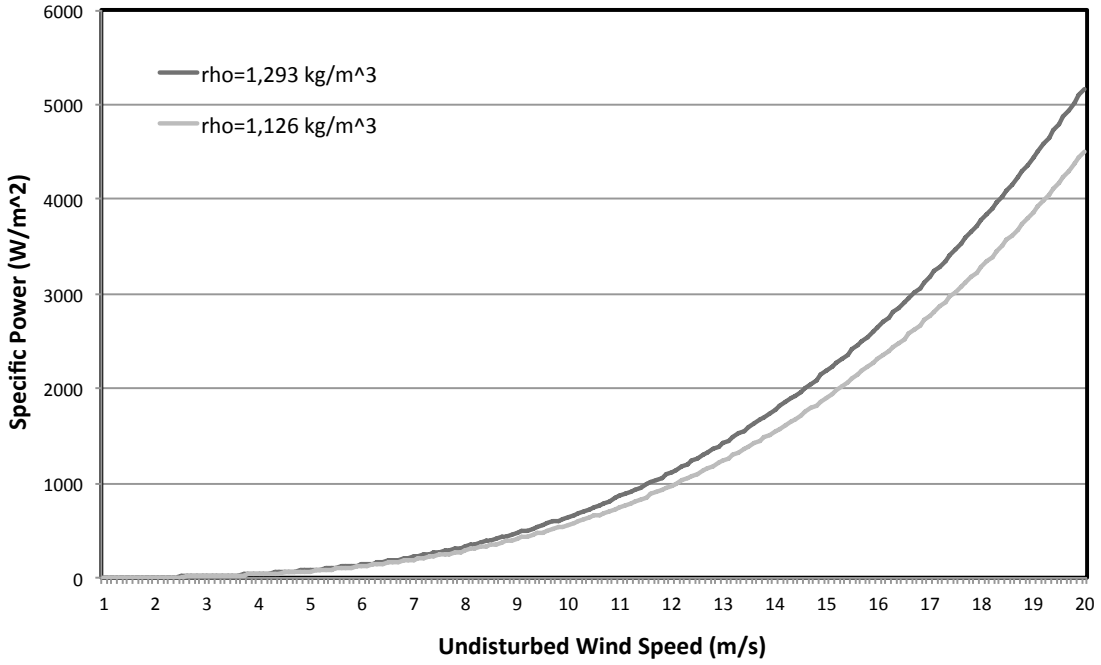

Figure 2.5: Specific Power vs. Undisturbed Wind Speed.

The turbine cannot absorb all the kinetic energy of the wind. We only are able to extract a maximum of 16/27 of wind power given by the equation (2.3), because of the Betz's Law [17]

The maximum extractable theoretical power, therefore is:

$$P = \frac{1}{2}\rho A V_\infty^3 \frac{16}{27} \tag{2.4}$$

In real operation, these machines try to follow the maximum theoretical power curve but owing to the rate power, efficiently and the control systems (concepts of which we will talk about in following sections), the real curves generated cannot capture completely the available wind power. As we can see in the fig. 2.6:

From equation (2.4) it can be seen that the available power is proportional to the air density, the area and wind speed. A small variation in wind speed is a great variation in the extractable power. Therefore to evaluate the energy availability of a location it is

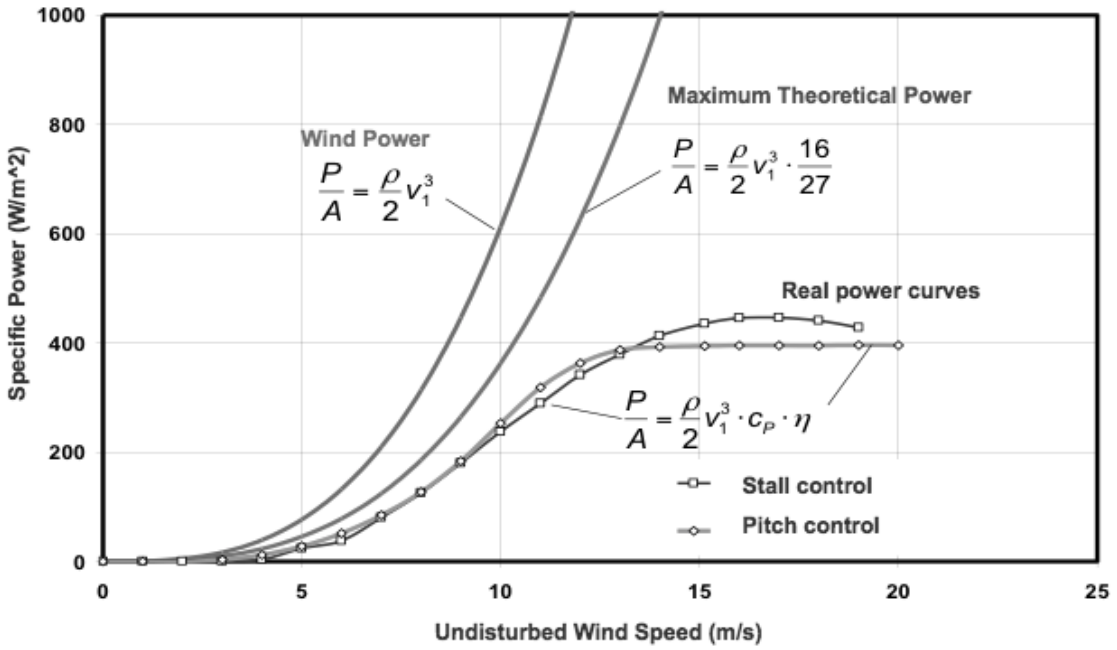

Figure 2.6: Specific Power vs. Undisturbed Wind Speed in different cases. Figure from [17].

crucial to know: the weather conditions, terrain roughness, wind speed distribution and frequency distribution, as we will see in the following section.

In this thesis, the area elected is too huge, because we have considered three different countries, and so that, we do not have the data of the final emplacement. However, there are some interesting steps to follow before setting the wind turbine in a location, provided that we have the essential tools:

2.3.1 Choice of possible locations

As we said before, there are two different classifications for wind regarding to the scale, the micro scale and global scale. In our case, we are focus on three countries, and so that the global scale is chosen.

Concerning the micro scale, it is interesting to select some different locations where the machine could be installed. It is know that wind varies in the space, so that; for the possible locations election, we have to take into account:

- Effects of orography and obstacles: The buildings or trees near the machine will generate perturbations and turbulence in the wind profile. Because of that, it is advisable to elect the locations far from obstacles.
- Select the highest zones in the village, since there the wind profile will be free stream or the terrain roughness is not too relevant in the profile of the wind.
- The site should also be relatively close to the point of consumption in order to save money in materials and have visual control of the machine. What is maybe in contradiction to the pursue recommendation.

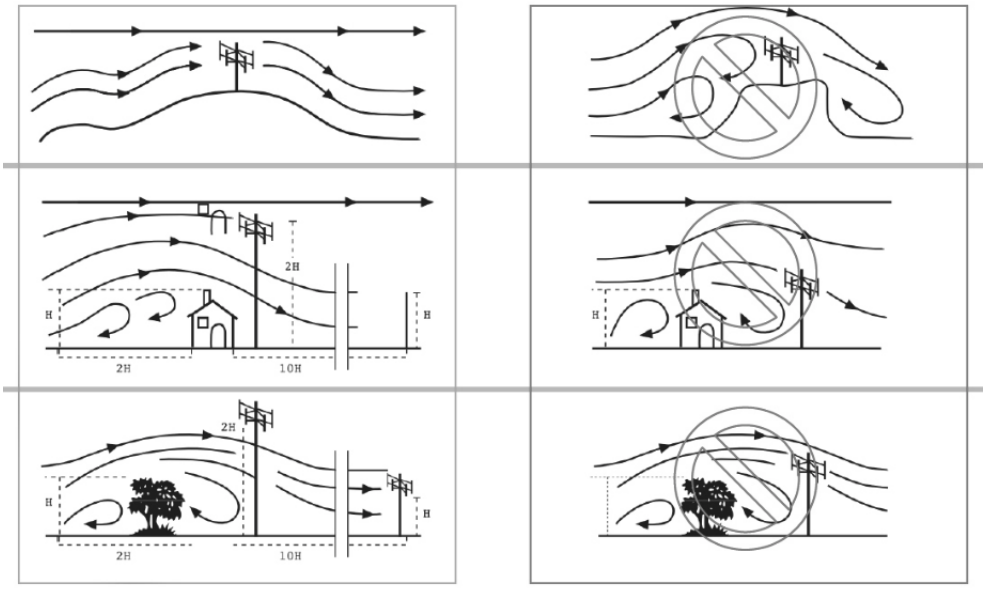

Figure 2.7: Good and wrong ways of choosing the possible location. Figure from [18].

2.3.2 Anemometers installation and data collection

Once the locations have been chosen, it could be interesting to install an anemometer in each of the places. With these devices we can measure the wind, collect some data and later analyze it. The more data we have on winds speed and direction, more representative and less biased the data analysis will be.

2.3.3 Data analysis

With all the data collected, we have to clear it up and do the following analysis:

Wind variations on time (daily, monthly, yearly...)

It is required to know how the wind speed varies during the time. The best ideal situation is to have no speed changes in the period or at least have soft variations, witch it means have almost all the time the same wind speed. It is successful owing to the fact that with no wind speed changes, the machine will not detect turbulence and it could work in a continuous and optimized way.

In the fig. 2.8, we can observe an example of two different places, where it is shown the relationship between the wind speed and the days of a month.

Thanks of this type of figure it is easy to interpret the data recollected, and to visually evaluate the results, order to observe the wind speed dynamic evolution.

Wind direction distribution, wind rose

The knowledge of the dominant wind directions and variability is important in order to find the arrangement of wind machines in uneven terrains because the best option is to find a location where the wind direction does not have significant variations. For studying the direction distribution, we will do a wind rose similar as the fig. 2.9, which shows us

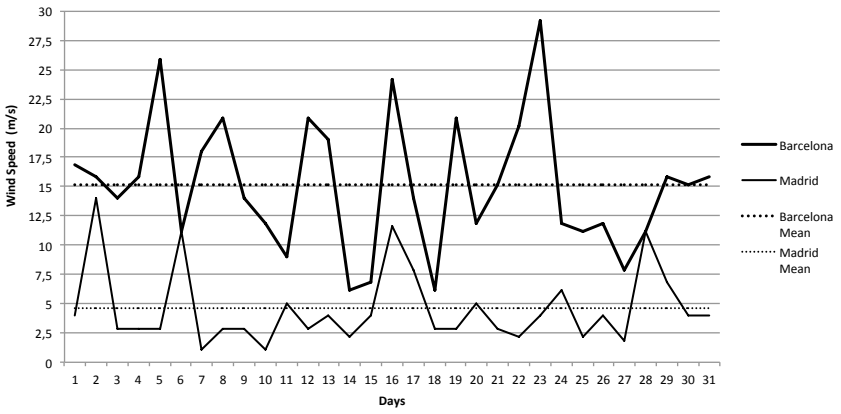

Figure 2.8: Wind speed vs. Days of January 2012 in Barcelona and Madrid. Adapted data from [19].

the wind direction. Take to account wind rose can be influenced by obstacles situated upstream of the wind turbine.

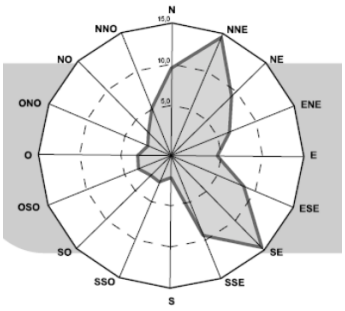

Figure 2.9: Example of wind rose. Data from [17].

Histograms and Weibull distribution function

With all the wind data collected, we can approximate it using a Weibull distribution, which is function of two parameters called A and K, or using the Rayleigh distribution function of a single parameter. This makes the first one is more versatile than the second, so that, we establish the first as a model.

Weibull probability density function is given by:

$$\begin{array}{ll} f(x) = \frac{k}{A}(\frac{x}{A})^{k-1}e^{-(x/A)^k} & x \geq 0 \ ; \ A > 0 \ ; \ k > 0 \\ f(x) = 0 & x < 0 \end{array} \tag{2.5}$$

If it is plotted, we get the fig. 2.10:

The scale parameter is given with A (Amplitude) and the parameter K defines the shape of the Weibull distributions.

This function describes the relative likelihood for this random variable to take on a given value. Thanks to this distribution we know how the wind behavior is and what the

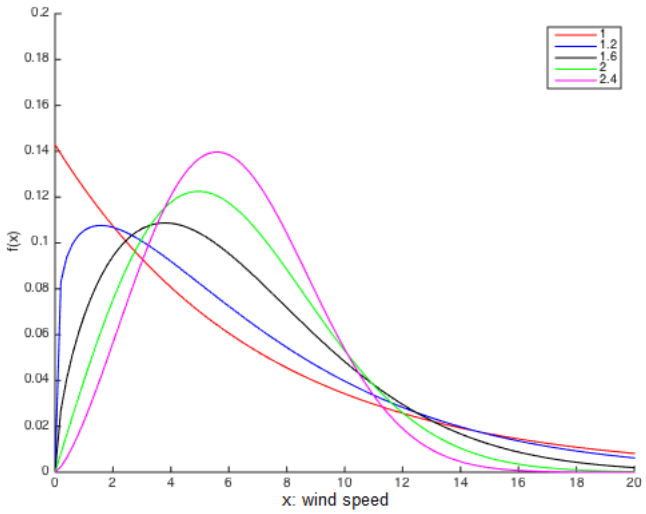

Figure 2.10: Weibull probability density function with A =7, and some different values of k. Fig. from [20].

most likely speeds are. Using the fig. 2.10, we can observe how this function changes if the parameter k changes its value. As bigger is the parameter k, as much in the right the peak of the function is.

Also, it is important to know that the peak of the function is not the wind speed mean, the mean is a little bit smaller than that value. The average velocity can be calculated from the equation (2.6) [17]:

$$\bar{U} = c\Gamma(1 + \frac{1}{k}) \tag{2.6}$$

where Γ is the gamma function.

And here the cumulative distribution function:

$$F(x) = 1 - e^{-(x/c)^k} \tag{2.7}$$

If it is plotted, we get the fig. 2.11:

With this type of graphic we can known the probability of the wind speed. Thanks to programs like Excel or Matlab, we can parameterize the distribution histogram obtaining a continuous function with the necessary parameters. Below, there is a example of one histogram and its Weibull function.

AEP (Annual Energy Production)

The wind turbine electrical potentiality can be calculated by the following expression [17]:

$$Potentiality = P * f(u) \tag{2.8}$$

where P: electrical power and $f(u)$: Weibull probability density function.

From this expression we obtain the Annual Energy Production like [17]:

$$\text{AEP} = N_h * \int_1^N P * f(u) \tag{2.9}$$

where N_h: number of hours in a year (about 8760) and N: number of bins

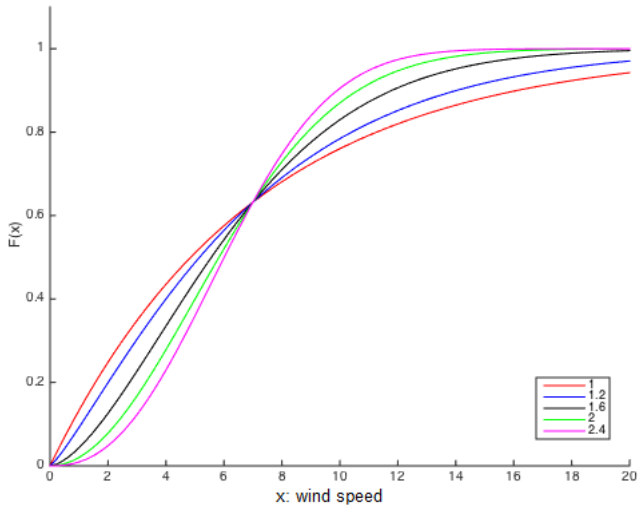

Figure 2.11: Cumulative distribution function with A=7, and some different values of k. Fig. from [20].

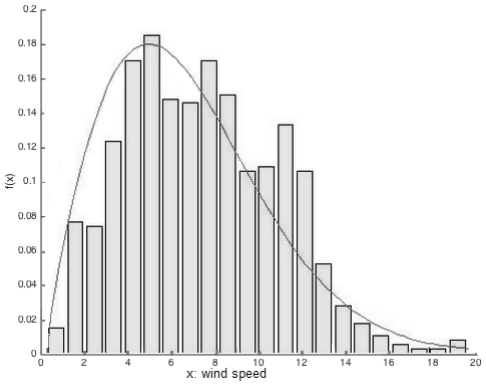

Figure 2.12: Weibull function from a histogram. Fig. from [20].

Thanks to the trapezoidal rule, a quadrature rule for approximating integrals, it follows that:

$$\text{AEP} = N_h * \sum_{i=1}^{N} [F(u_i) - F(u_{i-1})] * \left(\frac{P(u_i) + P(u_{i-1})}{2} \right) \tag{2.10}$$

where AEP: Annual Energy Production, N_h: number of hours in a year (about 8760), N: number of bins, u_i: normalized and averaged wind speed in bin i and $P(u_i)$: normalized and averaged power output in bin i, $F(u_i)$: cumulative distribution function in bin i 2.7.

The energy produced depends on the power curve and not on the peak power. This in turn depends mostly on the turbine's physical size (diameter) and the site distribution of wind speeds. Most of the energy will be produced while the turbine it is generating less than it's rated maximum power. In these everyday winds, the power depends on the size of the turbine and the wind speed, and not it's power rating. This parameter gives

a global idea of how much energy a wind turbine can produce during one year. So when some places are taking into account this parameter will give the final decision to instal the machine in one place or another. The higher is this value for one place, the best is that location to place the wind turbine.

2.3.4 Final election

This project and the design of the wind turbine is done for the micro-turbines, and because the wind speed will be low, it would be very interesting to develop the machine with the cut-in speed close to 3 m/s. Also, we have to take into account the wind variation on time and the wind direction distribution. The optimal situation is not to have variations neither on time nor on the direction distribution.

About the direction of the wind it is better not to have a lot of variation in it. Although as we will see later (Chapter 8) the yawing system would direction the machine towards the wind speed, the cables in the wind turbine could curl and break down. That is one of the main reasons why it interesting not to have a lot of variation.

Using the Weibull distribution for winds, we are interested in the curves situated with the peak in the right. This indicates high probability of strong winds and low probability of light winds. This is because the generated power would increase increasing the wind speed.

Chapter 3

Goals and dimensioning

To be able to do a correct design of the wind turbine, it is crucial to have a clear idea about requirements needed, which describe the requested behavior of the wind turbine. The most essential desired properties are:

- Low cost machine
- Use of recycled material
- Use of low cost material
- Easy manufacturing
- Easy assembling
- Easy maintenance
- Low noise
- Integration with the culture and society
- High security (Active - Passive)
- Standardized tool to do the manufacturing, assembling and maintenance
- Low cut-in point
- Environmental resistance
- High mechanical strength
- 10 years minimum life cycle (If the materials chosen have good qualities)
- Modular design
- Adjustability of a wide range of wind speeds

Not all the requirements factors are equally significant in the machine design. We highlight some of them as the most important.

- High security (Active - Passive)
- Integration with the culture and society
- Standardized tool to do the manufacturing, assembling and maintenance

- Low cost machine

Once the requirements are known, it is time to do a first dimensioning. One of the strongest idea about dimension is that the machine should be able to be handled by maximum 2 people. That is, the dimensions like measures or weight have to be less than the ones that two people can bear.

- Rotor blade dimensions: 0.75 - 2 m
- Tower height: 5 - 8 m
- Cut in point: 2 - 3 m/s
- Cut out point: 10 - 12 m/s

Chapter 4

History and existing technology

Although the use of the wind turbines to generate electricity is more or less recent, windmills exist since the first century AD when the Greek engineer Heron of Alexandria invented it to power a machine [21]. We can see his invention in fig. 4.1.

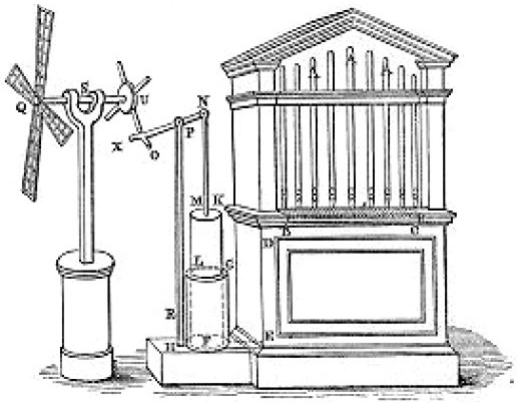

Figure 4.1: Heron of Alexandria's wind turbine. Figure from [21].

The first wind turbine with the purpose of generation of electricity was built by Professor James Blyth of Anderson's College, Glasgow in July of 1887 [21].

So, at the beginning of the invention of the wind turbines the objective was to build the biggest turbine ever. Nowadays, taking into account offshore machines, it is also very important to make as big and robust wind turbines as they can: the company Senvion SE started on the beginning of this year to install the 6.2M152. The company announced it on November of 2013, this is the biggest one ever built, its rotor diameter measures 152 m and it has 6.2 MW of power [22].

But bearing in mind onshore turbines, it is not so important how big you make it, but is more important to have a good one with good efficiency and sometimes, small enough to place it in a neighborhood. That is one reason why nowadays there are lots of companies researching the small wind turbines technology.

But, let's focus on homemade sector:

There are lots of people trying to make their own wind turbines using scrap or useless items and transforming them into a machine that can generate electricity. In this way, they can achieve electricity without paying for it. This is really interesting, above all, if there is no grid around their houses and the unique way to obtain energy is using fossil fuels.

There are a lot of different homemade wind turbines, we will name here a few of them:

William's wind turbine

William Kamkwamba is a Malawian man who built his first machine in 2002 at 14 years old. His purpose was to bring electricity and running water to his village, and when he saw a picture of a wind turbine he decided he should build one himself [23].

He made it assembling bicycle parts, a tractor fan blade and an old shock absorber and he fashioned the blades from plastic pipes.

In fig. 4.3 we can see William Kamkwamba and his turbine.

Figure 4.2: William Kamkwamba and his first wind turbine.

Navas I

The designer of this wind turbine is a professor at the University of Valencia, named Joaquín Navasiquillo Hervas. It is a PMSG, permanent magnet synchronous generator. The blades and almost all the turbine is made of wood. He built the generator using two iron discs and neodymium magnets and to make the coils of the generator, he used pegs and enclosed them with copper threat [24].

Homebrew 10' Wind Turbine

The people of Otherpower [25] are who made experimentally the design of this project. The main materials are wood, iron and metal.

The rotor measures 10 feet (3.08 m). They have thought about the common pine to the design of the blades and it should be as dry as possible. The generator is a PMSG, made of steel, NdFeB and fiberglass.

Hugh Piggott's wind turbine

Hugh Piggott has lived off-grid in Scotland since the 1970s. He built his own machines and nowadays the whole population of Scoraig, the village where he lives, gets electricity from his turbines [26].

Many organizations worldwide use Hugh's designs to produce small wind turbines. They can easily build their own machines because of the books he has edited: *Wind power workshop* [27] and *A wind turbine recipe book* [28] are the books we have been able to read and use.

The wind turbine is a horizontal axis, 3 bladed and upwind, and if we talk about the generator, is a PMSG.

Figure 4.3: Hugh Piggott's designed wind turbine built by the society Ti'eole in Valence, France. January 2015.

The blades are made of timber, the shape of each blade can be easily formed from a piece of wood. To balance and fix them, they use two pieces of wood in the middle screwing each one in one side of the blades.

Secondly, the generator is, above all, made of steel for the rotor's discs, magnets, cooper wire to build the coils, composites to join everything together and wooden molds to be sure that they give the good shape to the generator.

The nacelle is made with parts of metal, cutting and welding them until it has the appropriate form for the dimensions of the rotor.

Finally, the tower is made of metal, and to balance and fix it to the ground steel wires are used.

The philosophy of Hugh Piggott and all the societies that teach their design is to achieve a cheap and sustainable way of obtaining energy. In this case, wind energy. In fig. 4.3 we can see a group of people in Valence assembling a wind turbine. That machine was manufactured and assembled in January of this year by 19 people.

Chapter 5

Rotor. Design, analysis and manufacture

The rotor is one of the most important parts of the wind turbine. It consists of one or multiple blades attached to a hub and it is where the wind energy is converted to rotational energy and, thanks to the generator, to electricity.

5.1 Types of rotors

We can classify the types of rotors taking into account different aspects such as the direction of the axis, number of blades and the rotor position regarding the wind direction.

5.1.1 The direction of the axis: Vertical or Horizontal axis

Regarding the direction of the axis, there are two different designs: Vertical axis and Horizontal axis.

There are two basic designs of vertical axis, Darrieus and Savonius, as we can see in fig. 5.1. And about horizontal axis wind turbines we will talk in the following sections.

(a) Darrieus rotor (b) Savonius rotor

Figure 5.1: Vertical axis wind turbines.

The vertical axis machines are a technology which is still being developed. Some characteristics of them are that they do not need any yawing system, the generator, gearbox and most of the heavier items can be placed at ground level, also, the machine does not need a tower. On the other hand the wind speed near the ground is slower, and in order to achieve as high speed values as possible these machines could have a tower. The efficiency is small and the use of these kind of wind turbines is lower if they are compared with the horizontal axis ones.

The horizontal axis machines have a much higher efficiency, so the technology is much more robust and generally, more secure.

5.1.2 Number of blades

Regarding the number of blades, we can find wind turbines with as many blades as you can imagine, in both designs, horizontal and vertical axis. There are turbines with one blade, two-bladed wind turbines and there are also machines with more than 10 blades. The multi blade rotors are useful for water-pumping windmills, because they were built to produce high torque. To generate electricity you need speed rather than torque.

The most common design in horizontal axis is three-bladed turbine.

5.1.3 The rotor position regarding the wind direction: Upwind or Downwind

This distinction is only suitable for the horizontal axis machines because the vertical wind turbines do not need to change their position to respect to the wind.

As we can see in fig. 5.2 the difference between these two wind turbines is the position of the rotor. In the upwind machines, the rotor is in front of the nacelle and in the downwind ones the rotor is in the back side of the nacelle. The advantage of upwind

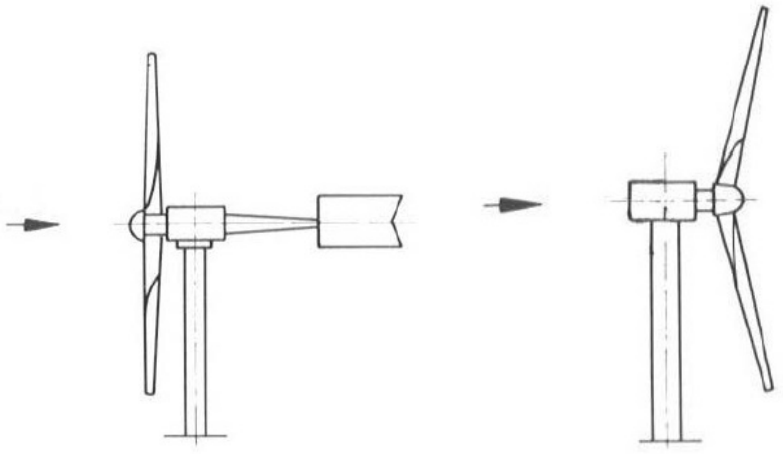

(a) Upwind rotor (b) Downwind rotor

Figure 5.2: Upwind and downwind rotors.

rotors is that there is not any interference in the wind because of the pass of it around the tower. The disadvantages are that it needs an orientation system (it could be passive or active) and that the material of the blades cannot be very flexible, because if the blades bend, they could crash with the tower.

In the downwind turbines, those problems do not occur, they can orientate themselves and the material of the rotor could be more flexible. But there is more turbulence in the wind in these kinds of designs.

5.2 Choice of the rotor

The pattern chosen to be designed and manufactured using low-cost resources is an horizontal axis machine, with 3 blades and upwind rotor.

In this choice we had take into account that the horizontal axis machines have a technology more developed than the vertical ones and also, that they are more efficient. We therefore opted for a horizontal axis wind turbine.

Regarding the number of blades, we chose 3 blades because the power coefficient with a three-blades rotor is higher than other configurations [17].

About the rotor position, the upwind machines have an advantage regarding to the downwind machines. The wind passes first through the turbine and then through the tower, which means there are less interferences in the wind and it is more uniform.

5.3 Design and materials

There are many different profiles on the market, often with characteristics that are well known. The challenge of this section is to create a blade using common and/or recycled material, in order to make it possible that the wind turbine is locally manufactured and maintained.

The blade design procedure is shown in fig. 5.3.

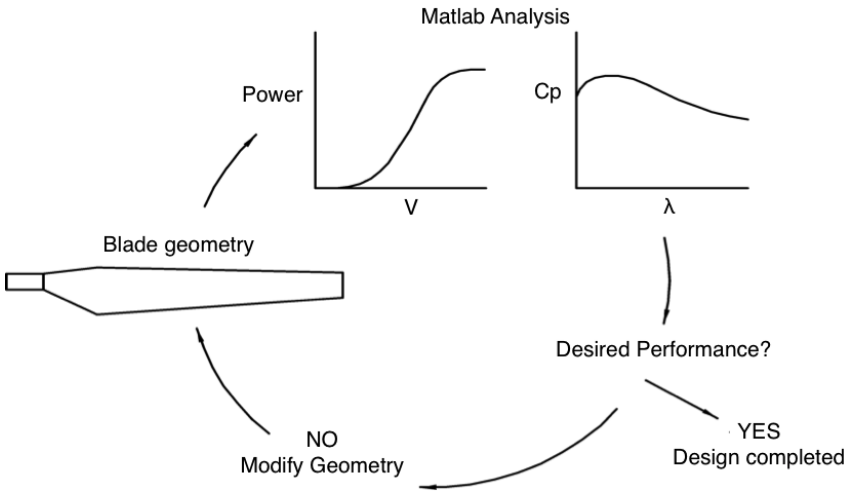

Figure 5.3: Analysis and design loop to optimize the blade geometry.

The blade geometry is streamlined using one Matlab programme, which is created specifically for this purpose. The loop starts with a first blade geometry, the blade geometry parameters will be the inputs in the Matlab code which is done using BEMT (Blade Element Momentum Theory, explained in the next section), and this will give us some outputs like power or turbine efficiency, which we will have to interprete in order to know if the geometry is good enough or if it has to be changed, and restart the optimization loop.

5.3.1 Aerodynamic theory overview

The design of the blade was done using Blade Element Momentum Theory (BEMT) [29], this is a theory that combines both blade element theory and momentum theory. But first of all lets develop some important aerodynamic ideas in order to be able after that to present and explain the Matlab code done.

Wind Power - Maximum wind power extractable - Betz's Law

Using a simple model with a control volume, whose boundary is the surface of a stream tube, we can observe and analyse the wind power, the maximum wind power extractable and the upper limit efficiency.

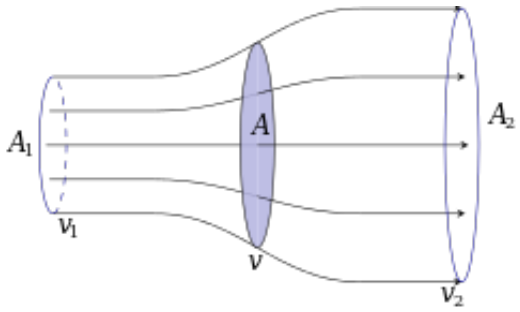

Figure 5.4: Stream tube around a wind turbine. A denotes the area and V denotes the speed, whereas the number (1 or 2) indicate the different locations. 1 is the position before the turbine and 2 after it.

The following assumptions are made.:

- The rotor is an ideal rotor, which means: the rotor does not have a hub, it has an infinite number of blades with no frictional drag.
- The flow into and out of the rotor is perfectly axial and the flow through the rotor disc is unconstrained.
- The flow properties: incompressible, constant density, homogenous and there is no heat transfer.
- Uniform thrust over the rotor area.

The power in the wind has been characterized in the previous sections, with the formula:

$$P = \frac{1}{2}\rho A V_1^3 \tag{5.1}$$

But regarding to the rotor power, the turbine does not absorb all the kinetic energy of the wind. The absorbed energy is the energy difference of input and output:

$$P = \frac{1}{2}\rho A (V_1^3 - V_2^3) \tag{5.2}$$

where P = Power, ρ = Air density, A = Area where the flow of the air goes through, and V_1 and V_2 the wind speed in locations 1 and 2.

($\rho = 1.225$ theoretical, $\rho = 1.26$ kg/m^3 in African conditions: Relative humidity: 45%, Temperature: 30°C and Air pressure: 1010 hPa.)

Thanks to equation (5.2) we find:

- To absorb all the power of the fluid vein, the output speed V_2 should be zero, which is impossible because would prevent the flow of the air downstream.
- If V_2 output speed equal to the input V_1 would imply no absorption in the wind turbine power.

Because of the first consideration, the wind turbine rotor performance is usually characterized by the next equation which only involves the wind speed upstream, the wind speed unperturbed, V_1:

$$P = \frac{1}{2} Cp\ \rho A V_1^3 \tag{5.3}$$

where Cp is the power coefficient.

The power coefficient, Cp, is a non-dimensional parameter which represents the fraction of the wind power that is extracted by the rotor. Using equations (5.1) and (5.3), the following expression is obtained:

$$Cp = \frac{P}{\frac{1}{2}\rho A V_1^3} = \frac{\text{Rotor Power}}{\text{Power in the wind}} \tag{5.4}$$

Using the previous assumptions, it is possible to calculate the maximum of the Cp, known as the Betz limit [30]. It shows the maximum possible energy that may be derived by means of an infinitely thin rotor from a fluid flowing at a known speed.

This value is:

$$Cp_{max} = \frac{16}{27} \approx 0.5926 \tag{5.5}$$

The Cp of the machine is different depending on the wind turbine design, the number of blades and the direction of the axis. Nowadays, the most modern and largest three bladed machines achieve peak values of Cp around 0.45 or even 0.5, while others like Savonious machines barely exceed 0.1.

Figure 5.5 shows the relationship between Cp and the tip speed ratio (λ, TSR). The tip speed ratio is the ratio between the tangential speed of the tip of the blade and the unperturbed wind speed:

$$\lambda = \frac{\omega R}{V_\infty} \tag{5.6}$$

where ω = rotor rotational speed in radians/second, R = the rotor radius in meters and V_∞ = the undisturbed wind speed in m/s.

Forces on a wind turbine rotor

The wind turbines uses the forces created by the wind to produce a rotational movement which is converted into electricity.

Because of the movement of the rotor, the wind which impacts in the blade, the apparent wind, is the vectorial sum of the unperturbed wind and the component generated due to the rotational movement, the tangential speed. See fig. 5.6.

As it is shown in fig. 5.6, the apparent wind is:

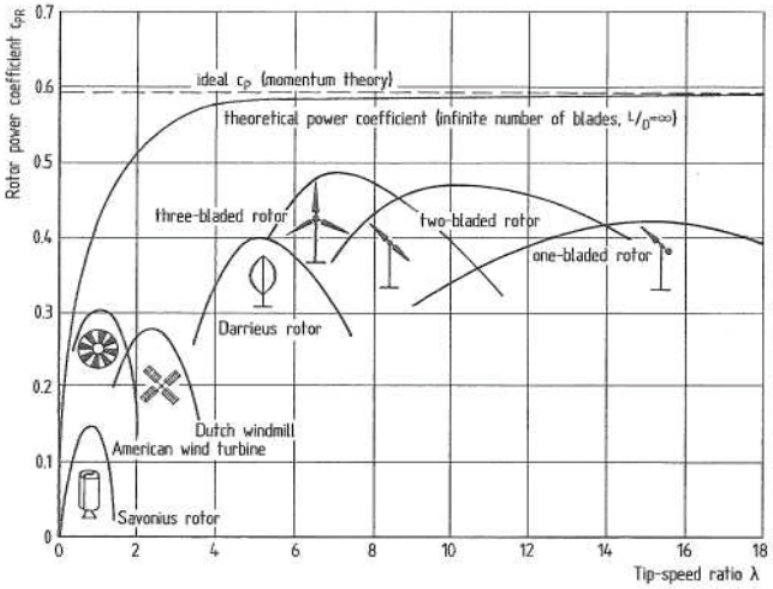

Figure 5.5: Cp vs. tip speed ratios for different designs of wind turbines and maximum power coefficient.

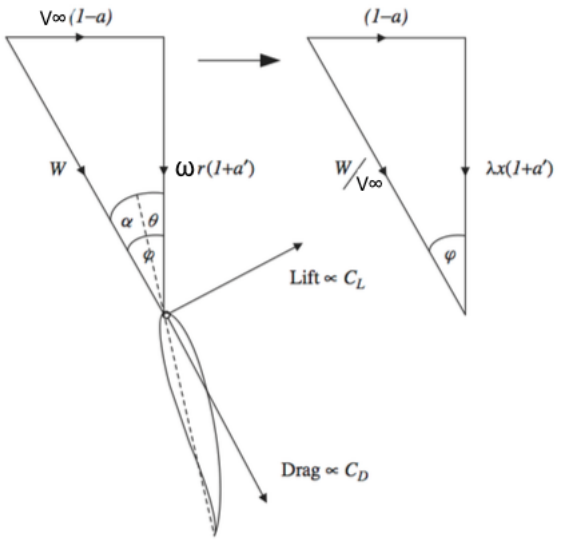

Figure 5.6: Geometry of the flow at the blade. From [29].

$$\vec{W} = \vec{V_\infty}(1-a) + \vec{\omega} r(1+a') \tag{5.7}$$

where a and a' are the axial and tangential induction factors respectively.

The axial induction factor, a, is defined as the fractional decrease in wind velocity between the free stream and the rotor plane. While, the tangential induction factor, a', is the value to take into account that if an axial flow imparts rotation on a rotor, then the rotor must also impart a counter-rotation on the flow, [29].

To obtain these two parameters, two different expressions for torque and for the thrust are equaled. The first equations, for thrust and torque, are derived from the momentum theory, explained later, and the second ones are expressed in terms of the lift and drag coefficients of the aerofoil.

Doing some algebra one obtains an expression for the axial induction factor (5.8) and for the tangential induction factor (5.9):

$$\frac{a}{1-a} = \frac{\sigma C_l[1 + \frac{1}{k}\tan\varphi]}{4F\sin\varphi\ \tan\varphi} \tag{5.8}$$

$$\frac{a'}{1-a'} = \frac{\sigma C_l[\tan\varphi - \frac{1}{k}]}{4F\sin\varphi} \tag{5.9}$$

where σ is the local solidity, defined the fraction of the rotor disc that is actually covered by the rotor blade, given by the next equation:

$$\sigma = \frac{B\ c}{2\pi r} \tag{5.10}$$

and k is the lift-to-drag ratio, defined as:

$$k = \frac{C_l}{C_d} \tag{5.11}$$

The effect of wind on blade profile generates: lift, drag, torque and thrust, as we can see in fig. 5.7.

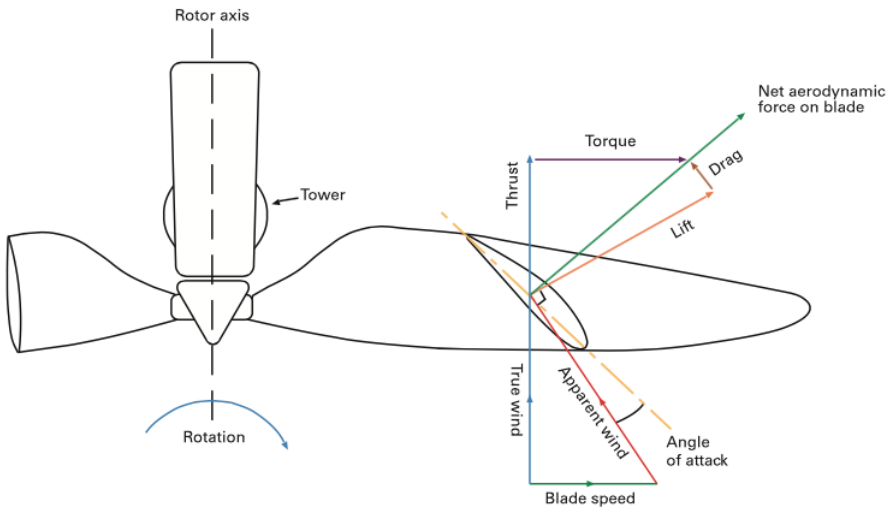

Figure 5.7: Forces on a wind turbine rotor. Figure from [31].

- Lift: It is consider the force that produces the rotor power and is perpendicular to the apparent wind flow.

  As we can see in fig. 5.8, the lift increases with the angle of attack (the angle between the blade and the wind). At very large angles of attack the profile stalls and the lift decreases. Therefore, there is, for every profile, an optimum angle that generates the maximum lift.

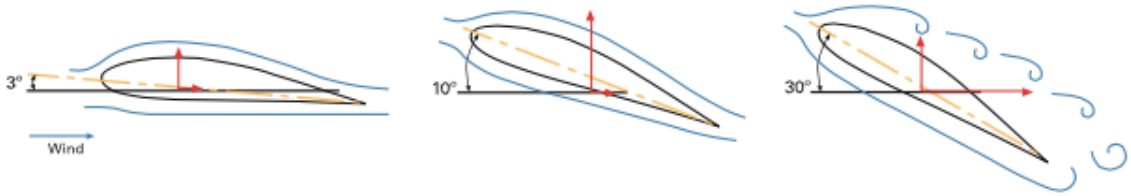

Figure 5.8: Example of the forces behaviour with different angles of attack (low, medium and high) using a determinate aerofoil profile. Figure from [31].

$$dL = \frac{1}{2}\rho W^2 C_l \, c \, dr \tag{5.12}$$

where c = chord of the section in the radius r.

- Drag: This force always exists, because of the movement of the rotor, and reduces the useful force on the rotor, which means that it reduces the torque. Its direction is perpendicular to the lift force. We can see how to calculate it in the following equation.

$$dD = \frac{1}{2}\rho W^2 C_d \, c \, dr \tag{5.13}$$

In fig. 5.8, we can see the drag behaviour for different angles of attack. The drag increases dramatically at very high angles of attack. Therefore, there is an operating point where the blade reaches the maximum lift/drag ratio.

- The third situation in fig. 5.8 where the angle of attack is higher than the optimum one, is a situation of stall, that has been introduces in the explanation of the lift and will be explained better in Chapter 7 Control.

From the decomposition of the above forces, lift and drag, torque and thrust can be obtained:

- Torque: The useful moment on the rotor, which delivers positive rotating motion in the turbines, its direction is perpendicular to the thrust force.

- Thrust: This moment has the direction of the unperturbed wind, tends to push the machine over. It has a direction parallel to the unperturbed wind.

With this aerodynamic concepts we can now explain the blade element theory and momentum theory.

Momentum theory

It is a theory describing a mathematical model of an ideal actuator disk.

Hypothesis:

- The rotor is modelled as an infinitely thin disc.

- The velocity along the axis of rotation is uniform.
- Stationary movement.
- Incompressible flow
- There is no air rotation

Under these mathematical premises of the fluid, there can be extracted a mathematical connection between power, radius of the rotor, torque and induced velocity [17].

$$dQ = \rho 2\pi V_\infty (1-a)\Omega 2\, a' r^3 dr \tag{5.14}$$

Blade element theory

It involves breaking a blade down into several small parts to be able then to determine the forces (see page 35) on each of these small blade elements. These forces are then integrated along the entire blade and over one rotor revolution in order to obtain the forces and moments produced by the entire rotor This relies on two main assumptions:

- There are no aerodynamic interactions between different blade elements.
- The forces on the blade elements are determined by the lift and drag coefficients

After some mathematical expressions we can obtain two equations that define the axial force (thrust) and tangential force (torque) in a function of the flow angles at the blades and aerofoil characteristics [17].

$$dT = B\frac{1}{2}\rho W^2 (C_l \sin(\phi) - C_d \cos(\phi)) c dr \tag{5.15}$$

$$dQ = B\frac{1}{2}\rho W^2 (C_l \sin(\phi) - C_d \cos(\phi)) c r dr \tag{5.16}$$

Twist

Regarding the apparent wind, the closer to the tip blade we are, the faster is the movement of the blade through the air, having a bigger apparent wind angle.

Accordingly, in order to maintain the angle of attack optimum along the blade, it needs to be turned further at the tips than at the root, in other words it must be built with a twist along its length, [31]. The typical twist of the blade is around 10° - 20° from the root to the tip.

Shape of the rotor blades

From optimum rotor theory, we obtain a equation to calculate the theoretical length of chord in every radius of the blade. This theory takes into account some assumptions such as: there is no wake rotation (a' = 0), there is no drag (Cd = 0), there are no losses to a finite number of blades, and the axial induction factor is the optimum one (a = 1/3).

$$c(\lambda, r/R) = \frac{16\pi R}{9B\lambda^2 x\, Cl} \tag{5.17}$$

where $x = r/R$, the relative radius coordinate.

This formula shows that the chord needs to decrease outward, giving a typical blade type with a fat root and a slim tip. The chord for the inner part of an actual wind turbine

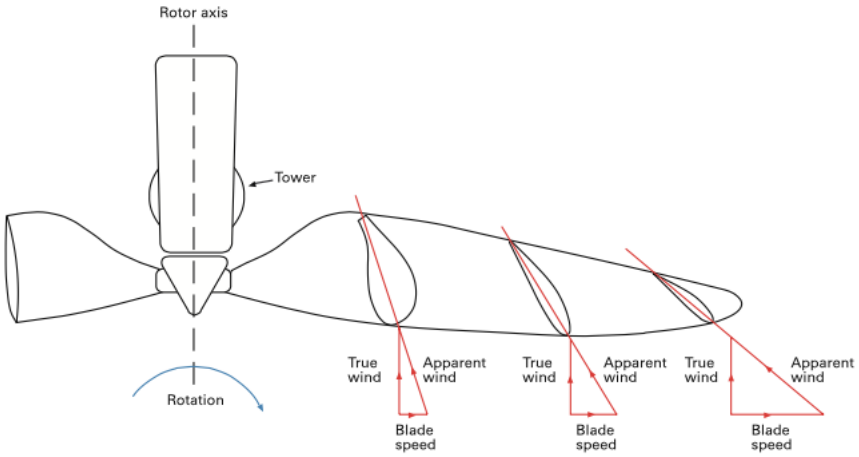

Figure 5.9: Blade twist as function of the radius. From [31]

blade will generally be quite different from the Betz optimum rotor, as the design of this part is more dominated by the structural than aerodynamics considerations [29]. The next figure 5.10 shows different shapes of rotor blade.

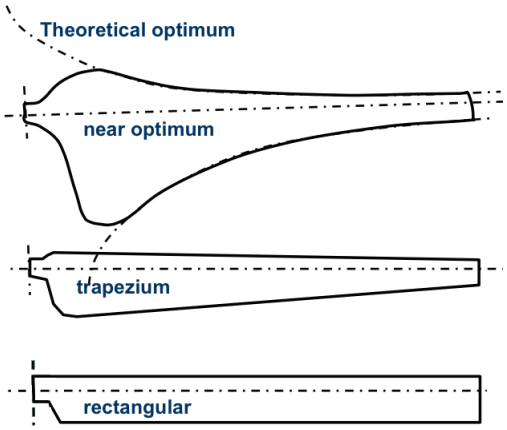

Figure 5.10: Different shapes of rotor blade. Above: the theoretical optimum blade shape and the near optimum one. In the middle, the trapezium blade, a simplification of the near optimum. Below, the rectangular, the simplest and easiest blade shape, far from the optimum shape. From [17]

5.3.2 Matlab Programme

In order to analyse the blade geometry, we have created a Matlab programme specifically for this purpose and this thesis. The codes are in the appendix 1.

During this subsection the Matlab programme is going to be analyzed explaining the most important ideas to understand the code. This Matlab code consists of a main programme, and 3 other files with subprogrammes.

1. **performance** - Main programme

Thanks to this code and helped by the three subprogrammes, it is possible to analysis the blades aerodynamic behaviour, outputs, given the input data.

INPUTS: lamdesign, V, nu, R, Rmin, N, B, liftdata, dragdata.

The inputs required are:

- lamdesign = The λ chosen to design the blades
- V = Undisturbed wind speed in m/s
- nu = Kinematic viscosity of air in m^2/s, at 300 K 1.568*10^{-}5 m^2/s.
- R and Rmin = Maximum and minimum radio of the blade in metres.
- N = Number of segments the blade is divided to do the analysis.
- B = Number of blades.
- liftdata and dragdata = There are two different .text files. Where the lift and drag data for every angle of attack in different Reynolds numbers are stored. Every design to be analyzed by the Matlab programme needs to have this files, and them will be different for each geometry. In them, the aeronautic behaviour is reflected in the numerical values of the lift and drag coefficients.

OUTPUTS: Figure 1, lammax, Cpmax, power.

The outputs obtained:

- Figure 1 = This is a graphic which shows lambda against power coefficient. Thanks to it, we can observe the numerical values of the Cp for different tip speed ratios, and also their trend and the maximum point.
- lammax = The lambda or tips speed ratio where the Cp is maximum.
- Cpmax = The numerical value of the maximum achievable power coefficient in the conditions given.
- power = The maximum extractable power in the conditions given. This results is provided in W.

Figure 5.11 shows the algorithm implemented in the Matlab code attached in the appendix.

Firstly, the programme achieves the geometry of the blade helped by the subprogramme bladegeometry. Once the geometry is defined, the code starts a loop to find the axial and angular induction factors, for every segments of the blade in different tip speed ratios, taking into account the effect of the tip loss and it correction factor.

With these induction factors, the Cp is calculated for every lambda and stored in an array. Thereupon, when all power coefficients for all lambdas are calculated, the code searches the higher Cp and the lambda associated with it. Both numbers shown as outputs: Cpmax and lammax. Also, the programme provides a figure, Figure 1, where it is possible to observe lambda against power coefficient, the trend and the maximum Cp point with a star, 5.13.

In addition, the programme gives the maximum extractable power as output. This is the theoretical maximum power which is possible to achieve using this blade geometry and in that conditions.

The equations used in the Matlab code are going to be shown below:

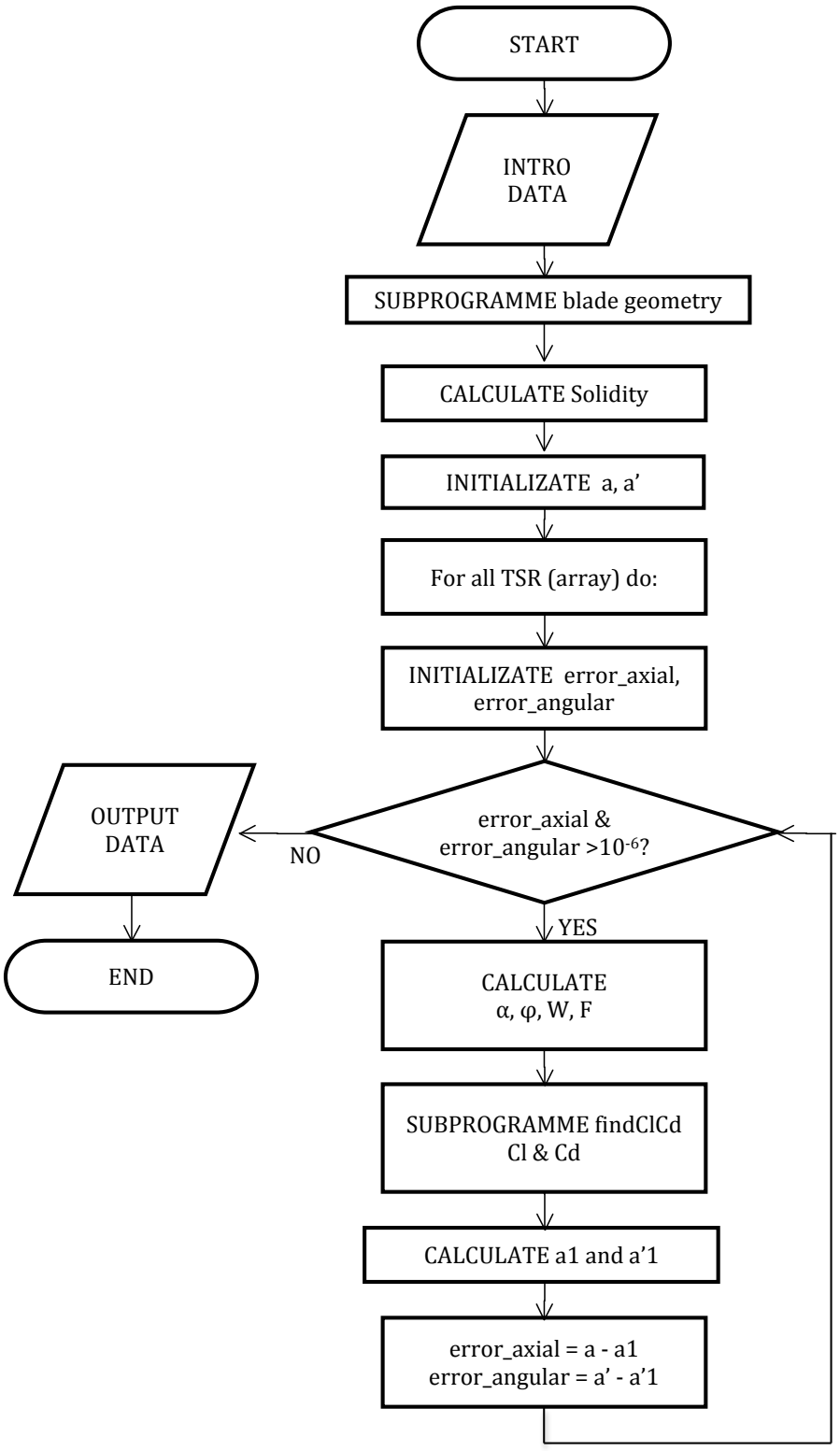

Figure 5.11: Algorithm of the main programme: performance.

The angle of relative wind φ, is calculate using the next equation:

$$\tan(\varphi) = \frac{1-a}{(1+a')\lambda x} \tag{5.18}$$

where a and a' are the axial and tangential induction factors.

The apparent wind speed and the angle of attack, α, can be known using trigonometry and analyzing the vectors shown in fig. 5.6. On one hand, apparent wind speed is:

$$W = \frac{V_\infty(1-a)}{\sin(\varphi)} \tag{5.19}$$

On the other hand, the angle of attack, α, is:

$$\varphi = \theta + \alpha \tag{5.20}$$

The losses in the tip of the blade have to be taken into account because they produce tip vortices on turbine blades. And as a result, this effect concerns the induction factors of the regions closed to the blade tip.

This correction factor is a function of the number of blades, the angle of relative wind, and the position on the blade. This correction factor F varies from 0 to 1 and characterizes the reduction in forces along the blade, [29].

The next equation give us the tip loss correction, F, based on Prandtl's method [29]:

$$F = \frac{2}{\pi}\cos^{-1}[\exp\{-\frac{(1-x)B\lambda}{2(1-a)}\}] \tag{5.21}$$

It is interesting to plot this function against the relative radius coordinate, x, for different tip speed ratios, λ, and number of blades, B, as it is done in fig. 5.12.

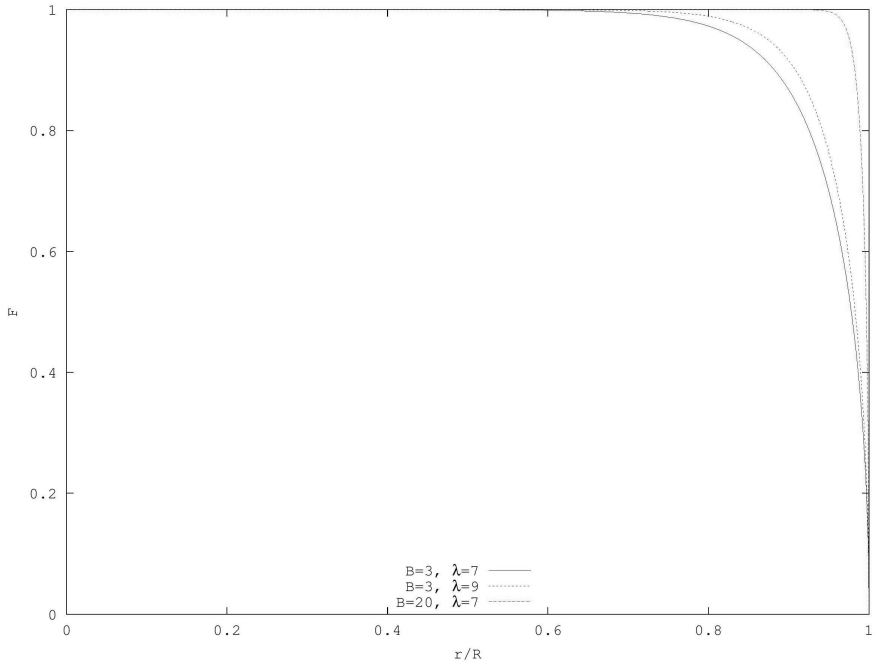

Figure 5.12: Tip-loss factor as a function of radius for different combinations of tip speed ratios and number of blades. From [29].

Also, the lift and drag coefficients are required, to obtain them in the different wind speeds and geometry situations it is used the subprogramme findclcd.

Regarding the induction factors, the code uses the same equations given in the aerodynamic theory overview, (5.8) and (5.9).

One of the most important outputs is the maximum power coefficient, Cp_{max}. To achieve it, the programme solves all the Cp for every lambda, using the equation (5.22), and then it chooses the highest Cp value. Provided as outputs the Cp_{max} and the lambda, lammax, where it is generated.

$$Cp = 8\ \lambda^2 \int_0^{\lambda} x^3\ a'\ (1-a)dx \tag{5.22}$$

To conclude, the programme provides us the maximum extractable power that can be achieve in the conditions given. The equation used is the one explained in the aerodynamic theory overview, (5.3).

2. **bladegeometry** - Subprogramme

This subprogramme calculates the optimum geometry of the blade with a profile done. It is able to estimate the best aerodynamics coefficients and give the optimum parameters of design back in order to obtain the best results in a situation determined by the wind speed.

Note: In this subprogramme the axial induction factor (a), and he tangential or angular induction factor (a') are considered 1/3 and 0 respectively. Besides, we implement the Optimum Rotor Theory, so that the geometry obtained will be theoretical and much better than the real one. The blade shape will provide more power and Cp than real wind turbine. But we can do this assumptions because we only want to estimate a geometry to start the loop, it is not the final blade geometry, and knowing that this design is the theoretical one, we will use it to compare the others.

INPUTS: lamdesign, V, nu, R, Rmin, N, B, liftdata, dragdata.
OUTPUTS: r, dr, c, gamma, phi, x.

The outputs calculated by the Matlab code for the subprogramme are:

- r: a vector where the coordinates of the centre of the blade segments in metres are stored.
- dr: the distance between 2 centres in metres.
- x: a dimensionless span coordinate which allows to reference a relative position: x = r/R.

The subprogramme calculates the theoretical chords (c) in metres, ussing the equation from the optimum rotor theory, where the chord is linked with the number of blades, the lambda and its coordinate, equation (5.17).

In this formula, we include a restriction to avoid the inboard section becoming to wide. Therefore the output is a N elements array with the chords in the different points stored.

Assuming the Reynolds numbers are similar in the whole blade and the number is approximated by its mean, it is possible to obtain all the Cl/Cd ratios, thanks to the

subprogramme: findliftdrag, and choose the best Cl/Cd ratio in order to optimize the angle of attack, α, in every segment of the blade.

With the inputs, the twist of the optimum Betz rotor can be calculated, φ.

$$\tan(\varphi) = \frac{2}{3\lambda x} \tag{5.23}$$

Knowing the relationship between this angle, the angle of attack, α and the pitch angle, θ. It can be calculated using equation (5.20).

And also its complementary, gamma (γ). ($\gamma = \pi/2$ - $\varphi + \alpha$)

Both angle outputs are N dimension arrays where the different angles (γ or φ) in every blade divisions are stored.

3. **findliftdrag** - Subprogramme

   The .text data inputs, liftdata and dragdata (explained in pag. 46), have all the lift and drag data for all the angles of attack and for some Reynolds numbers. Therefore, the goal of this subprogramme is to find the correct lift and drag data (liftdataRE and dragdataRE) for a Reynolds number given (RE1). If the Reynolds number input is different than the ones stored, the subprogramme interpolates or extrapolates the data in order to find the most suitable one.

   INPUTS: RE1, liftdata, dragdata.
   OUTPUTS: liftdataRE, dragdataRE.

4. **findClCd** - Subprogramme

   This subprogramme finds the Cl and Cd coefficients from an angle of attack. It needs to know the Reynolds number, so it is necessary to introduce the subprogramme inputs such as: the chord, the kinematic viscosity of air and the apparent wind speed in the working point.

   To achieve the outputs, the code uses the subprogramme findliftdrag to load the data, and afterwards it search the Cl and Cd values of the angle of attack given, using a linear method.

   Also, the code gives as an output the Reynolds number calculate.

   INPUTS: nu, alpha, c, W, liftdata, dragdata.
   OUTPUTS: Cl, Cd, RE.

5.3.3 Matlab Analysis

Once the Matlab code is programmed, it is time to compile it and analyse the results. As we said in the explanation and fig. 5.3, we are going to start with a known profile , in this case, a NACA0012. The first inputs in the loop:

- lamdesign = 5
- V = 6 m/s
- nu = 1.568*10^{-}5 m^2/s
- R and Rmin = 3 and 0.1 m.

- N = 10.
- B = 3.
- liftdata and dragdata = During our analysis, we use a data from a NACA0012 in two files: NACA0012lift.text and NACA0012drag.text. In its files, we have stored the Cl or Cd values for 6 different Reynolds numbers (160000, 360000, 700000, 1000000, 2000000, 5000000) in all the angles of attack (0° - 360°) in a 5° interval. So that, we obtain a matrix as it is shown in the appendix A.

The code provide us the results:

- lammax = 6.
- Cp = 0.4306.
- power = 1.6867e+03 W.
- Figure 1: Shown in fig. 5.13.

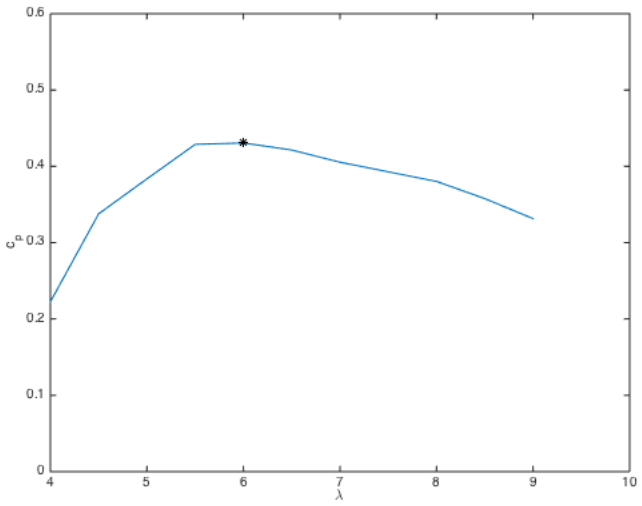

Figure 5.13: Lambda against power coefficient, the star shows the maximum power coefficient point.

Regarding these results, we can obtain some conclusions. Firstly, we have to take into account that the blade geometry used to obtain these values is near to the optimum blade shape, so that, these results are much better than the ones we could obtain.

For example, the maximum power coefficient obtained is 0.4306, which means that, it is close to the peak values achieved by the most modern and largest three blades wind turbines. Due to the value of the power coefficient, the power extractable for the wind is 1.61 kW, value much bigger than the extractable in real conditions.

Once we know the rotor behaviour with NACA0012 profile blades, it is time to design our own blade profile to be tested. When we have the blade design done, we have to create other two files .text with the different values for lift and drag coefficients with every angle of attack and in different Reynolds numbers for the new profile (this data could be obtained by a wind tunnel analysis). And restart the loop with the new geometry, taking

into account that this geometry have to be introduced by the user instead of using the subprogramme bladegeometry, and the .text files have to be loaded in the main programme.

In our case, the test in the wind tunnel exceed our working area because, not only it takes long time to study it but also, we are doing an optimization loop so we would have to repeat the analysis several times. To solve this problem, we are going to take the Cp of our design around 0.2. We have chosen this value because we prefer to be conservatives with the results given.

5.3.4 Materials

There are different material sources depending on the area, because of the region or the country where we are focusing on, we propose two different materials to manufacture the blades:

- PVC pipes: One material elected to create the blades is PVC, in fact, PVC pipes. These type of pipes are commonly used in water supply systems and drains, so that they can be reused and recycled or bought at low cost. Besides, the PVC properties are good to be used as blades: they have good resistance and high stiffness and mechanical strength, also these pipes are lightweight and easily machinable.

- Wood: Other common material to be used is wood. The timber is easily found in many places in Africa, if it is the case, the blades can be manufactured using this material. It mechanical properties depend on the type of wood concerned, their status, their age and the quantity of water it has. But in a general way, wood is a suitable material to manufacture the blades, because it is light, strong and resistant to fatigue. The most important inconvenient is to find enough amount of quality material.

5.3.5 Final design

The goal is to design a three bladed rotor as much efficient as possible using the materials and the tools available. To do that, the blade pattern has to be as close as possible to the theoretical ones.

Figure 5.14 shows a perspective of a blade, with the different areas.

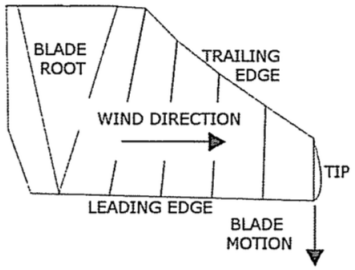

Figure 5.14: Perspective of the blade where it is possible to recognize the blade shape with two different edges. From [28].

The blade has four different regions:

- Root: The inner part at the hub.
- Tip: the outer part at the hub.
- Leading edge: The blade edge that strikes the wind first.
- Trailing edge: The streamlined part that leaves the air behind.

Our blade design has to follow the aerodynamic theory. So that:

The blade tip is narrower than the root. A very narrow blade is all we need to catch the power of the wind when the blades are turning fast. On the contrary, closer to the root the blades move more slowly and so that, they should be wider and more steeply angled to the wind. But the outer part is the most important because the root part does not sweep much wind compared to the part near the tip, [28]. It is known that the first third of the blade, the close part to the hub, do not achieve a lot of wind power [29] so that, in that area, the design is determined more by the construction, the structural integrity and the durability than by the aerodynamic concepts.

The edges, need to have a streamlined airfoil shape to spring fast with the minimum drag possible. The leading has to be ready to cut the wind and face the wind shake. Trailing edge has to be thin in order not to produce flow vortex behind the blade.

Other important idea to bear in mind is the direction of the rotation. Our design is a three blade rotor rotating clockwise. So that, the shape of the blade is conceived to turn in this way.

During this thesis, we have manufactured two different rotor, with different blade design ideas. The first one of wood and the second of PVC tubes:

Wooden blades:

The blades design made of wood is not our design, they are done following the indications provided by the book [28]. But, the profile also follows all the classical concept about how to design these elements, as it is discussed above.

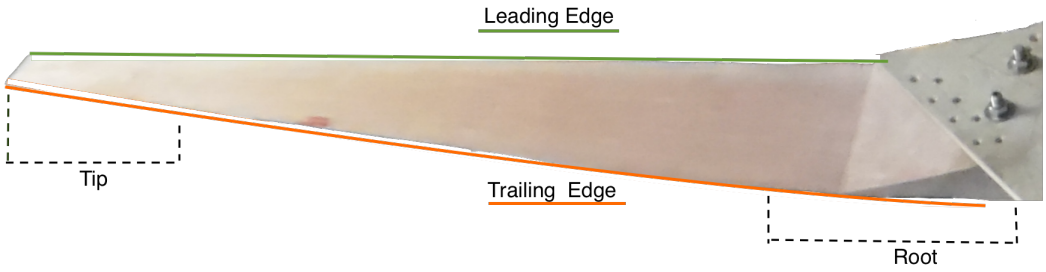

Figure 5.15: Picture of the wooden manufactured blade, where it is possible to recognize the blade shape with two different edges, the root and the tip. Also, on the right, there is a portion of the rotor assembling.

PVC blades:

The challenge in this part of the thesis is to be able to create a blade profile close to the aerodynamic theory using PVC pipes.

The first step is to know how big will be the blades. They dimensions are limited by the generator and the expected wind speeds. The generator we have was designed and created for the wooden rotor. The blade length chosen is therefore the same as for the wooden blades, 1.2 m.

Ones the length of the blade we want is known, it is time to chose the PVC pipe. To achieve the correct twist, the pipe diameter has to be around one fifth [32] of the length of it, therefore in our case:

$$D_{pipe} = \frac{1}{5} L_{pipe} = \frac{1.2m}{5} = 0.24m \tag{5.24}$$

where D_{pipe} is de diameter of the PVC pipe and L_{pipe} is the length of the PVC pipe.

Because of the standard dimensions of the pipes and because having a bigger diameter we can have a bigger twist, the diameter elected is 0.25 m. The thickness of the pipes is fixed by the supplier, in this case 5 mm.

Table 5.1: PVC pipe characteristics:

	Dimension (m)
Length	1.2
Diameter	0.25
Thickness	0.005

Knowing the length of the blade, the diameter and the thickness of the pipe, using a computer-aided design application for creating a 3D digital prototypes, in our case Autodesk Inventor, we developed an outline and the final design of the blade. This is shown in the appendices, in sheet 1.

In order to obtain a shape as similar as the theoretical one, we had to take into account the aerodynamic concepts discussed above, and the rotational direction. Our wind turbine has a clockwise rotation, what strongly affects the design of the different areas of the blade.

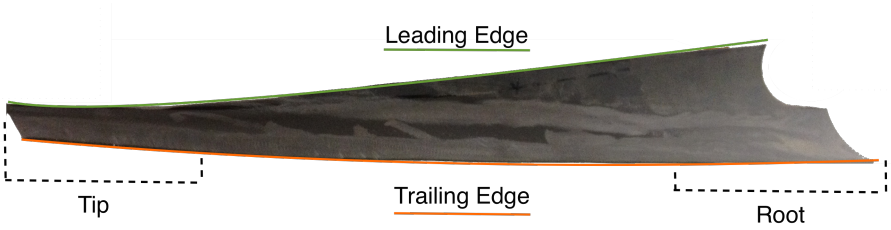

Figure 5.16: Figure of the PVC manufactured blade, where it is possible to recognize the blade shape with two different edges, the root and the tip.

- Blade areas: Using fig. 5.16 the blade should turn right. So that, the leading edge has to be in the above and the trailing one in the below. The leading edge has a square shape while the trailing edge is smoothed down to obtain a thin edge in order to let the wind flow leave the blade.
- Shape of the blades: From the theory shown before, we know that the blade part near to the hub (the root) has to be much fatter than the tip. Therefore, we designed a prototype following this principle and taking into account the proportions. In the

end, we will have a edge that follows a straight line and other which follows a curve making a near optimum shape.

- Twist: The blade design is important to have a twist in it, to achieve as much wind power as possible, optimizing the angle of attack. In our case, since the blade is done using a pipe, if we want to achieve a shape of the blade as the one mentioned, we also achieve a twist. The blade profile in every section is an annulus arc, in the root bigger and more twist and in the tip smaller and almost flat.

(a) Picture taken in Fablab.

(b) 5.17a Picture retouched.

Figure 5.17: Real and retouched picture of one blade perspective, where is possible to observe the twist it has.

The trick is to know in which edge we want to have included the straight line and the curve that defines the shape. The main difference in this design against the typical or classical profile is that, in our case the trailing edge follows a straight line and the leading edge is bent. To see the difference compare figures 5.15, which maintains a classical blade profile, and fig. 5.16, the design creates using a PVC pipe. This way allows to maintain an angle of attack close to the optimal one along the whole blade. As fig. 5.18 shows.

To be able to achieve this blade profile, we did some templates with the geometry of the blade. Thanks to this, the manufacturing of the PVC blades is easier. The user has to cut these templates, position them in the pipe and draw the profile, as you can see in the next section: Rotor manufactured.

Blades - hub assembly

This assembly should ensure the correct rotational transmission from the blades to the hub, where is fixed the rotor of the generator.

There are two options in this case. We thought about manufacturing a hub with the shape of the fig. 5.19.

With this design we want to have the two elements completely attached, designing the hub with the same shape as the root of the blade. It would be made in wood and therefore, the tools used would be the ones appropriate for this material. We will talk about it in the section of manufacturing of the rotor (page 53).

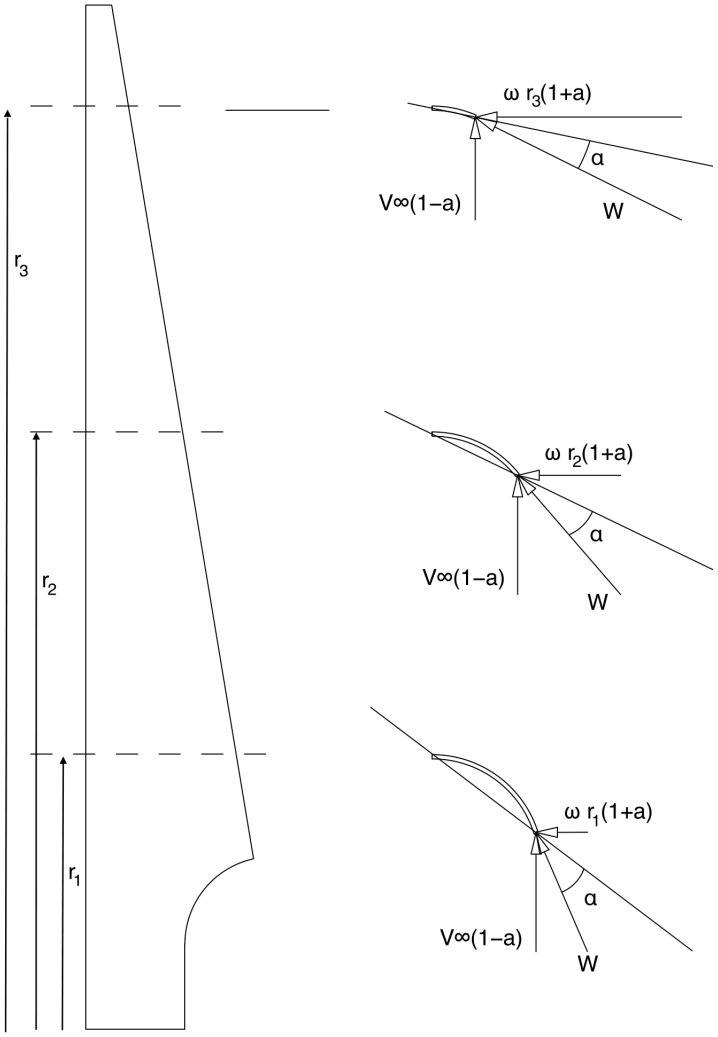

Figure 5.18: Different blade profiles of the PVC blade and the behaviour of the flown onto the them.

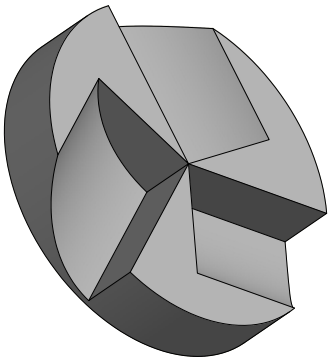

Figure 5.19: One of the designs for the hub of the wind turbine.

We want to give to the user the possibility to change the curvature of the design in order to generate new angles of attack for the same blade. In this case, one should cut down only in the curvature of the element.

We did not have enough carpentry tools to manufacture this element, so we thought about another option.

The second design consist on a wooden disc. The diameter of this wooden disc is 150 mm, in order to have enough space to assemble the blades on it, taking into account that the hub has 4 main screws to fix all the components on it. Figure 5.20 gives us an idea of the assembling blades-hub and the design of the disc and the blade assembling with all the dimensions are given in the appendix 2 sheet 7.

We have to distinguish two assemblies:

- Blades - disc assembly: To put together the blades and the disc, it can be used different metrics of screws and nuts. In this case, although we have not made any shear stress analysis or fatigue studies. We decided because of the space in the blade and the material available to use 3 metric screws 6 and 8 lock nuts per blade. Two of the screws are placed in the root, close to the trailing edge and the other also in the root but in the middle of the blade shape. (See fig. 5.20 or the plans/sketches in the appendix 2 sheet 7). Combining the lock nuts in the different screws (the fixation) we can achieve alternative angles of attack.

  The fixation we propose generates the highest angle between the blade and the disc. In this way, the trailing edge is adjacent to the wooden disc. It is possible to achieve it fixing the screws close to the trailing edge with 1 nut, and the other one with 3 nuts. As it is explained in the next part, rotor manufactured.

  But, the user is able to change this layout, generating new angles of attack for the same blade.

  The most important factor we have to take into account in this assembling is that it must be balance, otherwise the rotor will star to vibrate and to shake generating an undesired performance. This behaviour is not desired not only because it is not good to the material properties but also because the rotational speed transmitted will not be good enough to produce a sinusoidal signal with the generator.

- Disc - hub assembly:

  The wooden disc is though to fix the blades on it and to be assembled to the hub. Therefore, it has some different holes. Four metric 12 holes creating a square in the middle of the disc, to leave the bolts of the hub pass. And other 9 smaller holes, metric 6, to fix the blades. As we can see in fig. 5.20.

5.4 Manufacturing

In the manufacturing how to manufacture the wooden and PVC blades is going to be explained, step by step.

5.4.1 Rotor with wooden blades

The most important issue in the production of the blades is the good measurements of them. Mark the blanks to specify what part of wood it has been to remove and, therefore, give the good shape to the blades.

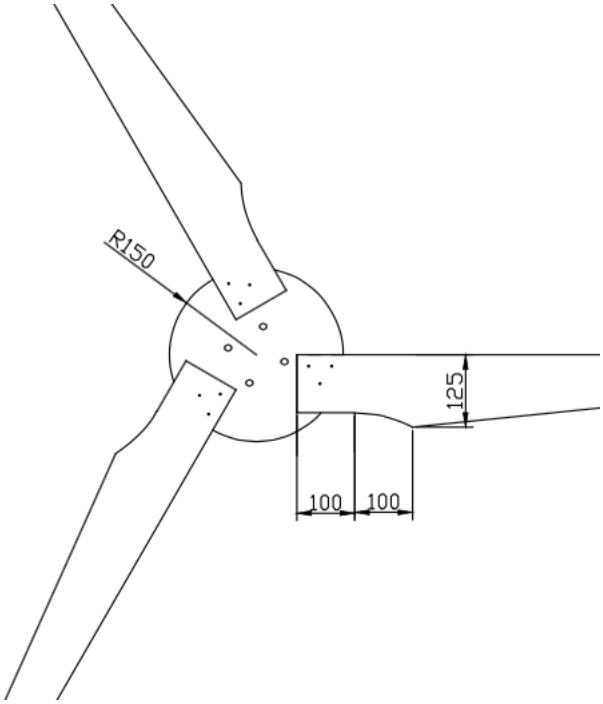

Figure 5.20: Sketch of the blades and the hub assembling with some relevant heights.

First of all, before starting to manufacture the blades, a beam of wood is needed. It is important to have it as well seasoned and free of sap as possible, because from this beam the three necessary blanks are going to be cut, to be able later to carve the blades.

Secondly, before marking the blades, made a plywood template of the blank shape of the blade. Make it with the measures specifies in the book [27] and, after that, start marking the blank. The key of manufacturing well the blades is making them as similar as possible. So, after marking them, and being sure that the marks were well done, start to cut.

To be sure that the trailing edges of the three blades are identical, place the leading edges of them in a surface and carve them until they are completely similar, as we can see in fig. 5.21. Finally, work separately with each one.

It is really important to measure and mark the blades, so start marking some stations at six equal intervals in the blade. These stations are helpful not only to measure well the blade, but also to have an illustrative way to know if the work is well done and all the measurements are as they have to be.

After that, the trailing edge can be marked. Measure some millimeters in each station, as the book specifies, connect them forming the trailing edge and start carving the blade.

For cutting out the wood here there are the most important woodworking tools that have to be used. We can see a picture of them in fig. 5.23:

- Draw knife: use this knife to cutting of when we a lot of precision is not needed. in the firsts carvings.
- Spokeshave: with this tool is used to carve with more accuracy. Use this tool once we had already arrived to the limit and to make thin layers of wood.
- Plane: this is an intermediate between the draw knife and the spokeshave.

Figure 5.21: Equalization of the three blades simultaneously.

Figure 5.22: Paula Íñiguez and Nerea Arraiza carving the blades.

- Chisel: there are two techniques to cutting of the wood. One is using the three other tools and the other one is with the chisel. With this one it is needed a hammer as well.

Once the intrados is carved, the flatness of the wood has to be verified. To confirm it, move one ruler along the intrados, from the trailing to the leading edge. If the whole intrados is flat, start measuring, and therefore, carving the extrados of the blade.

Before starting marking and carving the extrados, make some measures taking into account the assembling of the blades. For that, as we can see in fig. 5.24 drew a circle, the center of that is too the centre of the rotor and the radio of it, as we are going to see later,

(a) Draw knife

(b) Spokeshave

(c) Plane

(d) Chisel

Figure 5.23: Most important woodworking tools used during the manufacturing of the blades.

is the size of the plywood plate which is useful for the supporting and the assemblage of the blades.

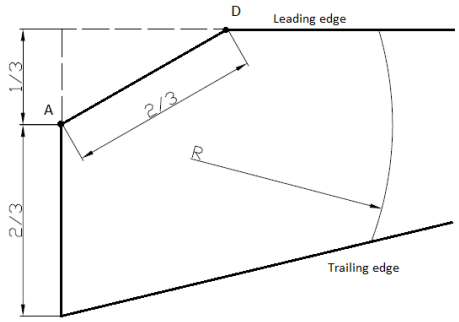

Figure 5.24: The center of the rotor of one blade. Adapted figure from [27].

Once the point B is drawn (the junction point between the circle and the leading edge) start marking the thickness of the blade. For that, as we can see in fig. 5.25, in each station and measuring it from the intrados, mark the mm given in the book. First of all do the trailing edge and, after that, measure the leading one. The measures are defined in the book.

Afterwards, continue cutting out. If it is supposed to be plane enough, measure with a thickness compass. After verifying that in each station is the correct thickness start with the assemblage of the blades.

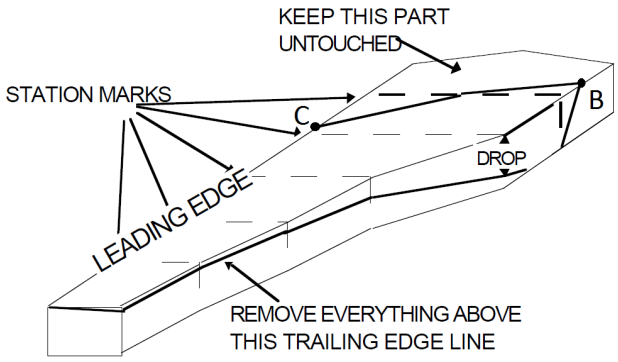

Figure 5.25: The zone that has to be removed in the extrados of the blade. Adapted figure from [27].

As we have said before, the centre of the circle in fig. 5.24 is the centre of the rotor, so to assemble the blades perfectly, make a slot of $360^o/3 = 120^o$ angle to fit the three of them. As we can see in fig. 5.24.

As for the assembling of the blades, supposing that the three blades are set up, the most important is to have them well supported and balanced. Regarding to the supporting of them the best is to make a sandwich with them. That is, put the blades between two plywood as we can see in fig. 5.26.

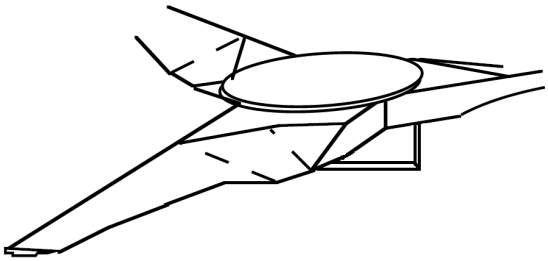

Figure 5.26: The way of assembling and supporting the blades. Figure from [27].

As we can see in fig. 5.26 on one hand, in the intrados of the rotor we have a triangle and on the other hand there is a disk. These two plywood plates are useful for the supporting of the blades. In both plywood plates two circles have to be traced, one of them of the same diameter of the rotor disk interior hole and the other of the same diameter of the hub. The first one is important to have the plywood plate well aligned and the second one is for not screwing in that zone.

After that, in the disk trace two other circles and two parallel lines in the triangle where the screws are going to be tight.

Regarding to the assembling of the blades, it is essential to have the center of them well positioned. Therefore, as we can read in the book, measure them until there is the same distance to the center. After that tight one screw, in this way we can move the blades until there are 120^o between them. To check it, measure the distance between the tips of the three blades, once there is the same distance, tight the rest of the screws.

Once the whole assemblage was finished the well balanced of the blades has to be ensured, therefore, we have to guarantee that making them spin, once they get braked they are in an equilibrium position, that is, that one of them is always in the vertical axe. If they are not balanced, we can level them attaching a metallic heavy plate to the lightest blade. This can be verified once the generator is fabricated.

5.4.2 Rotor with PVC blades

For the PVC blade, as we have said (page 49), the length of the blade will be 1.2 m and so the diameter of the PVC pipe 0.25 m. The necessary templates and dimensions are in appendices. Here how to shape the PVC pipes in order to achieve the good form of the blades is going to be explained.

First of all, we have to divide the pipe in four equal parts. Make the cuts as perpendicular as possible, in order to give the good shape to the trailing edge. For this part an square and a compass could be useful. Draw the contour of the pipe in a paper. Once having drawn the circle, divide it in four equal parts and place the pipe again in the circle drawn. To draw the lines where the cut will be done, a plane, straight and large item is needed. We used a wooden blank, placing it in the floor to ensure the perpendicularity of the line with regard to the floor. Once the pipe is drawn, it is time to start to cut. To do so, we used an angle grinder. We can see the final result in fig. 5.27b.

(a) The pipe drawn (b) The pipe cut

Figure 5.27: The PVC pipe divided in four equal parts.

Once the four parts are cut, take one-quarter and start drawing the shape of the blade. In order to make it easier there are some templates in appendices, sheets 3 to 6. Take the sheets, cut them and stick them forming the paper template of the blade, see fig. 5.28a. After that, position it in the PVC and start drawing the profile, see fig. 5.28b. Make it always in the interior of the PVC pipe, because it is there where it's diameter measures 250 mm.

Once the profile is drawn, it is time to cut it down. Here it is useful to fix the quarter pipe to the table, in order not to allow the pipe to move. In fig. 5.29 we can see how we cut it. To make the cut smoother, it is better to sand the edges, and in the root, for instance, it is difficult to follow the template. What we did there was to make a straight cut and after that sand until we arrived to the required shape, but this depends on the grade of familiarization with these tools.

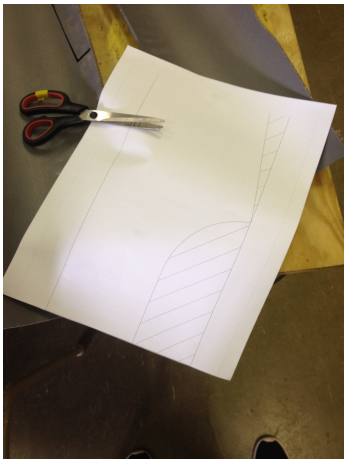

(a) Cut the template. Sheets 3 to 6 of the appendices.

(b) Draw the profile in the PVC to be able, after that, to cut it.

Figure 5.28: Shaping the blades.

Figure 5.29: Shaping the blades.

As we have told in the theoretical analysis, the trailing edge has to be sharp. So mark in the edge 1 mm and sand the pipe from the interior of it until you arrive to the line. Try to do it smoothly. Finishing it we will have the blade done and ready to assemble to the hub.

Hub

For the hub a wooden board is needed, in this case we used a plank of 20 mm of thickness. Take it and draw a circle of 300 mm of diameter in it, once the circle is drawn, cut it with a electric saw (fig. 5.30a). As we have in the generator 4 bolts that come from the hub, we have to let them go through the hub, so measure the dimensions of them and drill he board, like in fig. 5.30b.

(a) Cut the circle that will be the hub.

(b) The hub with the 4 holes on it.

Figure 5.30: Shaping the hub.

Assembling

For the assembling,the blades have to be screwed to the hub. In appendices, sheet 3 or 7 there is a template which is useful to make the holes of the blades in the correct place. Put the template in the root and mark with a permanent marker the position of them. As we can said in the previous section (page 52) we need 3 metric screws 6 for each blade so drill the PVC pipe with a bit of this dimension. For the hub, in sheet 7 we have the correct position for the blades and therefore, for the screws, make the holes of the same dimension as in the blades. Now we have made the holes, it is time to assemble the two parts.

First of all insert the screws in the hub. As we said in the designing of it, the angle of attack can be changed changing the number of nuts in each screw. In this case, we decided to insert 3 nuts in the screw 3 and 1 nuts in the screws 1 and 2 (see fig. 5.31) as we have said in the previous section, to obtain the highest angle of attack.

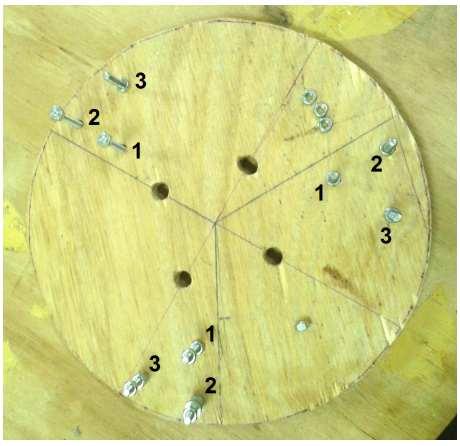

Figure 5.31: Hub with the holes and the screws. Enumeration of the screws in order to explain better the assembling.

Insert the blades, tighten the nuts with a wrench and once the generator is built, mount the rotor on it. Once, the assembling is done the balancing of the blades has to be realized. To do so, it is the same as in the wooden blades (page 57). In fig. 5.32 the final result of the rotor with PVC pipes can be seen.

Figure 5.32: Final result of the rotor with PVC pipes.

5.5 Suggestions for improvement

The main suggestion to improve the rotor design is to be able to achieve all the aerodynamic data we need to study the blade behaviour. Because, if it is possible to obtain them and do some .text files similar as the ones we used with the NACA profile, we could be able to restart the optimization loop and improve continuously the blade design, as we theoretically suggest. Also regarding to the blades, it could be interesting to analysis the mechanic behaviour of them, in order to know the PVC blade performances. We suggest for this purpose to test the fatigue, the stress and the buckling.

Other interesting idea to improve the rotor design is linked with the blade-hub assembling. The dimensions of the screws, bolts and nut taken are done based on the experience, but make some calculations such as: shear stress analysis or fatigue studies, and optimize their dimensions could be a good idea to improvement this design.

Chapter 6

Generator. Design, analysis and manufacture

The generator is a very important part of the wind turbine. It is here where the mechanical energy is converted to electrical energy.

The operating principle of electromagnetic generators was discovered in the years of 1831 and 1832 by Michael Faraday. The principle, later called Faraday's law, is that an electromotive force is generated in an electrical conductor which encircles a varying magnetic flux.

6.1 Types of generators

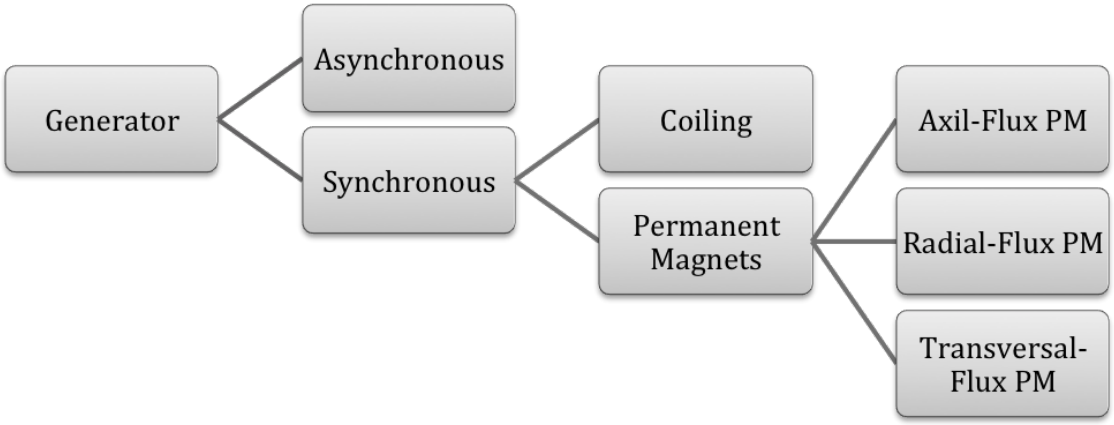

Figure 6.1: Types of generators. We only focus on synchronous as it is explained later.

Fig. 6.1, shows a way of classifying the different kind of generators. An induction machine requires externally supplied armature current; it cannot start on its own as a generator. Because the rotor field always lags behind the stator field, the induction machine always consumes reactive power, regardless of whether it is operating as a generator

or a motor. So that, there is no point in focusing on this kind of design.

The characteristics of the synchronous generators are more suitable for the project we are carrying out, for the following reasons:

- Although they can have one, they do not need a gearbox: In the gearbox occur most of the failures and it is an expensive and a heavy item.
- Suitable in off grid cases: The frequency is controlled by speed and the voltage amplitude is controlled by rotors excitation current.

There are two ways of obtaining the excitation current, therefore, as we can see in fig. 6.1 we can classify the synchronous machines by the way of obtaining it, by coiling or by permanent magnets. The first ones need a permanent excitation current (Ir) to generate the magnetic field (B) of the rotor. The second ones, the brushless generators, they generate the magnetic field by permanent magnets.

There are some advantages and disadvantages of each one. Brushless generators need less maintenance, have high efficiency, better refrigeration and there is the possibility of designing a multipole machine. But it has a big disadvantage, that is the advantage of the generator excited by coiling, as the voltage amplitude is controlled by the excitation current, if the generator does not have an excitation current the voltage cannot be controlled.

6.2 Election of the generator

Because of the advantages and disadvantages of each kind of generator and, because we are designing a wind turbine for low power, we have elected the synchronous, permanent magnet generator.

We can achieve it in three ways:

1. Buying it: it is too expensive and the possibility of buying wind turbines in developing countries are small.
2. With a car's alternator, there are 4 reasons why this option is less suitable: it has low efficiency, it is designed to be lightweight and run at very high rpm, the alternator field coil needs to be supplied with power to excite the magnetic flux and the internal regulator in the alternator is not suitable for charging a remote battery.
3. Handmade generator: Although it can be hard to make, finally it is cheaper, and the most advantage is that it can be designed and, therefore, manufactured as the designer wants, with the materials and tools available.

We have decided to create a handmade permanent magnet generator. As we have seen in fig. 6.1, there are 3 different designs for permanent magnets: Axial-Flux PM, Radial-Flux PM and Transversal-Flux PM.

In the following lines, these 3 types are going to be explained, in order to be able in the end of them to elect the most suitable configuration for our machine.

The transversal-Flux PMG ,fig. 6.2, is a machine which has a radial orientation of the air gap and the stator has a transverse orientation. This transverse orientation in the stator allows the area of the coil to be independent of the choice of the pole pitch. Therefore, the pole pitch may be reduced and thus the current increases to very high values. This generator design is a very innovative and it has not been commercialized yet. See fig. 6.2.

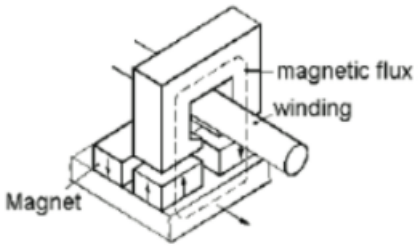

Figure 6.2: Transversal-Flux PMG. Figure from [33].

The Radial-Flux PMG, fig. 6.3, creates the flux in the air gap in radial direction to the pivot axis. The most common configuration is with the arrangement of the magnets axially on the cylindrical surface of the rotor and the stator slots also axially in the inner stator surface, but there are other configurations as we can see in the figure.

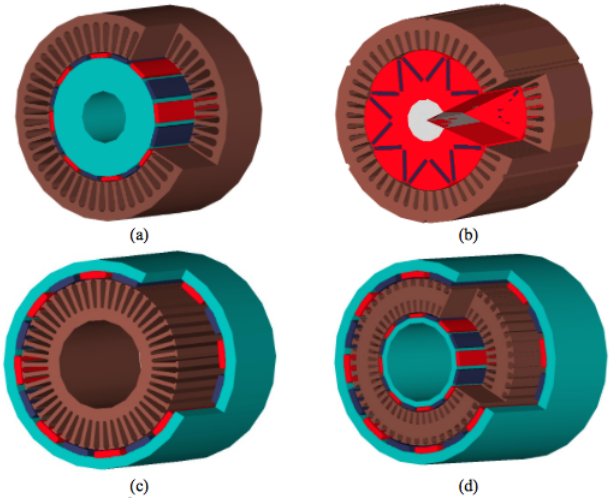

Figure 6.3: Radial-Flux PMG configurations. (a) and (b) are internal rotor structures with surface- mounted magnets (a) and buried magnets (b). Structure (c) is a drum motor which has only low demands for the fixing of the magnets, and structure (d) is a double rotor configuration with internal toroidally wound stator. Figure from [34].

The Axial-Flux PMG, fig. 6.4, is characterized in that the air gap flux takes an axial direction relative to the rotation axis. The rotor is disk-shaped, with the magnets arranged along the perimeter, and the stator is slotted radially where the coils are located. There are some different configurations depending on the number of rotors and stators, as we can see in the figure.

As we have shown, the main difference between the basic designs is the flux direction, and therefore the layout of the magnets. The most compact and simpler one is the Axial-Flux PMG. Therefore, our machine to design is: Axial-Flux Permanent Magnet Generator.

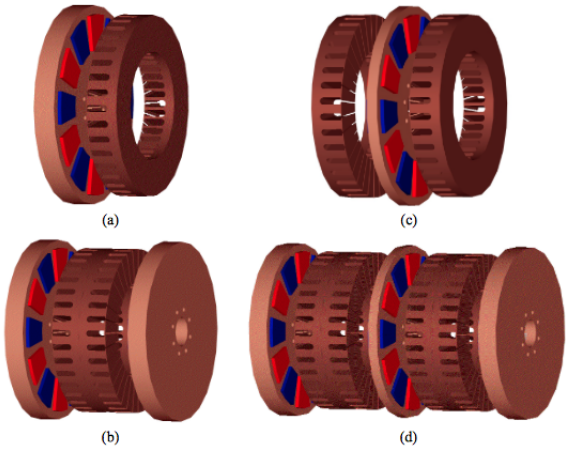

Figure 6.4: Axial-Flux PMG configurations. (a) Single-rotor single-stator structure. (b) Two-rotors single-stator structure. (c) Single-rotor two-stators structure, called hereafter also as AFIPM machine (Axial-Flux Interior rotor Permanent-Magnet machine). (d) Multistage structure including two stator blocks and three rotor blocks. Figure from [34].

6.3 Design and materials

For the design, the generator is split up in two different components: the magnetic rotor and the stator. This is shown in fig. 6.5.

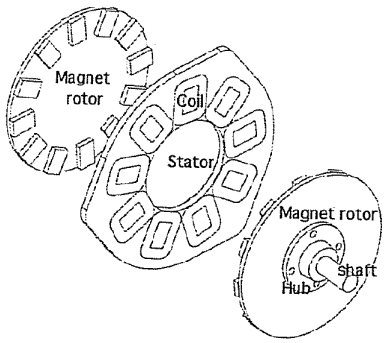

Figure 6.5: Sketch of the generator with: 2 magnetic rotors with 12 magnets on each disc, 1 stator with 9 coils, the shaft and the hub. Figure from [28].

The link between the design of the stator and the rotor is the magnets-coils relationship, which is 4x3 [28]. Regarding to how many magnets and coils would be the perfect relation, the three phase generators can be strongly complicated because there are a lot of configuration choices. But the general guideline is to use 4 magnets per 3 coils, giving the relationship 4x3. [28] [35] [36]. This relationship is the most used in the technical literature of small wind turbines due to the fact that it allows to optimize not only the space but also the magnetic flux crossing the coils over time.

6.3.1 Magnetic rotor

The rotor is responsible for creating the magnetic field, which crosses the stator and its coils, generating a magnetomotive force in the coils.

In order to achieve this result, we use two metallic surfaces where we can position the magnets and which are going to help the magnetic field to circulate. (Theoretical analysis given below)

The magnets are one of the key elements of the wind turbine since they influence directly the amount of energy produced. In order to convert as much mechanical energy as possible into electrical energy, we decided not to use recycled magnet but to purchase new ones. This will of course impact directly on the final cost of the machine. The magnets chosen are NbFeB (Neodymium-Iron-Boron). [28]. These magnets are often used in electric machines as they have a higher value of magnetic induction (B), and greater value of magnetic field intensity (H) compared to Alnico or Ferrite. [37].

The surfaces to fix the magnets on can be made from recycled material. One of the best elements that can be used as rotor surface, is a brake disc because its dimensions are suitable, the geometry and the thickness are appropriate, it is done by steel, and it can be found in all cars.

From a quick research about the most used cars in the countries elected, we conclude that one of the most widespread car brands is Toyota.[38] In particular the following models are the most widespread: Corolla, Avensis and Land Cruiser. Fig. 6.6 shows an example of brake discs we can find in a second hand market to build our generator. Each model has its own geometry for the brake discs:

- Toyota Corolla: Diameter = 266 mm, Thickness = 9 mm
- Toyota Avensis: Diameter = 280 mm, Thickness = 10 mm
- Toyota Land Cruiser: Diameter = 312 mm, Thickness = 18 mm

Figure 6.6: Second hand brake discs of Toyota Corolla.

We assume (because we do not know yet the number of turns per coil that we need and so, the area of each coil) that it will be possible to have 12 magnets in each disc, and 9 coils in the stator, in order to optimize the space, as we have saw in the sketch in fig. 6.5. This leads to the following configuration:

- 24 Magnets (12 magnets x 2 discs). Material: NdFeB, Dimensions: 46x30x10 mm (a_mxb_mxl_m) (Length x Width x Thickness)

- 2 Metal disc. Material: Steel 1010, Approximate dimensions: Diameter = 280 - 300 mm, Thickness (l_r) = 8 - 12 mm
- Gap. Space (air) where the stator is located. Dimensions: Thickness (l_g) = 20 mm. [28]. Also, it could be possible other dimensions, as it is analyzed after.

We choose as metal disc the brake disc of Toyota Avensis because its dimensions suits our requirements. A different brake disc could also be chosen. The only requirement needed is that the diameter of the chosen disk is equal or bigger than the Avensis one. This is because, as we will see later, the disc diameter limits all the geometry: the coil arrangement and the magnets.

The challenge of the magnet rotor design is to maximize the magnetic flux density in the gap between the two rotors, which is strongly dependent on the geometry and the material properties. Firstly, we have to calculate the flux density in the magnets. Once we have it, we will be able to calculate the flux density in the gap.

The magnets will create a flux density thanks to their working point. This working point is the intersection between the demagnetization curve and the load line, both explained below. [39]. This is shown in fig. 6.10. What it means, the point of the demagnetization curve that will operate the magnet once placed in a given magnetic circuit.

The demagnetization curve depends on the magnet material. In order to achieve this curve, we start with the hysteresis loop, fig. 6.7:

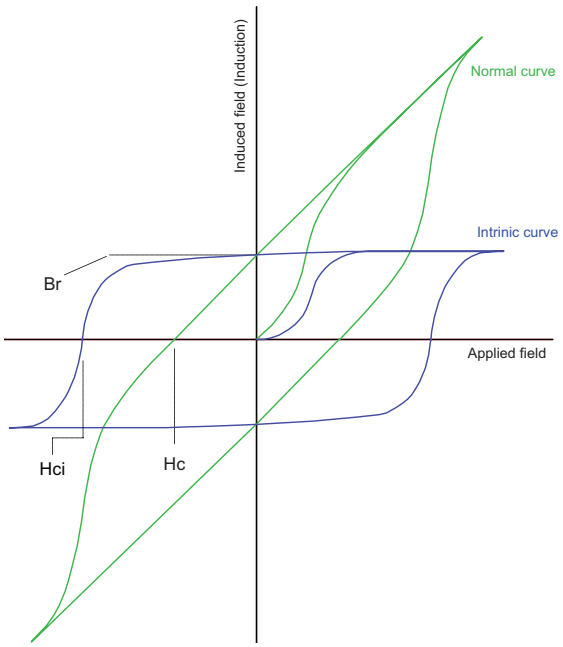

Figure 6.7: Hysteresis Loop all the quadrants. Figure from [37].

In the applied field axis, the magnetic field intensity H represents the magnitude of an externally applied field to the magnet and the inducted field axis, the flux density B represents the magnetic output either of the magnet. The Intrinsic curve shows the magnetic material induction, it is calculated the output due only to the magnet. Whereas, the Normal curve represents the observable induction, the measured, combined the value of B of both fields, the applied field and the contributed by the permanent magnet. Also, there are some terms:

- Br is the remanence, the magnetic induction corresponding to zero magnetizing force in a magnetic material after saturation in a closed circuit.

- Hc is the coercive force. This is equal to the demagnetizing force required to reduce remanence or residual induction, Br to zero in a magnetic field after magnetizing to saturation, in this point there is not observable field.

- Hci is the intrinsic coercive force, that indicates the resistance to demagnetization.

The magnet circuit we want to create is not in closer or shorted, in fact the flux has to go though the gap. So that, the magnet, in operation, works only within the region known as the 2nd quadrant of the hysteresis curve.

It is important to remember that the curve is representative of the specific material used to make the magnet, and it is independent of the geometry and layout of the magnets. Depending on the material, the Hci will be more or less close to the vertical axis. If the intrinsic coercive force is less than 25 Oersted the material is called: soft, if this parameter is bigger the material is hard.[37] See fig. 6.8.

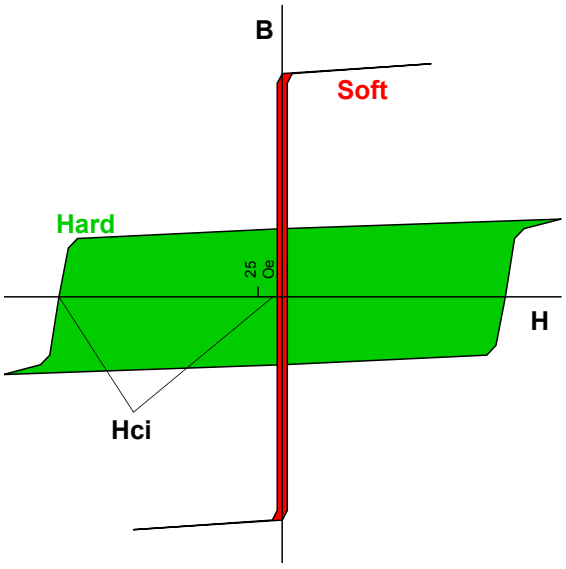

Figure 6.8: Soft vs. Hard Permanent Magnetic Materials Hysteresis Intrinsic Loop. Figure from [37].

The material of the magnets chosen is NbFeB, which has a Hci much bigger than 25 Oersted, and has more remanence (the magnetization left behind in a ferromagnetic material after an external magnetic field is removed. It is also the measure of that magnetization. The remanence of magnetic materials provides the magnetic memory in magnetic storage devices). We have chosen a Hard material because we need that this material cannot be demagnetized easily. And, so that, to have the demagnetization curve as flatter as possible, in order to obtain the working point with the bigger B possible. As we will see after.

Thanks to fig. 6.9 and supposing that, in our case, the temperature is almost 20°C, we can obtain the magnetization curve, the relation between B and H:

$$B_{mc} = 1.30 * 10^{-6} H_{mc} + 1.24T \tag{6.1}$$

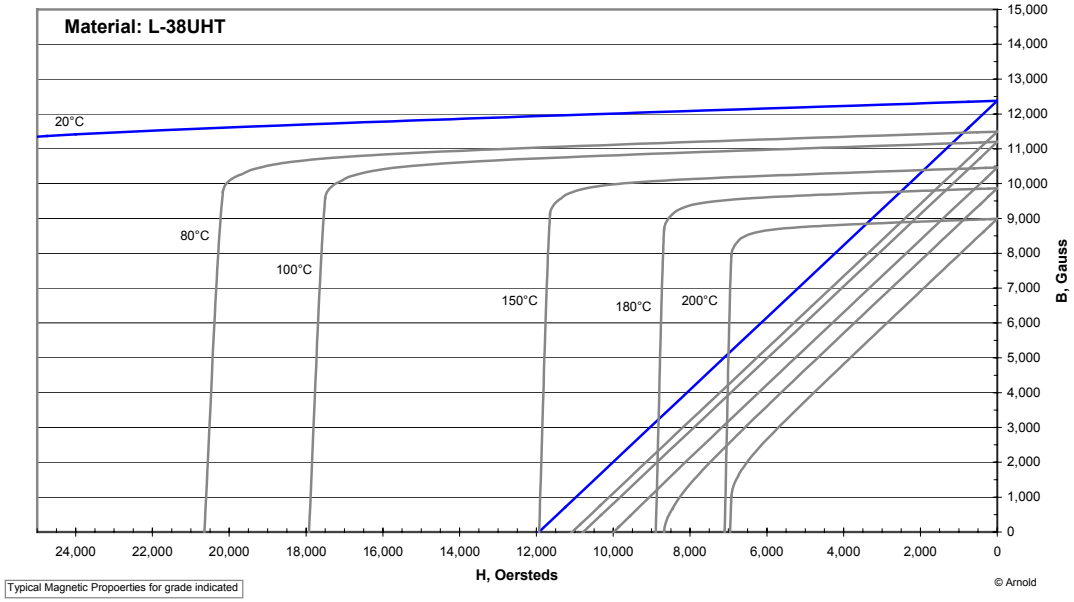

Figure 6.9: 2nd quadrant of the hysteresis curve of NdFeB in different temperatures. Figure from [37].

This equation is in SI, and includes the subscript mc in both parameters (B_{mc} and H_{mc}) to refer that they are parameters of the magnetization curve.

The point of the demagnetization curve where the magnets are going to work once they are installed in the magnetic circuits, depends on the magnets geometry and the gap. In other words, it depends on the load line. Fig. 6.10 is an example of how the operating point is fixed by a load line and a specific material.

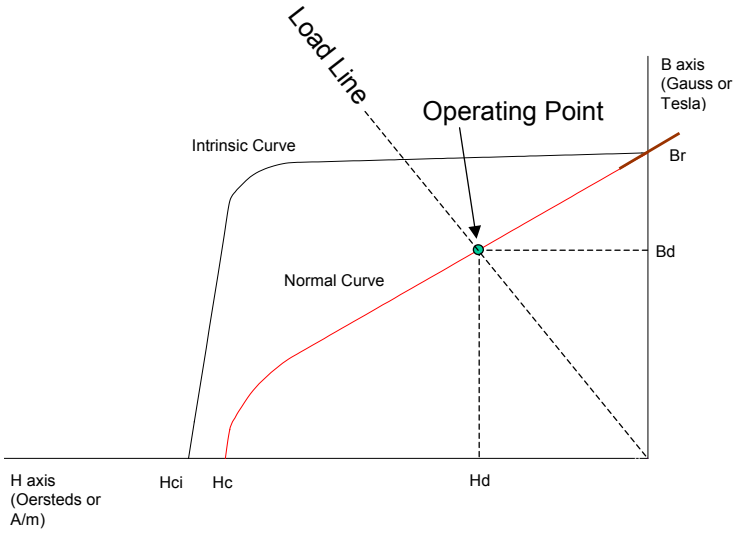

Figure 6.10: An example of the working point of the magnets for a specific material and a load line. Figure from [37].

The load line depends on the geometry of the magnets and the gap. It can be calculated thought Ampère's Law (6.3), Faraday's Law (6.5) and Gauss's Law (6.6). Fig. 6.11 shows a simplified top view of the generator. Where it is possible to observe the two rotors, the stator and the gap, the space between the magnets disposed face to face. Also, there is a line, which simulates the flux way. It is important to take into account that this figure is only an sketch and so that the dimensions are only approximated.

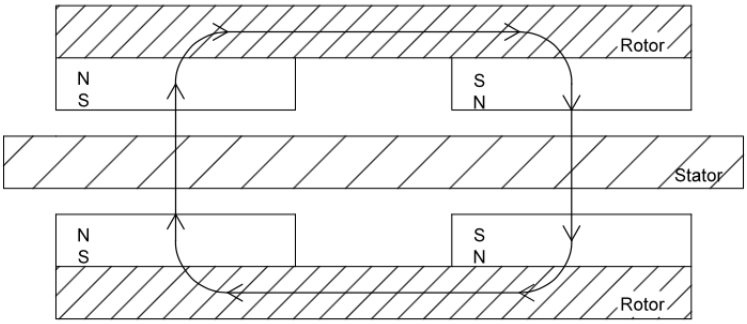

Figure 6.11: Simplified sketch of the generator.

Ampère's Law determines the magnetic field associated with a given current, or the current associated with a given magnetic field, while the electric field does not change over time. One of the integral forms of this law is:

$$\oint_C \vec{B} \cdot \vec{dl} = \mu_o \iint_S \vec{J} \cdot \vec{dS} = \mu_o \, i_{enc} \tag{6.2}$$

where μ_o is the vacuum permeability.

This equation explains that the line integral of the magnetic flux density (B), around closed curve (C) is proportional to the total current, free and bound current, (i_{enc}) passing thought the surface S, enclosed by C

Other alternative integral, which is linked only with the free current is:

$$\oint_C \vec{H} \cdot \vec{dl} = \iint_S \vec{J_S} \cdot \vec{dS} = i_{f,enc} \tag{6.3}$$

This equation explains that the line integral of the magnetic field intensity (H), around closed curve (C) equals the free current ($i_{f,enc}$).

Due to the fact that the permanent magnet is magnetized in the absence of free current [39], applying the Ampere's law (6.3) it is obtained:

$$H_m l_m + H_g l_g = 0 \tag{6.4}$$

where, H_m is the field intensity in the magnet, H_g is the field intensity in the gap, and l_m and l_g are the thicknesses of the magnet and of the gap.

We suppose that the magnetic core permeability is much bigger than permeability in the gap: $H_g l_g > H_r l_r$, where H_r and l_r are the parameters linked to the rotor (brake disc or magnetic core), can be respected.

On the other hand,the magnetic flux through a surface is proportional to the number of field lines passing through that surface:

$$\phi = \iint_S \vec{B}.d\vec{S} \tag{6.5}$$

In this case the surface is closed. So, following the Gauss's law for magnetism states: the total magnetic flux through a closed surface is equal to zero [39], we find that:

$$\phi = \iint_S \vec{B}.d\vec{S} = 0 \tag{6.6}$$

Therefore,if we study what happens between the magnets and the gap, the input magnetic flux in the surface has to be the same as the output flux:

$$\phi = B_m S_m = B_g S_g \tag{6.7}$$

where B_m is the magnetic flux density in the magnet, B_g is the magnetic flux density in the gap, and S_m and S_g are the surfaces in the magnet and in the gap traversed by the flux density.

From the equations (6.4) and (6.7) we find the equations (6.9) and (6.8):

$$\frac{B_g S_g}{H_m l_m} = \frac{B_m S_m}{-H_g l_g} \tag{6.8}$$

$$\frac{-B_g S_g H_g l_g}{H_m l_m S_m} = B_m \tag{6.9}$$

The magnetic permeability in the gap is constant and almost the same as in the vacuum; $\mu_o = 4\pi * 10^{-7}$ N/A^2. Using the relation between the magnetic flux density and the field intensity, we obtain:

$$\mu_o H_g = B_g \tag{6.10}$$

In addition, using equation (6.7) and changing it, we can write:

$$B_g = \frac{B_m S_m}{S_g} \tag{6.11}$$

According to the relation (6.10), $H_g = \frac{B_g}{\mu_o}$. Replacing this field intensity and the magnetic flux density in the gap, equation (6.11), in (6.9) we obtain the load line:

$$B_m = \frac{-\mu_o S_g l_m}{S_m l_g} H_m \tag{6.12}$$

Observing this load line, we can notice that it is situated in the second quadrant, where it was supposed to be. [39].

As we can see, this line is strongly dependent on the geometry. Below, we give numerical values for our particular case:

- $S_g = (a_m b_m) * 1.25 =$ (46 mm * 30 mm)*1.25 = 1725 mm^2 = $1.725 * 10^{-3}$ m^2 The surface in the gap traversed by the flux is consider as 1.5 times the magnet surface because of the edge and dispersion effects, and taking into account the thickness of the gap. (See the simulation in the fig. 6.14).
- l_m = 10 mm = 0.01 m

- $S_m = a_m b_m$ = 46 mm * 30 mm = 1380 mm^2 = 1.38*10^{-3} m^2
- l_g = 20 mm = 0.02 m

Finally, we obtain the load line in the case studied:

$$B_m = -1.5025 * 10^{-6} H_m \tag{6.13}$$

where the slope of the line is given in Tm/A.

Once both curves are known, it is possible to find the intersection between them, and find the working point. In fig. 6.12 we calculate the intersection between the load line (6.13) and the magnetization curve (6.1).

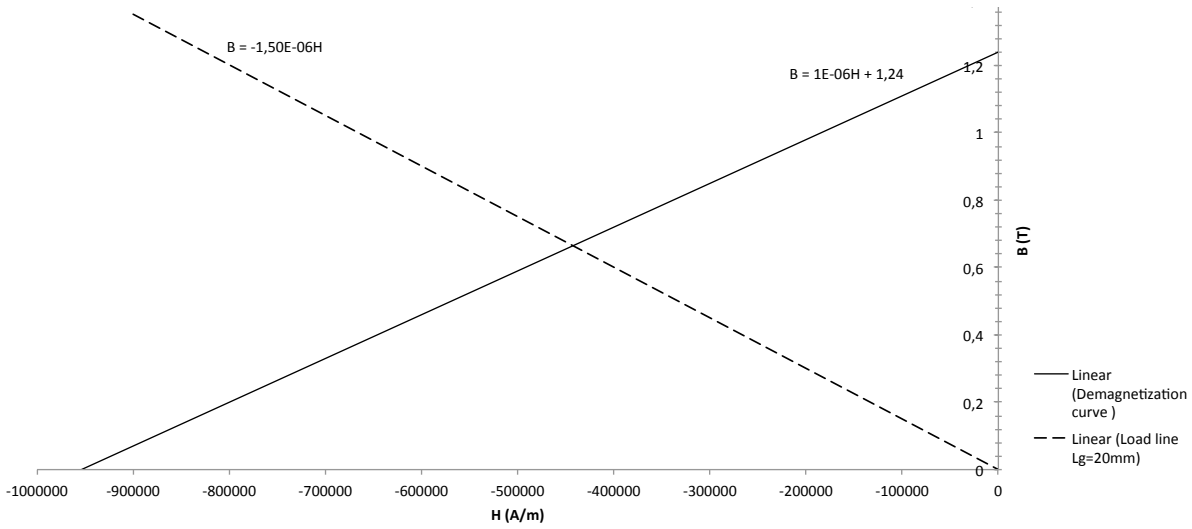

Figure 6.12: Intersection between Load line and Magnetization curve

The operation point or working point is:
B_m = 0.664 T
H_m = - 442462.087 A/m

Once we have the B_m, we can calculate B_g thanks to the relationship shown in (6.11). This gives:
B_g = 0.531 T

During this explanation we did not take into account the rotor material, and it behaviour. At this point, we might question the status of the rotor material, which means, the magnetic saturation of the brake discs (B_r).

This analysis can be done using a similar equation to (6.7) but in this case we include B_r and S_r, parameters linked with the rotor, instead of B_g and S_g.

$$\phi = B_m S_m = B_r S_r \tag{6.14}$$

Also, we know: $S_r = a_m l_r$ = 46 mm *10mm= 460 mm^2 = 4.6*10^{-4} m^2, because is the area in the rotor traversed by the flux density, when it is developed.

Solving for the unknown, magnetic flux density in the rotor:

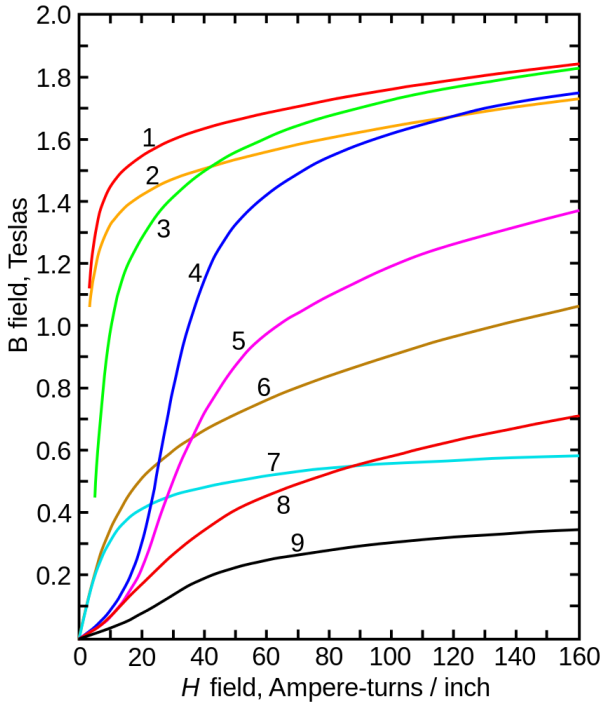

Figure 6.13: Magnetization curves of 9 ferromagnetic materials, showing saturation. 1.Sheet steel, 2.Silicon steel, 3.Cast steel, 4.Tungsten steel, 5.Magnet steel, 6.Cast iron, 7.Nickel, 8.Cobalt, 9.Magnetite. Adapted figure from [40].

$B_r = 1.992$ T

As we can see in fig. 6.13, if we assume we have a carbon steel (1010 or similar), the maximal magnetic flux density that it supports before getting saturated is between 1.2 T and 1.6 T [40]. So that, we can conclude that these brake disc metals are saturated, also that in the equation (6.4), and we should have taken into account it. So that, if the discs are considered saturated, as in the case, the result of B_g will be lower than the calculated. Using the equation (6.14) and assuming that the B_{rmax} is 1.6 T, it is possible to recalculate the B_m (B'_m) and after that, the new B_g (B'_g) thanks to (6.11):
$B'_m = 0.533$ T
$B'_g = 0.426$ T

We have assumed that B_{rmax} is 1.6 T in order to be conservative with the result. Because of that, we have a bigger possible value of B_g, B'_g, with which we will design the other components of the generator.

Thanks to the programme FEMM, Finite Element Method Magnetics [41], we could simulate our case, solving it as a low frequency electromagnetic problem (problems that can be described by a diffusion equation rather than by a wave equation [41]) on two-dimensional planar domains.

To do this, we have drawn the top view with all the geometry and materials already given, and have simulated it, fig. 6.14.

In fig. 6.14 we can see the magnetic simulation of our case, with some flux density lines. It is important to take into account that this figure is a sketch, where we can simulate the magnetic flux behaviour and gives us an approximate idea about the dispersion of the flux. The material disposition is the same as the fig. 6.11.

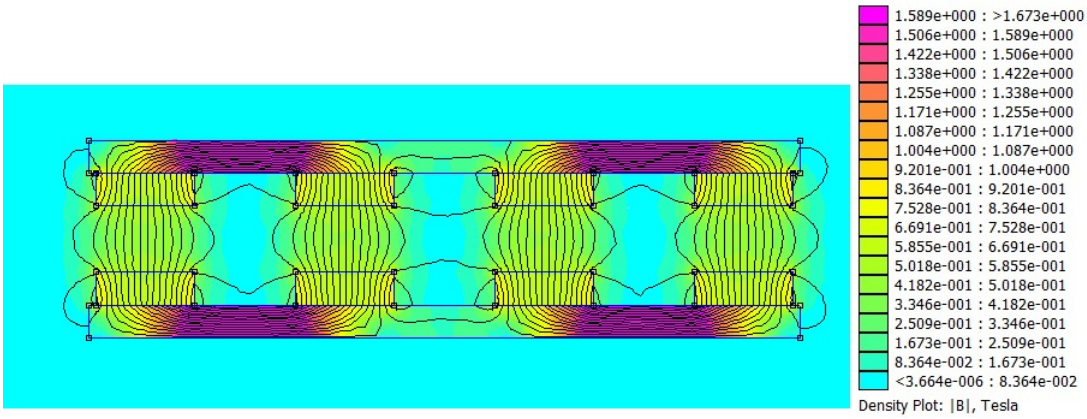

Figure 6.14: On the left: magnet rotor simulation (simplified top view). Sketch with the 2 brakes disc, 8 magnets and the gap. On the right: colour bar for the magnetic flux density.

In the gap, we can see some distance between the field lines, this means that the flux density in this zone is weaker than in the brake discs. The flux lines go through the gap generating an area, S_g, traversed by the flux. Thanks to the simulation, as it is not possible to do it theoretically, we can suppose that this area is 1.25 times the magnet area.

Also, the different colours shown in the figure give us a numerical value of the flux density. The colours in the gap are green and green-yellow, so if we consider the caption it means the flux density can be between 0.4 T and 0.5 T. The colours in the brake discs are pink, being the flux density higher than 1.5 T, that involves that the metal of brake discs is saturated, as we said before in a numerical way. In the magnet, the flux lines are closer than in the gap but not as much as in the brake discs and the colour in this area is yellow. If we use the caption, we can conclude that the magnetic flux density in the magnets is around 0.6 T or 0.5 T.

Another possibility to design the magnetic rotor is to build it with two brake discs but only one face with magnets.

The principal advantages are:

- The cost is lower, because we need only half of the magnets we needed before
- This model is easier to build

It will be also the option we use in the university in order to build the machine and to study its behavior.

The characteristics of this generator design are:

- 8 Magnets. Material: NbFeB, Dimensions: 46 x 30 x 10 mm (a_mxb_mxl_m)
- 2 Brake disc. Material: Steel 1010, Dimensions: Diameter = 280 mm, Thickness = 10 mm (l_r)
- Gap. Space (air) where the stator is located. Dimensions: Thickness = 20 mm (l_g)

With regard to the flux density study, this case follows the same steps as the previous one but with an essential difference: in the first case we had 2 magnetic faces (see fig. 6.11) and in this one, we only have one (fig. 6.16).

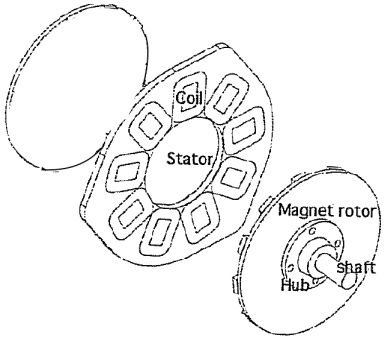

Figure 6.15: Sketch of the generator, with 12 magnets and 9 coils. Modified figure from [28].

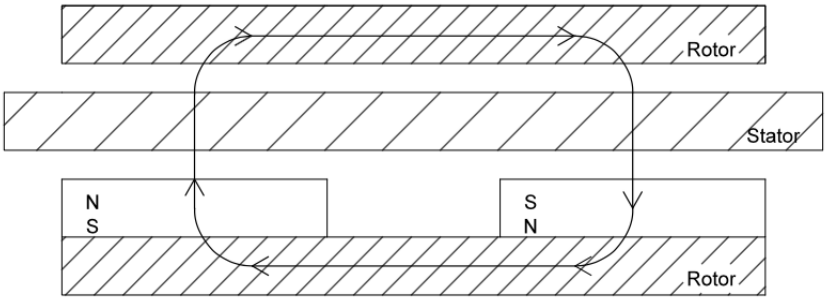

Figure 6.16: Simplified sketch of the generator with only one magnetic rotor.

To estimate the values of the flux density, we used the same programme FEMM [41], as we can see in fig. 6.11 but with four magnets instead of eight.

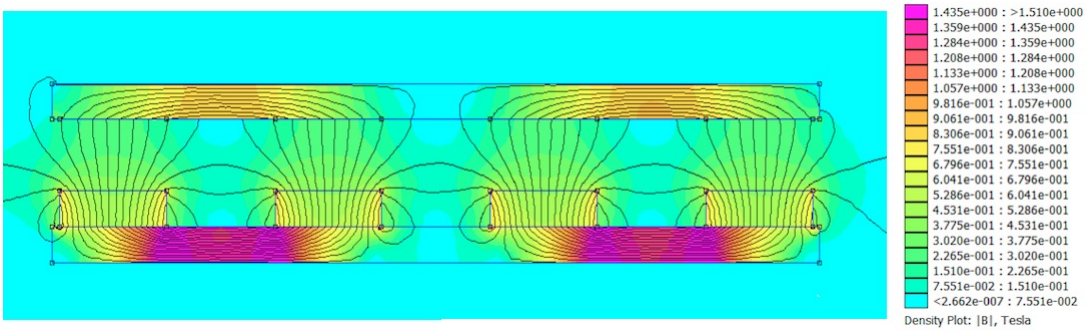

Figure 6.17: On the left: Magnet rotor simulation simplified top view. Sketch with the 2 brakes disc, 4 magnets and the gap. On the right: Caption which shows colours linked with different values of magnetic flux density.

As we can see, in this case, the magnetic field is not homogeneous even on the length of the gap, because the zone close to the magnets has a stronger flux value than the zone near the brake disc without magnets. Having the non magnetic rotor here is important,

because it allows the field to have a better way than the air to end the loop. This means that we have a stronger field in the gap if it is compared with not having this brake disc.

To conclude, the flux density in the gap, as we have only magnets in one disc, will be smaller than $B'_g = 0.426$ T, flux density with magnets in both discs.

Using the simulation fig. 6.17, we can say that the flux density in the gap in this case will be between the interval: 0.302 T and 0.528 T. Both values are taken from the caption in the figure, the first one corresponds to the situation near the brake disc and the other one, the situation close to the magnet. The flux density we have in this situation will be smaller than the previous situation because, now, the magnetic force is less strong.

6.3.2 Stator

Thanks to Faraday's (6.5) and (6.16), and Ampère's Laws, we can achieve the intensity in the stator, and thus, the final electricity.

The design of the stator is basically focus on the coils: the number of turns per coil and wire dimensions.

These parameters are linked to the rotational speed and the output voltage. The rotational speed is given by the Matlab programme throughout the tip speed ratio. In the section of the rotor have been explained that the outputs of the Matlab programme are the Tip Speed Ratio (TSR) where the Cp is maximum, the Cp and the power. So it should be normal to think that the design of the generator has to be done with this Tip Speed Ratio. It would be like this if the rotational speed would be variable, in order to maintain always the required rotational speed for the optimum Cp. But in this case, the rotational speed is fixed because the generator is directly connected to the batteries via a rectifier, as we will see in Chapter 9 Electronics and conversion systems.

If we take into account that the Cp should be maximum for the most possible wind speed, a good solution to this problem would be to choose a higher TSR to design the generator [28]. This is because the wind turbine is going to start to generate electricity at a wind speed slower than the most probable wind speed, cut-in speed. And it is here were we have to decide the value of the rotational speed related to this cut-in speed, and so the rotational speed for the turbine.

In this case, for instance, if we have a TSR for the maximum Cp of 6 the TSR for the starting and designing point would be around 7.5. Also, if we want to start generating energy at a wind speed of 3 m/s, the rotational speed would be, thanks to the equation. (5.6), where $V_\infty = 3$ m/s, TSR (λ)= 7.5 and R will be different in the two blade designs:

- Wooden rotor: R = 0.9 m:

$$\omega = \frac{\lambda V_\infty}{R} = \frac{7.5 * 3}{0.9} \rightarrow \omega = 25 \text{ rad/s} \simeq 240 \text{ rpm}$$

- PVC pipe rotor: R = 1.27 m:

$$\omega = \frac{\lambda V_\infty}{R} = \frac{7.5 * 3}{1.27} \rightarrow \omega = 17.71 \text{ rad/s} \simeq 170 \text{ rpm}$$

So that, with this rotational speed at a wind speed of 6 m/s (the most probable wind speed) the TSR would be lower than 7.5.

The designing rotational speed for the designing of the stator would be, 240 rpm in wooden rotor case and 170 rpm in the plastic one, although at the most probable wind speed (6 m/s) we do not have the optimum TSR, it is closer than if the designing TSR would be the one done by the Matlab programme.

We have exposed two rotational speed depending on the design of the rotor and the blades we use. In order to continue, we elect one of them, 240 rpm.

The output voltage has to be fixed, in our case, a little more than 24 V, around 25.4 V. Due to the fact that we want to charge 24 V batteries, it is necessary to include a rectifier which will need some voltage, it is estimated that 1.4 V. As we will see in the section of Electronics and conversion systems, Rectifier (page 100), the voltage in one diode usually is around 0.7 V, here, as we have two diodes in series, the voltage will be 1.4 V See fig. 6.18.

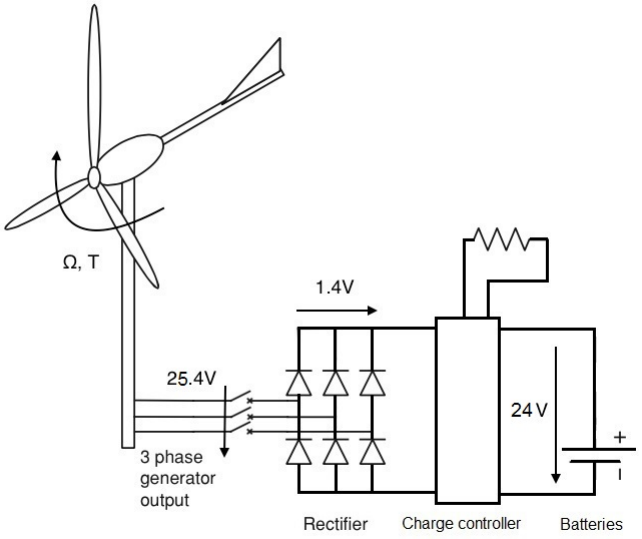

Figure 6.18: General sketch of the elements and voltage distribution. Figure from [42] modified.

Once we know the rotational speed and the output voltage, it is possible to start the design.

The number of turns per coil

In order to determine this parameter, we are going to mach two voltage equations. The first one expresses the required voltage:

$$V_{req1} = V_{batt} + V_{rect} \tag{6.15}$$

where V_{req1}, is known and equal to 25.4 V.

The second equation (6.21) is the voltage produced by the generator, which is dependent on the number of turns. To achieve it, we follow the next analysis :

We have three phases, and in every phase we have N_{cp}, number of coils per phase. Also, we have a total number of turns of wire per phase, N_s, so that we can say that in every coil we have N_s/N_{cp} windings. (In the first case, we have 9 coils which means N_{cp}=3, and in the second case, the case with one layer of magnets, we have 6 coils, so that N_{cp}=2)

The following study is done for the second case with 6 coils, 2 per phase. Fig. 6.19 shows the coils distribution. A, B and C represent the 3 phases of the generator. As we have two coils per phase, the subscript represent the number of coil.

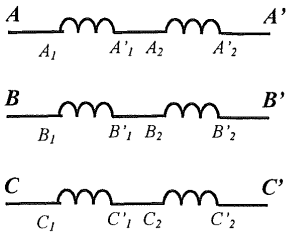

Figure 6.19: Coils distribution of the generator. From [17]

Now, if one of the coils per phase A, A_1A_1', is analyzed in order to know the voltage:

$$E_{A_1A_1'} = -\frac{N_s}{N_{cp}}\frac{d\phi}{dt} \tag{6.16}$$

With the rotation of the magnetic rotor the value of B_g, as it depends on the angle which is related to the angular frequency, changes in the time. Being the magnetic flux density during the time $B_g(\theta)$ and θ the angle linked with the speed rotation and the time: $\Omega(rps) * t(s)$. Knowing this, and using the Faraday's law (equation (6.5)), we can obtain $\phi(t)$:

$$\phi(t) = \int_0^{\pi/p} B_g(\theta) S_{tm}\, d\theta = \int_0^{\theta} -B_g S_{tm}\, d\theta + \int_{\theta}^{\pi/p} B_g S_{tm}\, d\theta \tag{6.17}$$

$$= B_g S_{tm}(\pi/p - 2\theta) = B_g S_{tm}(\pi/p - 2\Omega t) \tag{6.18}$$

where: S_{tm} is the sum of the surfaces in the magnets traversed by the flux density and p: number of pole pairs, in this case 4.

Deriving and using the equation 6.16 [28]:

$$\mid E_{A_1A_1'} \mid = \frac{N_s}{N_{cp}} 2 B_g S_{tm} \Omega \tag{6.19}$$

which implies that the total voltage in the phase AA' is the sum of the voltage in every coil in the phase. The 3 phases voltage is given by:

$$\mid E_{AA'} \mid = \mid E_{A_1A_1'} \mid + \mid E_{A_2A_2'} \mid = N_s 2 B_g S_{tm} \Omega \tag{6.20}$$

If we are in the first, the case with two layers, we should include $+ \mid E_{A_3A_3'} \mid$ in the equation (6.20), because there are three coils instead of one.

As we want to know the number of turns per phase of the stator, we should take into account the peak tension value. Equation (6.20) gives us the average voltage in a group of coils for a given speed of rotation, so that we need to increase it with:

- $\sqrt{3}$: necessary because our system is a three phases system and we need to change the phase voltage into line voltage.
- $\pi/2$: in order to change the average value into the peak value assuming a sine wave output.

This term leads to:

$$V_{req2} = 2 B_g S_{tm} \Omega N_s \sqrt{3}\pi/2 \tag{6.21}$$

where: B_g = magnetic flux density in the gap, Ns = total number of wire turns per phase of the stator, Ω = rotational speed done in revolutions per second (rps) and S_{tm} = sum of the surfaces in the magnets traversed by the flux density.

Ones we have the equations (6.15) and (6.21), we are able to know N_s:

$$N_s = \frac{25,4}{2B_g S_{tm} \Omega \sqrt{3}\pi/2} \tag{6.22}$$

Wire dimensions:

Also, the dimensions of the wire are important, we need to determine the wire diameter and the length of the wire.

- The wire diameter

The coils may be arranged in two ways, as it is shown in the following figure:

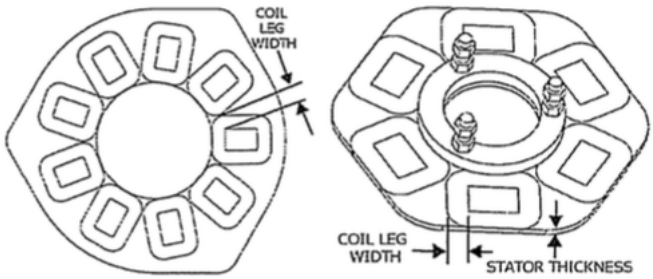

Figure 6.20: Different coils dispositions. Figure from [28].

The layout model on the left is used for the design with 9 coils, while the right is used when there are 6, always to optimize space and minimize power and heating losses.

On the one hand, the coil leg (see fig. 6.20) width is limited by the size of the coils that fit next to each other, and on the other hand, the coil thickness is limited by the stator thickness fixed before. Therefore, this will be different in both cases and it is necessary to calculate them in order to know the measures of the final coils we will have.

Helped by the book "A wind turbine recipe book" [28], and knowing the dimensions of the coil winder and the magnetic rotor, we can do some sketches to estimate the available space for the coils we have in both cases. Achieving the results shown in table 6.1:

Table 6.1: Coil characteristics.

Machine	**9 Coils**	**6 Coils**
Coil leg width (mm)	17	30
Coil thickness (mm)	13	13

Ones we know these dimensions, the cross-sectional area of the coil can be calculated from the relation:

$$\text{Cross-sectional coil area} = \text{Coil leg width} * \text{ Coil thickness} \tag{6.23}$$

This area is traversed by the copper $\frac{N_s}{N_{cp}}$ times, but we have to take into account that in this area there is a lost space which depends on how tight the turns are. To determine the ratio of the volume occupied by the wire in the coil, to the total volume of the winding, we use space factor. This factor will depend on how tightly the cooper is wound. The typically used one are between 55% to 60%, [28]. So that, we can consider:

$$\frac{N_s}{N_{cp}} * \text{Wire area} = \text{Coil leg width} * \text{Coil thickness} * 0.55 \tag{6.24}$$

This formula shows that the cross-sectional area covered by the wire is 0.55 times the area: coil leg width x coil thickness. And, as we know all the parameters, we can calculate the wire area, and choose the closest size of wire available, aided by table 6.2.

Table 6.2: Standard wire diameters. Source: [28].

Diameter (mm)	**Area (mm^2)**
0,71	0,40
0,75	0,44
0,8	0,50
0,85	0,57
0,9	0,64
0,95	0,71
1,00	0,79
1,06	0,88
1,12	0,99
1,18	1,09
1,25	1,23
1,32	1,37
1,40	1,54
1,50	1,77
1,60	2,01
1,70	2,27
1,80	2,54

For example, in the case we have manufactured, it was a 6 coils machine: coil leg width = 30 and coil thickness=13 and 120 turns per coil:

$$\text{Wire area} = \frac{30*13*0.55}{120} = 1.7875 \text{ mm}^2$$

Once, we knew the area, helped by table 6.2, we obtained the diameter: 1.50 mm.

- The length of wire

In order to know the total length of wire, firstly it is necessary to calculate the average length of a turn of wire in a coil [28]:

$$\text{Average length of a turn of wire} = 2 * (a_m + b_m) + \pi * \text{Coil leg width} \tag{6.25}$$

The total length of wire in a coil will then be this number times $\frac{N_s}{N_{cp}}$ (coil turns):

$$\text{Wire length per coil} = \text{Average length of a turn of wire} * \frac{N_s}{N_{cp}} \tag{6.26}$$

Keeping up the previous example, the total wire length required is:

Average length of a winding = 2∗(46 mm+30 mm)+π∗30mm = 246.24 mm

Wire length per coil = 246.24 mm ∗ 120 = 29548.8 mm = 29.55 mm

Coil and stator resistance:

The coil resistance is important for working out the performance of the generator when it is working, and so that, producing current. Once we know the resistance of the coils, and also we know configuration of them, the stator resistance can be calculated.

The resistance of the coil depends on the length, and the thickness of the wire. As much longer and thinner it has more resistance, as we can observe in the next expression:

$$R_{coil} = \frac{\text{Wire length per coil}}{\text{Wire area}} * \frac{1}{\sigma} \tag{6.27}$$

where σ is the conductivity of the copper. (Take into account that the conductivity of the copper is strongly dependent on the temperature, so there is no a single answer.)

Once the resistance of the coil is known, we can achieve the stator resistance thanks to the next equation:

$$R_s = 2 * \text{Number of coils per phase} * R_{coil} \tag{6.28}$$

The equation (6.28) has been taken from the book [28], and it has some approximations. *"A simplified way to consider the current in the stator is to say that it only uses two of the three wires at any given time, and passes through two phases in series. In fact there will be some sharing of current at times between all three wires, but this is hard to allow for and secondary in magnitude."*

Continuing with the same example, in this case:

$R_{coil} = \frac{29.55}{1.77*10^{-6}} * \frac{1}{54*10^{6}} = 0.309\ \Omega$

$R_s = 2 * 2 * 0.309\ \Omega$

6.4 Manufacturing of the generator

In the course of Valence where we went a permanent magnet generator with axial flux was built. In this case we followed the instructions of the book [27]. As during the whole section has done, here, the manufacturing is also going to be split up in two different components: the stator and the magnetic rotor. In fig. 6.15 we have an exploded view of the machine we built.

6.4.1 Magnetic rotor

Two steel discs were needed, one to assemble there the magnets and the other to direction the flux. The only engineering that they needed was making some threaded holes to be able, later, to assemble them and in order not to oxidize because of the rain, painting them with a stainless paint.

In each disc the magnets needed to be fit, so to make it easier, a mould was built. We measured the diameter of the steel disc and knowing the number of magnets and the measures of them, we could be able to make the geometry necessary to make the mould.

The most interesting in this part was the setting up of the magnets. We had to take into account that in each rotor the poles of the magnets had to be intercalated, therefore,

if the first magnet situated was with the north face in the steel disc, the next magnet had to be the contrary. The two rotors had to be symmetric, consequently, in front of a north face it had to be a south one. To fix well the magnets to the steel disc we added a bit of glue.

On the other hand, as we can see in fig. 6.21, a resin to the steel disc with the magnets has to be incorporated to assure that they were well attached to it and to protect them from corrosion. Therefore, a mould had to be done. To fabricate it, we had to take into account the sizes of the steel discs, the diameter, the width of the steel disc with the magnets....

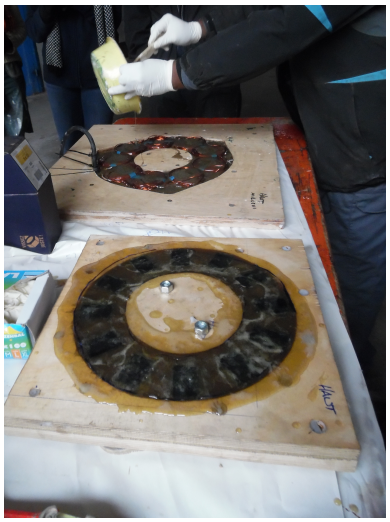

Figure 6.21: The magnetic rotor and the stator when the resin was being added.

Finally, the grout had to be mixed to, as we have said before, fix the magnets to the steel discs and protect them, but before it we had to spread the mould with wax to make it latter easier to unmould them. We also needed that substance in the stator, so it will be explained in the next section.

6.4.2 Stator

With regard to the stator, as a PMG was being manufactured, we begun with the coils, here in the stator we had 6 coils. It is easy to make a coil only rolling wire around a template of the same shape of the magnets, but to build them easier and more effectively we fabricated a coil winder. It is explained in the book [27] how to make it. It is important to make the coils as compact as possible, because in this way, the generator will be more effective, and it is also important to make all the coils as similar to each other as possible, because in this way the three phases of the stator will be similar too.

Once the coil winder was made, we rolled the cooper wire as many lap as the book specified, making the required coils.

Otherwise, the mould for the stator had to be fabricated. This one, as the rotor mould, is important because once we added the resin and it got dry, the stator finally kept the mould shape. In this case, the measures of the nacelle, the way we were going to assemble to it, the measures of the rotor and that some wires were going to get out from it had to be taken into account, so the shape of fig. 6.22 was made.

As we can see, there are three protrusion where the stator was going to be screwed

to the nacelle and the cover of the mould had a hole, so that, the wires could get out. To decide at what radio the coils had be to fixed, we had to think that the hole of the magnets shape in the coils had to be aligned with the magnets of the rotor.

For doing that effectively we drew 6 magnets in the stator, in such a way we could align the coils and the magnets, taking into account that the interior hole of the coils has to be face to face with the magnets.

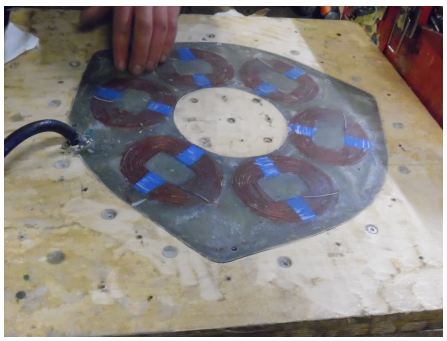

Figure 6.22: Stator of the wind turbine.

Afterwards, we connected the coils, in this case, in a star connection. In order to do so, we peeled the wires and we welded them with tin.

Before adding grout we had to test if all the phases had the same resistance. To do that, we used a multimeter. If all the phases had more or less the same resistance, it meant that the coils where well done and well connected.

Finally, we added the resin. We had to keep in mind that the wires could not cross the three protrusions, inasmuch as we had to screw it to the nacelle from there.

As we have said before, how to mixed the chemical constituents to create the grout is going to be explained. There are some issues to bear in mind in synthesizing the resin:

We summary the magnetic rotor needs a grout to protect the magnets from the corrosion, and also, needs a resin that conducts well the heat.

Here there are the steps necessaries to make the grout:

1. Synthesize the resin. We made a polyester resin because it is convenient for both, the stator and the rotor.

2. Add the catalyst to the resin.

3. Mix the resin with talcum, that is because it is cheaper and it helps to conduct the heat. Remove it until it becomes denser. Take into account that there should not be air bubbles.

4. Pour in the mixture in the waxed mould. Watch out with the magnets and the coils.

5. Put the fiberglass in the mould: one piece for the rotor and two for the stator.In the stator we have to put one fiberglass before adding the mixture and another one after adding it.

6. Cover the mould and wait some hours until it is dry.

7. When it is dry unmould it.

6.5 General characteristics and analysis of the generator

On the present subsection we summarize the characteristics of the three-phase generator we manufactured (table 6.3).

Table 6.3: General characteristics of the generator. Source: [28]

	Data
Power	620 W *
Cut-in speed	3 m/s
Cut-out speed	10 m/s
Output Voltage in AC	25.4 V
Design TSR	6
Cut in TSR	7.5
Cut in RPM	240 rpm
Nº of magnets	8
Magnet material	NbFeB
Length of the magnet	46 mm
Width of the magnet	30 mm
Thickness of the magnet	10 mm
Nº of coils	6
Nº of coils in series per phase	2
Coil thickness	13 mm
Coil leg width	28 mm
Coil area	364 mm^2
Coil wire material	Bonded coating copper
Turns per coil	120
Coil wire area	1.77 mm^2
Coil wire length	26.5 m
Total wire weight	2.6 kg
Rotor Thickness	16 mm
Brake disc diameter	260 mm
Brake disc thickness	6 mm
Stator Thickness	13 mm
Gap. Space Rotor-Rotor	20 mm (approx.)
Magnetic flux density in the gap	0.44 T

* Power different to the power given by the bibliography, due to the fact that it is achieved with pipe blades design and different profile as the proposed in the Piggott's book [28].

Once these characteristics are known, it is interesting to achieve in a practical way some theoretical expressions done before, such as: coil resistance, stator resistance and the voltage performance against the rotational speed in vacuum.

6.5.1 Coil resistance:

The resistance of the coil is a characteristic easy to calculate, using the equation (6.27). To apply it we need to determine the following quantities:

- Average length of a turn of wire: To obtain this parameter, we use the equation (6.25):

$$\text{Average length of a turn of wire} = 2 * (a_m + b_m) + \pi * \text{Coil leg width}$$

= 2*(46 mm + 30 mm)+ π* 28 mm = 239.9 mm = 0.2399 m.

- N_s/N_{cp}: It is the same as turns per coil, it is: 120. Data from table 6.3.
- Wire area: 1.77 mm^2= 1.77*10^-6 m^2.
- σ: The conductivity of the copper, as it is said, depends on the temperature. If we suppose to have 14ºC, it is 56*10^6 S/m.

This gives for the resistance in the coil, $R_{coil} = 0.290\ \Omega$.

6.5.2 Stator resistance:

This parameter can be obtained thanks to the equation (6.28) and knowing R_{coil}:

$$R_s = 2 * \text{Number of coils per phase} * R_{coil} = 2*2*0.290 = 1.16\ \Omega$$

6.5.3 Voltage performance against the rotational speed in vacuum:

The relationship between the voltage and the rotational speed (Ω, revolutions per second) in vacuum can be achieve using the equation (6.21) which gives:

$$V = 2 * 0.44 * 0.011 * 240 * \sqrt{3}\pi/2\ \Omega = 6.32\ \Omega \tag{6.29}$$

where Ω is the rotational speed in revolutions per second.

If Ω is done in RPM, revolutions per minute:

To determinate the chars of the generator we measure the voltage produced in the generator's terminals, at different rotational speeds. To do this analysis, we used a multimeter to measure the output voltage and a sensor to quantify the rotational speed in every moment. And also, it could be possible to use a machine which generates different rotational speeds, as a small electric engine.

Table 6.4 shows the measured values:

Table 6.4: Data obtained.

Rotational speed (RPM)	**Voltage (V)**
15	1.8
29	3.2
36	4.4
60	6.7
72	7.6

During the test we could not obtain higher rotational speeds, because of the limitations of the tools, and therefore, we could not obtain more data points. But, it would be interesting to achieve some more points in order to have more data and create a trend line more accurate.

Using the 5 points measured, we can fit trend line as shown in fig. 6.23.

The trend line obtained is:

$$Y = 0.1113X$$

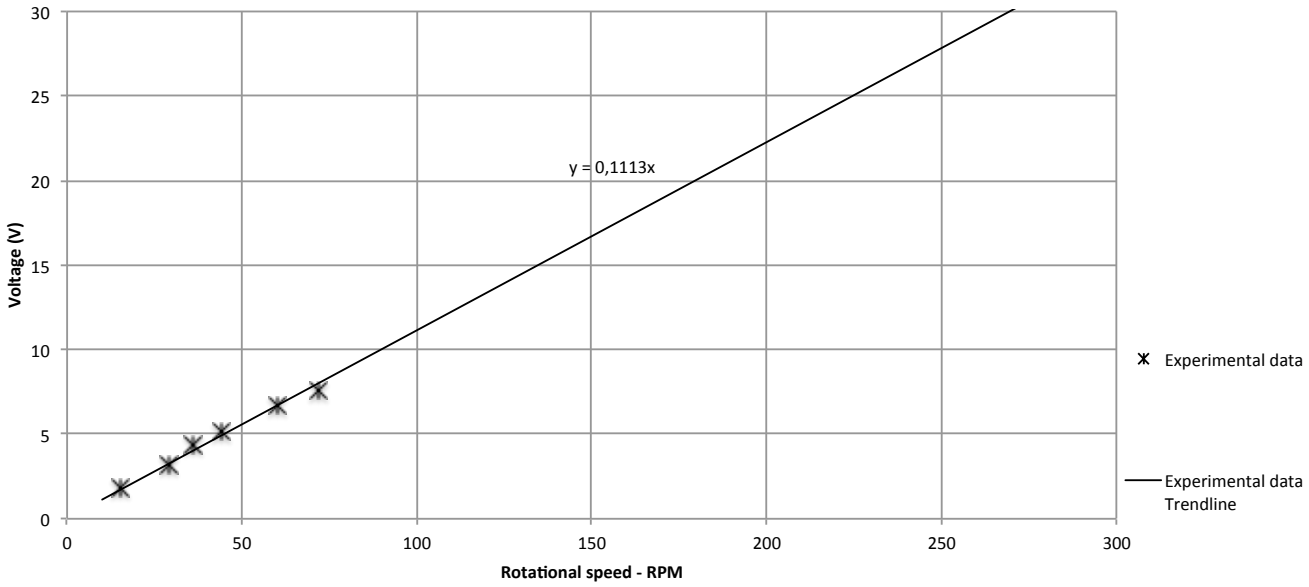

Figure 6.23: Rotational speed against Voltage. Values achieved in a experimental way. The trend line with it equation.

where Y is the Voltage (V) and X the Rotational speed (RPM).

In this point, this line cannot be compared with the theoretical one obtained in 6.29 because the theoretical one is given in revolution per second and this new one is given in RPM. To can compare, we change the theoretical line into RPM:

$$V = 0.1053\Omega$$

where Ω is in RPM.

Now, if it is compared the constant value in both lines, it is different. In order to giving a better idea of the agreement, in fig. 6.24 both lines are represented.

In fig. 6.24 we can observe both different lines. The theoretical one is smaller than the practical one. It may be due to imprecisions in the measurement or/and the theoretical calculations. We have to take into account that, on one hand the theoretical value is achieved using the estimated magnetic flux density in the gap. And on the other hand, the practical values have been achieved testing the generator manually, what it involves it could have been experimental errors.

6.6 Suggestions for improvement

Once design and material have been selected, there is a chance to suggest some improvements, and also to explain why the design chosen is better than other ideas that at the first moment could have appeared correct. To do so, we have divided this section in two different parts, as we did in the previous section.

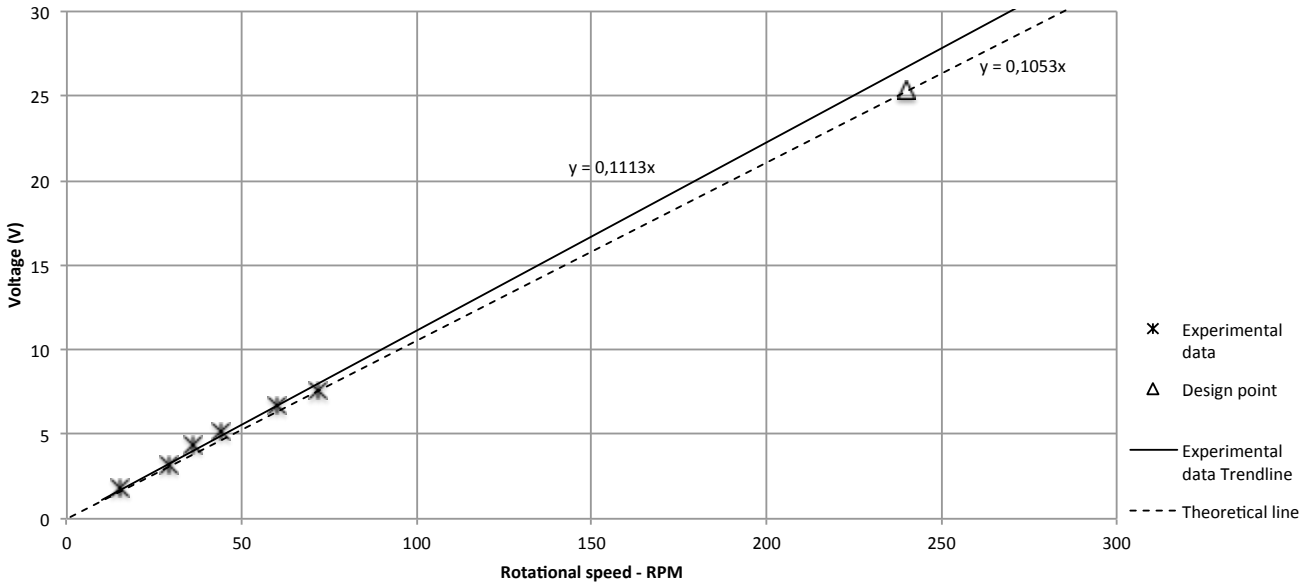

Figure 6.24: Rotational speed against Voltage. The experimental trend line and theoretical line with their equations.

6.6.1 Magnetic rotor:

The challenge of the magnet rotor design is to maximize the magnetic flux density in the gap, which depends on the geometry and the material properties. Therefore, there are some improvements associated with geometrical and/or material changes.

Assuming that we cannot change the material elected, the only possibility to improve the design is to change its geometry.

The geometry changes that could produce an improvements are:

- To increase the thickness of the brake disc
- To reduce the thickness of the gap

Increase of the brake disc thickness:

This improvement means to use other brake discs with a bigger thickness than the elected. If we consider this option, we will have to do the same steps till the equation (6.14) where the S_r will be different and higher. This change involves to achieve a magnetic flux density in the rotor (B_r) smaller. Implying that there is the possibility that the material will not saturate and the to that, we could take advantage of the maximum B_g.

To know what brake disc would be the closer to the ideal, below we calculate the thickness from which the material does not saturate. According to equation (6.14), knowing the next relationship $S_r = a_m l_r$ we find:

$$l_r = \frac{B_m S_m}{B_r a_m} \tag{6.30}$$

The numerical values of S_m, B_m and a_m are the same as before because they are not influenced by the disc thickness. About the value of B_r, we want to work in a point no-saturated. This gives 1.3 T in order to be conservative with the result. Getting:

l_r = 15.3 mm

It implies that if our new brake disc has a bigger thickness than 15.3 mm, we could benefit all the magnetic flux density in the gap created.

The disc of Toyota Land Cruise has the thickness = 18 mm and also the diameter is valid for the design of the magnets disposition: Diameter = 312 mm. So that, if we use its brake disc, according with the equation (6.14) the magnetic flux density in the discs will be 1.11 T, which means the material is not saturated and there is the B_g = 0.531 T as we have calculated before.

In order to verify all the theoretical calculations, we have simulated this new cases using the FEMM programme and getting fig. 6.25.

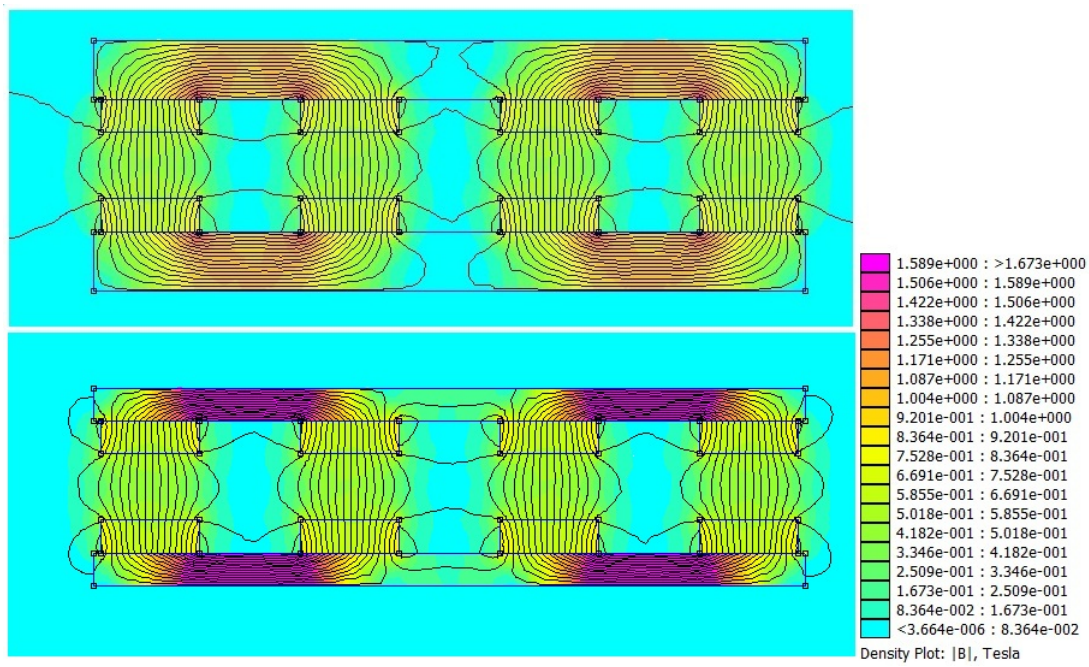

Figure 6.25: On the left: Magnet rotor simulations. Above: Magnetic rotor with a Land Cruiser brake disc. Below: Magnetic rotor with an Avensis brake disc. On the right: Caption which shows colours linked with different values of magnetic flux density.

Apparently, this second election is better than the first one at issue on electromagnetic field, but also, it is necessary to take into account that these new discs have bigger diameter and bigger thickness that implies having a heavier magnetic rotor. To give a rough idea, if the disc material is carbon steel, with a density like 7850 kg/m^3, the weight increases by 123.5 %.

Due to the fact that we have to find a compromise between mechanics and magnetical aspects, finally, we decided to keep the original design of the research.

Reduction of the gap thickness:

A improvement point could be to reduce the gap thickness. As it is mentioned before, the load line has a strong dependence on the geometry, and if the gap thickness is reduced, the load line changes, and with it, the intersection point between the new load line and the magnetization curve.

Fig. 6.26 shows different load lines depending on the gap thickness and their intersection with the magnetization curve:

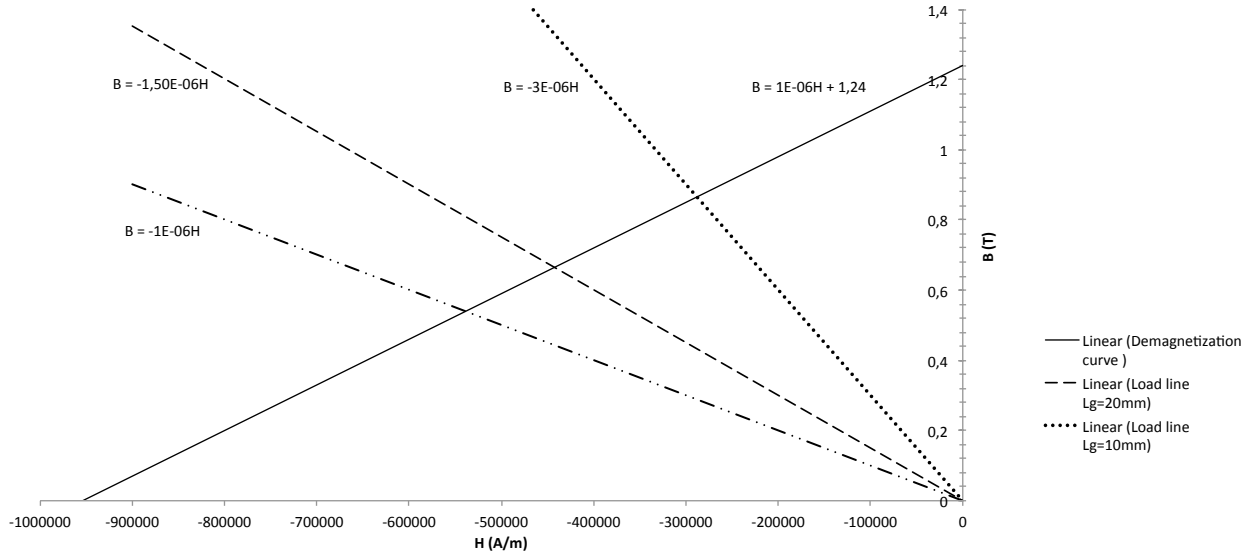

Figure 6.26: Intersection between some Load lines and Magnetization curve.

As we can see, the smaller gap thickness gives the best working point, because it has the biggest B_m and therefore B_g. Although reducing the thickness seems to be a good improvement, we have to take into account that in this gap, the stator will be introduced, so that, this space should suit the stator dimensions.

So that, to conclude this analysis, we say that it is not possible to reduce the gap thickness owing to the total design of the machine.

6.6.2 Stator:

We are going to highlight only one improvement in the stator, the coil shapes. The coil characteristic and geometry are fundamental to achieve the maximum flux density in the coils, and to obtain the maximum intensity. The optimum winding will be the one which fits more the space available on the rotor and produces more with lower resistive and inductive losses.

Chapter 7

Control. Design and analysis

In this section, all the possible events that need control are going to be exposed in order to try to design the wind turbine as secure and controlled as possible. The control involves the whole machine, so that, this is a sum up of the elements that have something in relation to this issue.

7.1 Control of the generated power

Generally, the small wind turbines have various kinds of control systems that act also as elements of limitation and protection. These are the types of control more applied:

7.1.1 Pitch control

Pitch-regulated wind turbines have an active control system that can vary the pitch angle (turn the blade around its own axis) of the turbine blades to decrease the torque produced by the blades in a fixed-speed turbine and to decrease the rotational speed in variable-speed turbines. This involves an active control system to sense blade position, measure output power and change the blade pitch when necessary.

In the figure 7.1 we can see the difference in the output power vs the wind speed between the Stall and Pitch controlled wind turbines.

7.1.2 Stall control

In stall-regulated wind turbines, the blades are designed in order to decrease the power production (decreasing the aerodynamic torque) with increasing wind speed above a certain value. The blades are designed so that they will perform worse (in terms of energy extraction) in high wind speeds to protect the wind turbine without the need of any active control. Decrease in power with increasing wind speeds is due to aerodynamic effects on the turbine blades.

In this situation the lift decreases providing separated flow from the airfoil and produces aerodynamic looses. Because when the unperturbed wind speed is too hight the angle of attack increases and the lift decreases and with it, it is possible to control the blade rotation and limit power in high wind speeds.

This is a very reliable mechanism because it does not need any moving part, so that it is, more robust and, therefore it will have fewer failures.

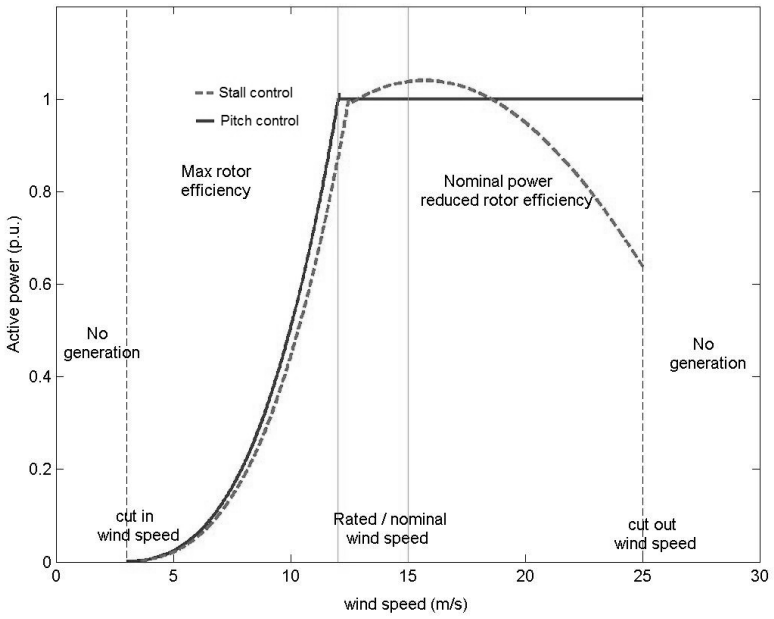

Figure 7.1: Difference in the output power vs the wind speed between the Stall and Pitch control. Figure from [43].

7.1.3 Furling

Furling is a passive mechanism used to limit the torque and the output power of small wind turbines in strong winds. This is the most frequently used mechanism [44]. At high wind speeds, the output power of the wind turbine can go above of the limits of wind turbine design, that is, the electronic devices or the generator. When this occurs, small wind turbines use mechanical control to turn the rotor out of the perpendicular direction of the wind, reducing the exposed rotor surface.

In the figure 7.2 an overview of the operating principles of a furling system can be seen.

This mechanism attends to a lot of different applications such as: breaking the rotor for maintenance, protecting the components of the generator in high wind speeds, reduces the cost of the tower and rotor, and adjusts the generated power as it goes increasing the wind speed.

7.1.4 Control with power converter

The control with power converter is a new system. This is based on power electronics, estimating the theoretical behaviour of the machine. It is a complicated and not robust nor reliable mechanism, so there is no point in focusing in this kind of control.

The two control mechanism that have been chosen are the stall control and furling. With the pitch control more failures could appear and so more maintenance might be needed, breaching one of the initial specifications. Due to the importance of the furling mechanism control, we have decided to explain it in a separated chapter, (Chapter 8, Yawing systems).

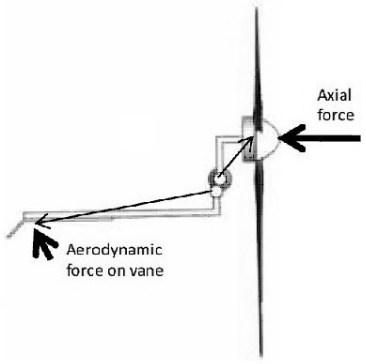

(a) Aerodynamic forces

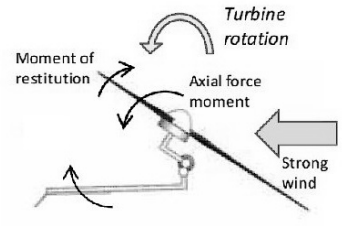

(b) Furling movement in strong winds

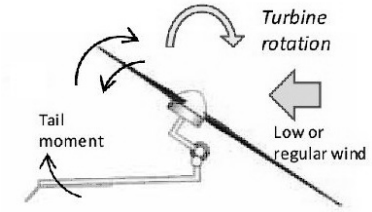

(c) Restitution of normal (aligned) operation upon reduction of the wind speed

Figure 7.2: Overview of the operating principles of a furling system. Figure from [44].

7.2 Control of the batteries charging

This element will be explained in Chapter 9, Electronics and conversion systems. The charging of batteries is controlled by the a charge controller (see Charge controller 9.2).

7.3 Breaking system

Sometimes the breaking system is used in stead of the furling system. But in this case, our purpose is to use it in order to block the rotor when maintenance or reparation. The breaking system will be explained in Chapter 9 Electronics and conversion systems (see Short - circuit break 9.5).

Chapter 8

Yawing system. Design, analysis and manufacture

The yaw system is responsible to rotate the nacelle around the tower axis. This system has different functions in the wind turbine:

- Increase the energy capture by pointing the rotor swept area steadily towards the incoming wind direction and thus maximize the general power input of the wind turbine
- Reduction of the structural load by letting the nacelle passively rotate. This rotation is in order to compensate yaw moments from aerodynamic loads.
- Control of the output power of the wind turbine, pointing the rotor swept area inclined from the incoming wind direction. Ass we mentioned in Chapter 7 Control.

8.1 Types of yawing systems

Roughly it can be said that there are two kinds of yawing systems:

- Active yawing system
- Passive yawing system

8.1.1 Active yawing system

The active yaw systems are equipped with some sort of torque producing device able to rotate the nacelle of the wind turbine around the tower based on signals from wind direction sensors. The various components of the modern active yaw systems vary depending on the design characteristics but all the active yaw systems include: rotatable connection between nacelle and tower (yaw bearing), an active variation of the rotor orientation (yaw drive), a restricting the rotation of the nacelle (yaw brake) and a control system which processes the signals from wind direction sensors (wind vanes) and gives the proper commands to the actuating mechanisms. In fig. 8.1 we can see an example of an active yaw system.

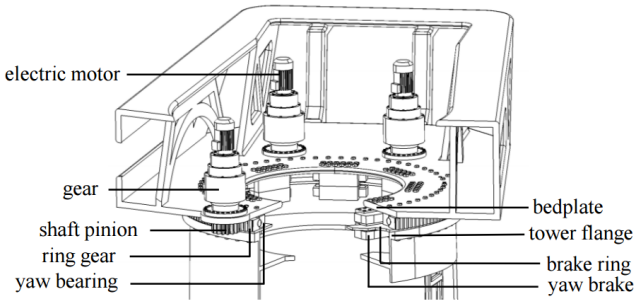

Figure 8.1: Example of an active yaw system. Figure from [45].

8.1.2 Passive yawing system

The passive yaw systems use the wind force in order to adjust the orientation of the wind turbine rotor into the wind. In their simplest form these system are comprise by a simple roller bearing connection between the tower and the nacelle and a tail fin mounted on the nacelle. This tail is designed to turn the wind turbine rotor into the wind by exerting a torque to the nacelle. Therefore the power of the wind is responsible for the rotor rotation and the nacelle orientation. Alternatively in case of downwind turbines the tail fin is not necessary since the rotor itself is able to point the nacelle into the wind.

The tail is commonly used for small wind turbines since it offers a low cost and reliable solution. It is, however, unable to cope with the high moments required to yaw the nacelle of a large wind turbine.

Passive yaw systems have to be designed in a way that the nacelle does not follow the sudden changes in wind direction with too fast a yaw movement, in order to avoid high gyroscopic loads.

In fig. 8.2 an example of a passive yawing system can be seen.

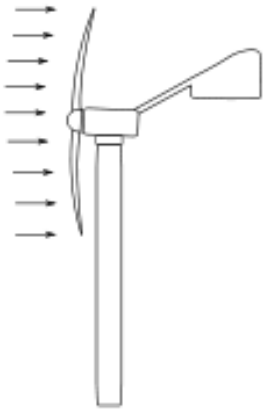

Figure 8.2: Example of a passive yaw system with a tail and a vane.

8.2 Choice

The most suitable kind of yaw system for small wind turbines is the passive one. In this case, as the price and the simplicity of the mechanism have to be taken into account too, the choice is easy to make.

8.3 Design and materials

The design of the yawing system is based on the book [27]. The tail and the vane can also be designed in order to control the output power of the whole wind turbine and to protect itself from overload. In this case, this is the way that has been chosen (a furling system), so the design of the yawing system has to take into account this ability too.

8.3.1 Yaw bearing

The yaw bearing is the connection between the nacelle and the tower. This element consists of two pieces of steel pipe, one inside of the other. We can see a sketch in fig. 8.3b. The recommended sizes of steel pipes for the yaw bearing can be seen in table 8.1 and in the subsection of manufacturing how to build it is going to be explained.

8.3.2 Tail

The tail consists of a plywood vane bolted to steel flat bars on a steel pipe. The tail has two functions. On the one hand, it has to have a large enough area to control the blades and overcome their tendency to turn away or the turbine will never be able to face the wind. As the wind gets stronger, the thrust force on the blades increases but so does the force on the tail, so the wind turbine keeps facing the wind.

On the other hand, at a chosen level of wind thrust (in this case the thrust generated at a wind speed around 10 m/s), the tail can no longer hold the turbine facing squarely into the wind. It swings, allowing the turbine to face away from the wind. For a correct furling what matters is the weight of the tail and its length. By making the tail heavier you can delay the furling and drive the turbine harder in stronger winds. A turbine with a light tail will furl sooner but therefore, produce less.

When the machine is furling, the blades continue turning and producing power but as the effective area is smaller the torque and so the output power decreases.

In fig. 8.3 and table 8.1 we can see the dimensions required to achieve the two functions of the tail and the vane in our turbine design.

Table 8.1: Steel pipe dimensions for the tail see fig. 8.3. Data from [28].

Boom	Length A	800 mm
	Diameter B	48.3 mm
Hinge outer	Length C	100 mm
	Diameter D	60.3 mm
Hinge inner	Length E	150 mm
	Diameter F	48.3 mm

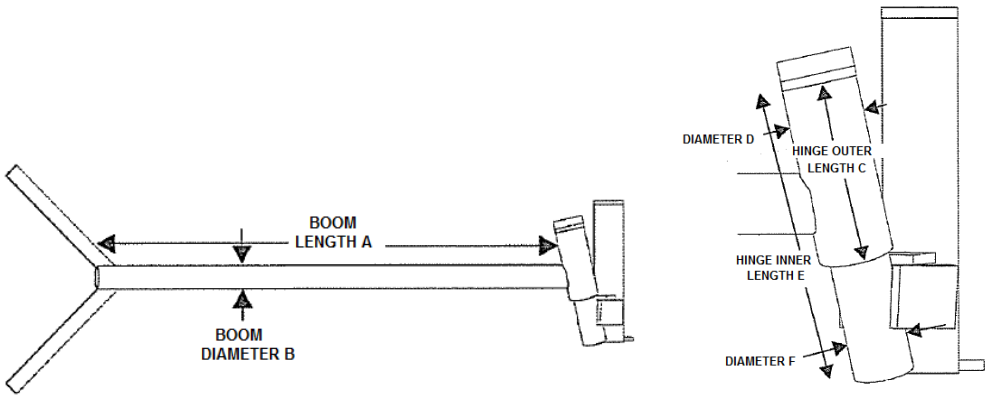

(a) Steel pipe for the tail (b) Yaw bearing

Figure 8.3: Tail boom. Figure from [28]. A clarifying sketch for table 8.1.

8.3.3 Tail vane and brackets

The tail vane can have any shape that the user wants, but it is important to bear in mind that the weight and the area of the tail controls the way the wind turbine behaves, so it is recommended to manufacture it using the size in table 8.2. About the brackets, the most used angle is 70º.

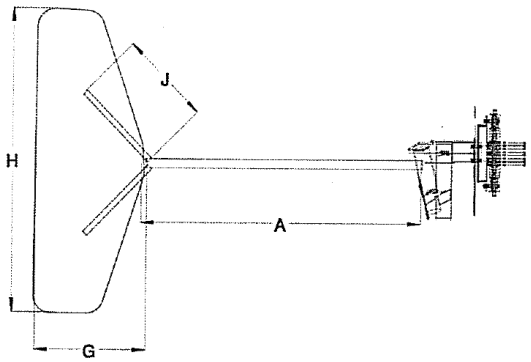

Figure 8.4: A sketch of the tail vane and brackets. Figure from [28]

Table 8.2: Dimensions of the tail vane and brackets see fig. 8.4. Data from [28].

Tail vane area GxH	40 x 100 cm
Thickness of plywood	6 mm
Brackets section	8 x 30 mm
Length of each flatbar J	Two at 30 cm

8.4 Manufacture

We have already talked about the geometry and the dimensions of each part of the yawing system. But now what has to be taken into account is how to manufacture and to assemble it.

The most important here is that there are some angles and some security issues that have to take into account when the manufacturing. The alternator frame is mounted onto the yaw bearing off-centre; this is in order to create a 'yawing moment'. To balance this tendency and to keep the turbine facing squarely into the wind under most conditions, the tail is deliberately angled 20° to the opposite side, see fig. 8.5. Another angle that has to be taken into account is the angle of 55° between alternator frame and the horizontal, this angle is in order to let the wind turbine rotate more smoothly in high variations of wind speed [27]. A good way to set it up when welding is to prop the frame of the machine up on the bench or the floor at 55 degrees to the horizontal and weld the tail hinge pipe on in a vertical plane, as we can see in fig. 8.6.

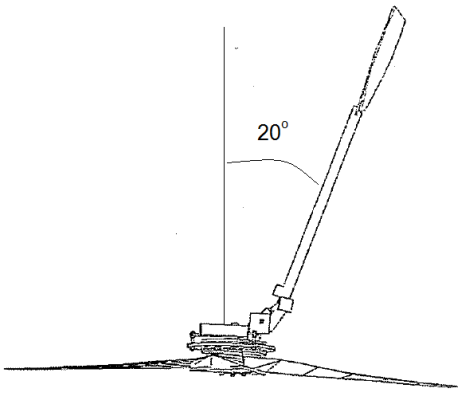

Figure 8.5: A top view of the wind turbine, where we can see the angle between the nacelle and the tail. Adapted figure from [28].

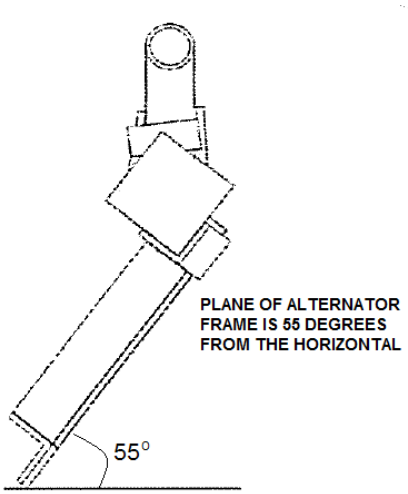

Figure 8.6: Angle between the alternator frame and the horizontal. Figure from [28].

For the security issues there are two things to bear in mind: on the one hand, that the outer pipe of the hinge needs a cap of steel plate on the top that can rest on the top of the inner pipe and also to keep rain out of the pipes. And on the other hand, the range of movement of the tail has to be limited, to do so there are some pieces of steel that have to be welded in order to stop the tail between the boom and the yaw pipe to prevent it swinging too far up into the blade.

Chapter 9

Electronics and conversion systems. Design analysis and manufacture

As the wind turbine design will be used in an off-grid installation, there are various subjects to take into account in the design of the installation and the signal conditioning. In this chapter, some electronic devices are designed, that not only condition the signal, but also to protect the machine, the batteries and, above all, the people. A scheme of the electronic system we are going to design is shown fig. 9.1:

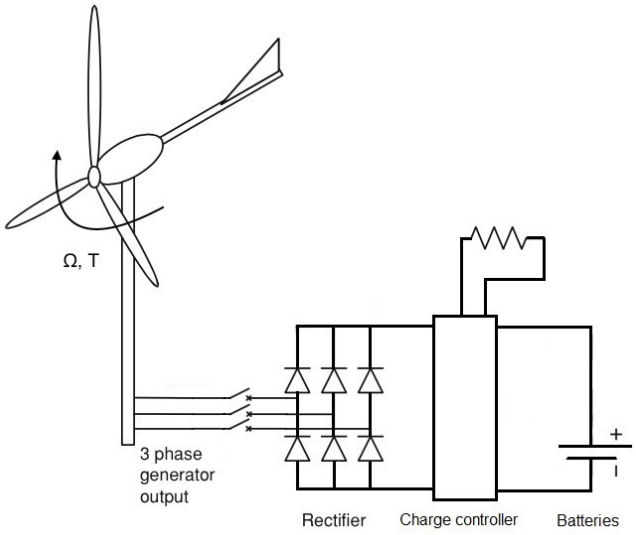

Figure 9.1: Scheme of the electronic system. Adapted figure from [42].

As we can see in fig. 9.1, all the energy generated is accumulated in the batteries. We recall that voltage of the batteries is 24 V. The installation capacity varies from one installation to another. Because it is an off-grid installation, we have to take into account that there could be some days without wind, and hence, without energy. That is what we have to have in mind calculating the storage capacity of the batteries.

We have decided to charge batteries because it is the simplest and cheapest way to store energy. The idea of having a rectifier (to pass the energy from AC to DC) and after that an inverter (to pass it from DC to AC) was considered but it was difficult to calculate

how much energy would they need and what to do with that energy when nothing is installed and when there is no wind. In addition, with this kind of electronic system, a controller should be needed to maintain the frequency in 50 Hz and the voltage in 220 V. Besides, the inverter is not robust enough to use in a country in development. According to [45] that system is usually the one that has the most of failures.

What we want to achieve is to charge batteries when there is wind and to use that energy whenever the user wants. Having more than one battery, the user obtains more independence, because when one is charging, the other one could be being used and vice versa. Above all, the user could have an energy supply when there is no wind.

In this kind of installations off-grid it is also normal to see various types of generation sources like photovoltaic or hydroelectric, combining them when one of the natural sources is not enough for the required energy.

First of all, there is one issue that is going to limit all the design of the signal conditioning. Because we do not have any controller, and as we have discussed during Chapter 5 Rotor, the rotational speed of the magnetic rotor of the generator, and so, of the rotor will be constant. But some electronic device has to control the charging of the batteries. This device is the charging controller. We are going to explain each component one by one.

9.1 Rectifier

The rectifier is an electrical device that converts alternating current (AC), in direct current (DC). The process is known as rectification. There are various ways of rectifying the current, but the one we are going to explain here is the simplest and cheapest one, and so, the one that is the most interesting for our project: the diodes bridge or more commonly named as bridge rectifier.

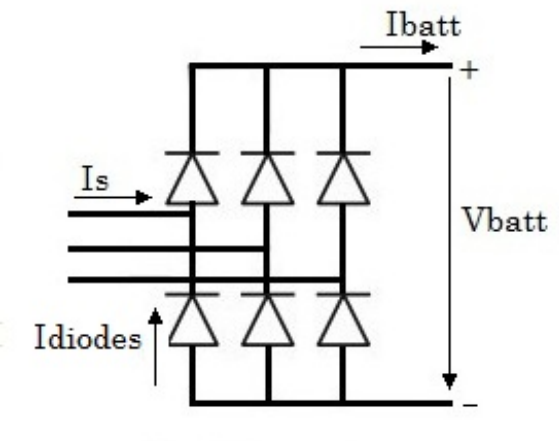

Figure 9.2: Diodes bridge. Adapted figure from [42].

To design this device we have to take into account the intensity in DC in the batteries. Once we know the maximum intensity in DC we have to confirm that the coils of the generator can bear that amount of intensity.

First of all, to know the intensity in DC in the batteries, the nominal power and the tension in the batteries have to be known. In this case, we have P_{nom} = 380 W and V_{batt} = 24 V.

$$\frac{P_{nom}}{V_{batt}} = I_{battmax} \rightarrow I_{battmax} = \frac{380W}{24V} = 15.83 \text{ A} \tag{9.1}$$

where: P_{nom} = Nominal Power, V_{batt} = Tension in the batteries, $I_{battmax}$ = Maximum intensity in the batteries.

As we can see in Chapter 2 of the book [46], the average value of the intensity in the diodes is:

$$I_{diodes} = \frac{1}{3} * I_{batttmax} \rightarrow I_{diodes} = \frac{15.83}{3} = 5.27 \text{ A} \tag{9.2}$$

where, as we can see in the figure 9.2: I_{diodes} = Intensity in the diodes.

As we have to design the rectifier keeping in mind that it can support the maximum intensity and without oversizeing it, we have to purchase diodes that can accept that intensity. But, the question is if the wires of the coils in the generator can accept that too.

In the design of the coils in the stator of the generator (Chapter 6, Generator, equations (6.24) and (6.23)) we design the area of the wire with which the coils have to be made. However, the surface of these wires also gives the maximum intensity they can accept without melting or developing any failure. In this case, the surface of the coils is: S = 1.77 mm^2 where we used Table 1 from the ITC-BT 19 (Instrucciones Técnicas Complementarias Baja Tensión sección 19), the normative book in Spain, we can see what is the maximum intensity that these wires can accept is 15 A. Therefore they will be able to accept the maximum intensity.

We have made some simplifications to know the intensity in the batteries. We have supposed the rectified tension between the terminals to be constant, and equal to the tension in vacuum. That is because the batteries impose their tension, so they impose the speed of the wind turbine too, decreasing the efficiency of the system.

Making this supposition we do not make a large mistake. As we can see in the fig. 9.3, if the impedance and the resistance of the system and the intensity are very small (in the case of this generator it is), we can say that both voltages are more or less the same.

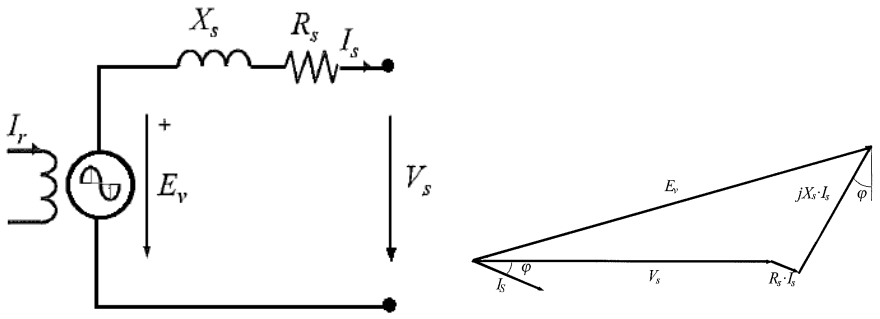

(a) Equivalent circuit of the synchronous machine

(b) Phase diagram of 9.3a

Figure 9.3: Equivalent circuit and it phase diagram.

Equation (9.1) is the simple way of calculating the maximum intensity is going to go

throw the cables. In reality, the equation is much more complicated because the whole wind turbine is involved. We could say that, the intensity is the one in the equation (9.3):

$$I_r = \frac{E_v - (V_{batt} + V_{rect})}{Z_s} \tag{9.3}$$

where: E_v = Voltage in vacuum, V_{batt} = Voltage in the batteries, V_{rect} = Voltage drop in the rectifier, Z_s = Impedance of the stator.

As we know from Chapter 6, Generator in equation (6.21) the E_v is dependent on the rotational speed of the generator:

$$E_v = 2B_g S_{tm} \Omega N_s \sqrt{3}\pi/2$$

If we consider both equations (9.3) and (9.1) and take into account, that the rotational speed of the generator does not change, the E_v would be constant and so, the intensity too. This is false. This is the mistake we make saying that the tension in vacuum and the tension in the terminals is the same. The only way of solving this problem would be simulating the whole wind turbine with some programme like PSIM or SIMPOWER. About this field, we think we do not need to do that, because what we want is to design the diodes and not to know exactly the intensity generated.

Apart from simulating the whole wind turbine with a programme, another way of improving this device would be installing a current controller or a speed controller, but taking into account the goals of this project it has no sense, because it would be more difficult to understand, make and less hard or robust, which is one of the initial specifications.

9.2 Charge controller

A charge controller is an essential part of any wind system to ensure the batteries are not overcharged or undercharged. This device monitors the battery voltage and switches them off when they are fully charged, or switches them back on charge when they reach a pre-set level of discharge. In particular they protect the batteries from overcharging, subsequent gassing, loss of electrolyte and possible plate damage. The overvoltage can reduce battery performance or lifespan, and may pose a safety risk. That is one of the reasons why it is important to have a charge controller.

It is not difficult to make a homemade charge controller, because the components needed are easy to find and the circuit is not really difficult to understand.There are some good explanations of how to manufacture a homemade charge controller in the bibliography. The one we have chosen [47] is one of the most interesting, because it is made by simple elements which you can find everywhere. An scheme of the circuit is in the figure 9.4.

As we can see in the figure 9.4, the components required are:

- IC1 - 7805 5 Volt positive Voltage Regulator
- IC2 - NE555 Timer Chip
- PB1, PB2 - NO Momentary Contact Push Buttons
- LED1 - Green LED
- LED2 - Yellow LED
- RLY1 - 40 A SPDT Automotive Relay
- D1 - 1N4001 or similar
- R1, R2 - 10K Multi-Turn Trim-Pots
- R3, R4, R5 - 1 KΩ 1/8 W 10%

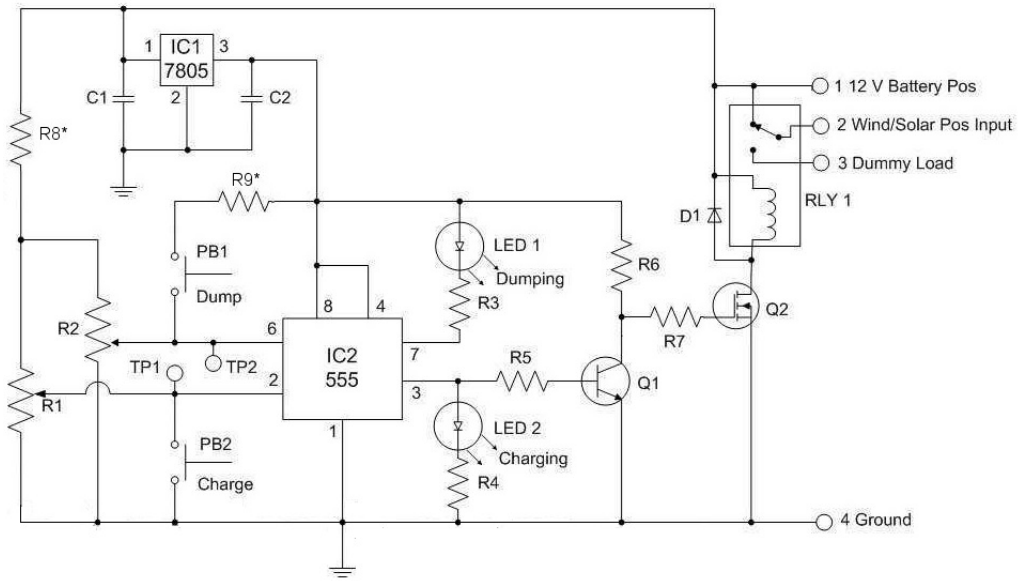

Figure 9.4: An electronic scheme of a 555 based, homemade charge controller. Figure from [47].

- R6 - 330 Ω 1/8 W 10%
- R7 - 100 Ω 1/8 W 10%
- Q1 - 2N2222 Or Similar NPN Transistor
- Q2 - IRF540 Or Similar Power MOSFET
- C1 - 0.33 μF 35 V 10%
- C2 - 0.1 μF 35 V 10%
- R8*-R9* - Optional 330 Ω 1/2 W Resistors

9.3 Dispenser-resistance

When the batteries are completely charged and the wind turbine keeps generating energy, that energy needs to be dumped. This is the goal of this resistance. The charge controller is the element that controls where is going to go the intensity, that is, if the batteries are completely charged or the intensity is too hight to them, the intensity would go to the resistance to waste that amount of energy. If we place the resistance in a tub with water, we could heat it and so, do not throw any energy, but convert that energy in heat.

9.4 Batteries

The energy generated by the wind turbine can be consumed directly or it could be stored in batteries. The storage capacity changes for every installation. In an off-grid installation the lack of wind has to be taken into account. It could happen that during some days the production of energy it is not enough and therefore, the batteries have to have autonomy of various days. It is known that the cost of the batteries is very high so the storage capacity has to be well calculated and the choice of the kind of battery has to be, also, carefully elected. In the market there are lots of different kinds of batteries such us lead - acid, alkaline, (Ni-Fe) or (Ni-Cd). Because of the goals of this project, the most suitable

ones are the lead - acid batteries.

9.4.1 Lead - acid batteries.

These kind of batteries can be easily found. This is because despite of having a very low energy-to-weight ratio and a low energy-to-volume ratio, its ability to supply high surge currents means that the cells have a relatively large power-to-weight ratio. These features, along with their low cost, make them attractive for use in motor vehicles. So that, they can be found easily and be cheap or completely free if you use the battery of a broken car.

Nevertheless, the charge and discharge transformation in this kind of batteries cannot be repeated indefinitely. After a while, the lead sulphate forms crystals, and it is not possible to reverse the process. It is at this point where the battery is sulphated and it is no longer possible to use it again.

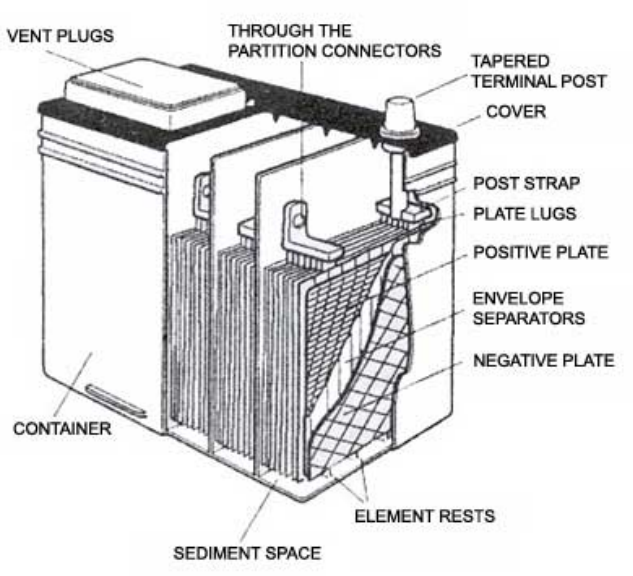

Figure 9.5: Internal and external structure of the lead - acid battery of one car.

This kind of batteries are generated by small batteries of 2 V, connecting them in series forming the storage capacity wanted. In the figure 9.5 we can see the internal and external structure of one car. There, we can see that the cells are connected in series. There are negative and positive lead plates too, the positive electrode (cathode) typically consists of pure lead dioxide supported on a metallic grid, whereas the negative electrode (anode) consists of a grid of metallic lead alloy containing various elemental additives that includes one or more of the following and sometimes others not mentioned, antimony, calcium, arsenic, copper, tin, strontium, aluminum, selenium and more recently bismuth and silver.

The plates are immersed in a liquid electrolyte consisting of 35% sulfuric acid and 65% water. It is the electrolyte that facilitates the chemical reactions that enable the storage and discharge of electrical energy and permit the passage of electrons that provide the current flow.

We can see graphically the voltage vs the state of charge of a 12 V lead - acid battery while they are under charge and discharge in the figure 9.6. There we can see that, although the battery is completely discharged, there is always at least 10 V of voltage. That is what we talked about during Chapter 6 Generator.

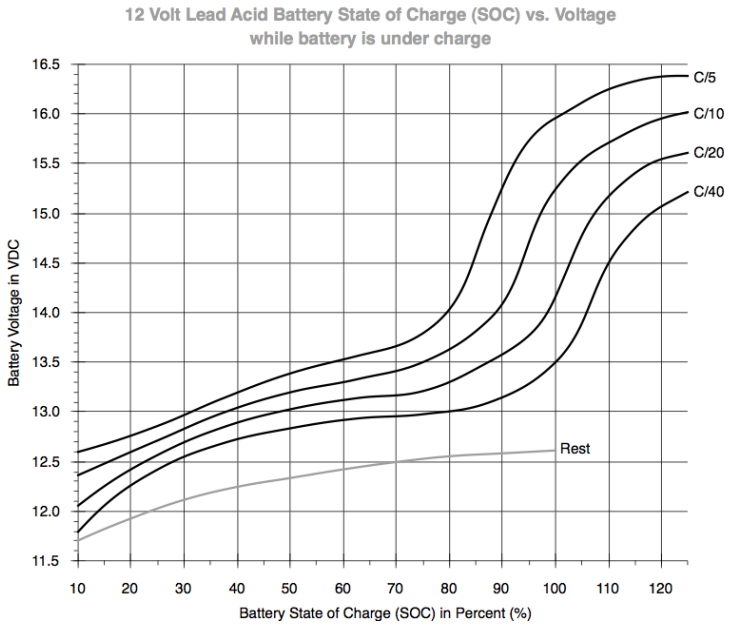

(a) Charge of a 12 V lead - acid battery.

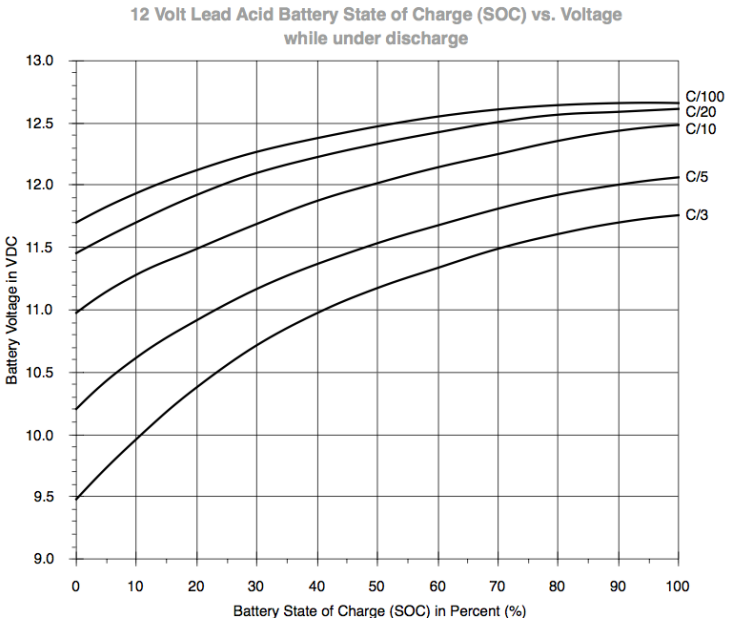

(b) Discharge of a 12 V lead - acid battery.

Figure 9.6: 12 V lead - acid battery state of charge (SOC) vs Voltage while the batteries are under charge (9.6a) and under discharge (9.6b). Figures from [48].

The car batteries have a voltage of 12 V. The lower is this voltage in the output of the wind turbine, the higher are the intensity in the rectifier, the charge controller, the stator and in the batteries, so, the loses in heat and, therefore, in energy will be more.

This is the reason why we have decided to rise the voltage in the output, in this case 24 V. To achieve that, we have to connect two car batteries in series. Normally, the capacity of the batteries is around 55 Ah, this indicates that to be completely discharged, a current of 55 A has to be extracted during 1 hour or that it can give a current of 1 A during 55

hours.

So, as we have put them in series, the capacity is not going to change, but the voltage is going to be 24 V and the stored energy will be twice more:

$$E_{batt} = V_{batt} * Ih = 12 * 2 * 55 = 1320 \text{ Wh} \tag{9.4}$$

9.5 Short - circuit break

In fig. 9.1, a short - circuit break can be seen. This delay is used to break the wind turbine when there is no wind, because if there would be wind a big torque would appear and so, the blades could break. It can only be used to break the wind turbine when it is going to be repaired in order to gain more security and more control of the machine.

Chapter 10

Tower and foundation. Design and analysis

A wind turbine tower is not only a support structure, but also it raises the wind turbine so that the blades can reach the cleaner and stronger winds at higher elevations. As we know (equation 2.3), the power output from a wind turbine is a function of the cube of the wind speed, so even small increases in wind speed have a big impact on energy production.

Another reason for having a taller wind tower is the turbulence of the air. While at higher elevations the wind is generally less turbulent, at lower elevations it can often become quite turbulent, this is due to obstructions from obstacles like houses or trees.

So, as a general rule it is better to go for as high a tower as makes economic sense. But, in this case, besides the price of the tower, we have to take into account the manageability of it. Generally, the height of the turbine is related to its size. There are many types of towers in the market today, they vary in size and structure and are designed for each case.

10.1 Types of towers

Here there are the most used types of towers [17]:

10.1.1 Guyed tower

A guyed tower is a tall thin vertical structure that its stability depends on guy lines, diagonal tensioned cables attached to the ground. The mast itself can support its own weight, but usually does not have the shear strength to stand unsupported. There are usually three or four guy lines made of steel cable which run from the top of the tower to guy. They are often the cheapest type of wind towers, but it has to be considered the space they need in the base because of the wires extension.

10.1.2 Guyed Tilt-Up Tower

These are a type of guyed tower which have a pivot joint at the base, so it can be easy to raise or lower the tower to set it up or to do maintenance on the turbine later. They can cost slightly more than a traditional guyed tower [49] but can reduce the hassle of setting up the turbine and maintaining it. As in guyed towers there is also needed to have space for the guy wires, and besides a space to lay down the tower if it is necessary.

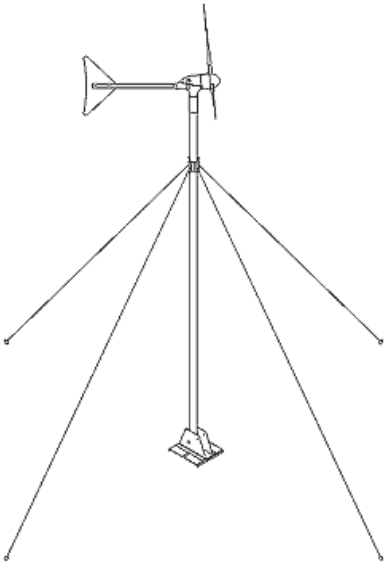

Figure 10.1: An example of a guyed tower. Figure from [17].

Figure 10.2: An example of a guyed tilt-up tower.

Figure 10.3: An example of a lattice tower.

10.1.3 Lattice tower

A lattice tower or truss tower is a freestanding framework tower. These kinds of towers were common in the past when the wind turbines were smaller, but are seldom used today.

They have the disadvantage that, as they use more material their cost is bigger than in the two previous ones, but the space necessary is less. The most important inconvenience is that these towers have a higher construction maintenance cost.

10.1.4 Tubular tower

Figure 10.4: An example of a tubular tower.

They are freestanding towers. These types of towers are constructed as a large tube often tapered at the base. For big wind turbines, they are the most commercialized towers. This is because the simplicity of its design. On most of them there is a ladder in the inside of the tube so that a worker can climb the tower to do repairs and maintenance on the turbine.

10.2 Choice of the tower

These machines above explained are the most common ones, but we have search about other kinds of towers and we have found another interesting one [50]: scissors tower. This tower has the simplicity of the Guyed Tilt-Up towers to set the machine up, the maintenance and cost, and the big advantages of the space they require, that is very low comparing to the guyed ones and the security in the lowering and rise of the turbine.

As we can see in fig. 10.5, the scissor tower has two differentiated parts, the first one is a support that is firmly anchored to the ground, with a concrete foundation, and the second one is a pipe structure. Between them there is a hinge that allows the central pipe structure to rotate about the support. With this kind of tower there is less risk when raising and lowering the machine because it is not going to fall to the floor, but it will hang on the support.

There is more to think and design about this part such us the diameters of the pipes, the materials, the length or volume of concrete necessary. But we will leave it for future work.

Figure 10.5: An example of a scissor tower

Chapter 11

Wind turbine design overview

	Name	characterisation
Nominal values	Peak power (wind speed 10 m/s)	620 W
	Average wind speed	6 m/s
	Speed rotation	240 rpm
	Scope of application	Out of grid rural areas
Operating speeds	Cut in point	3 m/s
	Cut out point	10 m/s
Rotor	Axis position	Horizontal
	Number of blades	3
	Position regarding the wind direction	Upwind
	Rotor radius	1.9 m
	Blade profile	No commercial design
	Blade materials	Wood/PVC pipes
Generator	Type	Axial-flux permanent magnet
	Number of phases	3
	Coils per phase	2
	Number of turns per coil	120
	Output voltage	25.4 V
Yawing system	Type	Passive system
	Vane area	0.4 m^2
	Materials	Steel and wood
Electronics and conversion system	Rectifier	6 Diodes > 5.27 A
	Voltage drop in the rectifier	1.4 V
	Charger controller	555 Based charger controller
	Batteries type	Lead - Acid batteries (Car battery)
	Number of batteries	2
	Voltage of batteries	12 V
	Type of batteries connection	Serie
Control	Number of controls	2
	Type	Stall
	Type	Furling
Tower and foundation	Type	Scissors tower
	Height	6 - 8 m, depending on the environment

Chapter 12

Safety and real practical shift

12.1 Environmental and social study

12.1.1 Environmental impact of wind energy

It is difficult to quantify the contamination generated by a wind turbine. On the one hand, it is difficult to evaluate the emissions generated during the whole process of the fabrication of the machine, because it has to take into account the material used and the energy spent during the process. On the other hand, it is more difficult to do so if we have to extrapolate the data to another country, because it has a lot of variation from one place to another [51]. According to [52], commercial wind turbines contaminate a median value of between 12 and 11 (g CO_2eq / kWh), in this case as we use recycled material it will be lower.

12.1.2 Interactions with fauna

There are two kind of risk in this section, the risk the wind turbine can cause in the fauna and vice versa.

On the one hand, the risks to birds caused by wind turbines are above all, because of collisions with blades or tower. Normally, in big wind farms it has to take into account the migration routes of those animals, but in this case, because of the small size of the machine there is no point in doing so. Also, it has to take into account the risk to the wind turbine caused by the animals in the site where it is placed. Sometimes, these machines are placed in fields where the cows or the cattle grazes. They can bump into it, so that, we purpose to circle the wind turbine with a barbed wire, and thanks of that, we avoid animals to reach the tower of the machine.

12.1.3 Interactions with humans

Visual impact

Regarding to visual impact, it is difficult to evaluate it, because it depends on the people perception and the needs. But in general way, it is thought that these machines are ugly and deteriorate the landscape. In order to avoid the negative visual effect the wind turbine could be painted in a suitable color and taking into account the orography of the place.

Noise

There are two sources of the noise. Mechanic origin, that in this case it only depends on the design of the generator, and aerodynamic origin that some parameters have to be taken into account: the rotational speed, the material of the blades, wind speed and its turbulence and the number of blades. The noise generated by a small power wind turbine is almost negligible because the blades are small and when the wind rises, the noise of the wind turbine too. But this is misrepresented because of the noise generated by the wind in trees or other obstacles in the area.

Possible damage to people

It is better to place the wind turbine in an area far away from the rural one, because of the noise, and because of the possible damage to people. If the wind turbine is circled with barbed wire the children could damage themselves. If there is any problem with the wind turbine and this falls down, we talk in the section 5.6. Tower and foundations that it would hang, but just in case, the machines falls completely down it is better to have it far away from the places where usually are people.

12.2 Maintenance

Amongst the maintenance works, it has to make a distinction between the preventive and corrective maintenance.

In this case, we are going to talk about the preventive maintenance, it recommended to make these annual inspections:

- Blade inspection
- Axis inspection
- Generator inspection
- Grease the connection between the tower and the generator.
- Electrical connections inspection

Chapter 13

Estimated budget

The budget can be split up in four main blocks: material for the manufacturing of the wind turbine, material for the construction of the templates and mould, the cost of the energy spent in the process and the cost of the hours of work in the fabrication and assemblage.

We are not going to take into account neither the cost of the energy spent in the process nor the hours of work in the design, fabrication and assemblage. About the energy spent, we do not know exactly the working conditions they will have. Maybe they only work during the day and the tools they use are not electric, so the cost of energy will be null or very low. Or just the contrary, but the energy spent in the process is not too high so the cost of it will be small. About the design, we are not going to collect money for it. And the fabrication and assemblage hours, they are themselves who build it, so they do not have to pay anything for it.

Although the prices of the material will change for one country to another, this is the estimated budget for the whole wind turbine [35]. The prices data have been rounded from the ones from Amazon or Ebay:

Table 13.1: Estimated budget of the materials for the manufacturing of the wind turbine

Material	**Quantity**	**Price**	**Total price (€)**
Generator			
Grout	2 kg	6 €/ kg	12
Talcum powder	1.5 kg	2 €/ kg	3
Fiberglass fabric	1 m^2	2.5€/ m^2	2.5
Brake disc	2	-	-
Magnets	8	17 €/ 20Pcs	7
Anti-rust paint	1Pcs	5 €/ 1Pcs	5
Cooper wire	1.5 kg	10 €/ kg	15
Elastic cable	20 m	0.30 €/ m	6
Tin wire	1 m	2 €/ m	2

Continues in the next page

Material	Quantity	Price	Total price (€)
Rotor			
PVC pipe (250 mm diameter)	1.5 m	39 €/3 m	19.5
Wooden plate	1 m^2	1 €/ m^2	1
Screws M6	9	2.5 €/ 25Pcs	0.9
Nuts M6	24	10 €/ 100Pcs	2.4
Paper for the templates	4	0.05 €/ paper	0.2
Tower and mechanic parts			
Steel pipe (48.3 mm)	800 mm	10 €/ m	5
Steel pipe (60.3 mm)	100 mm	10 €/ m	6
Angled steel (30x30x5) mm	300 mm	20 €/ m	6
Wooden plate (400x1000x6) mm	1	1 €/ m^2	1
Steel pipe 7 m)	1	10 €/ m	70
Nacelle			
Car hub	1	-	-
Angle steel (50x50x6) mm	649 mm	30 €/ m	20
Steel plates	some mm^2	-	-
Screws M6	7	2.5 €/ 25Pcs	0.7
Nuts M6	30	10 €/ 100Pcs	3
Bolts M12	4	2.5 €/ 10Pcs	1
Nuts M12	16	6 €/ 100Pcs	1
Electronic and control			
Batteries	2	-	-
Diodes 6A	6	3 €/ 10Pcs	1.8
Cable	5 m	0.3 €/ m	1.5
Resistance	1	5 €	5
Charge controller			
7805 5 V Regulator	1	5 €	5
NE555 Timer Chip	1	7 €/ 10Pcs	0.7
Green LED	1	7 €/ 10Pcs	0.7
Yellow LED	1	7 €/ 10Pcs	0.7
40 A SPDT Automotive Relay	1	3 €	3
1N4001	1	6 €/ 100Pcs	0.06
10K potentiometer	2	2 €/ 50Pcs	0.08
1 KΩ 1/8 W 10%	1	1 €/ 50Pcs	0.02
330 Ω 1/8 W 10%	1	1 €/ 50Pcs	0.02
100 Ω 1/8 W 10%	1	1 €/ 50Pcs	0.02
2N2222	1	1€/ 50Pcs	0.02
IRF540	1	2.5€/ 10Pcs	0.25
0.33 μF 35 V 10% capacitor	1	2 €/ 10Pcs	0.2
0.1 μF 35 V 10% capacitor	1	2 €/ 10Pcs	0.2
330 Ω 1/2 W Resistors	2	5 €/ 100Pcs	0.1
TOTAL			209.57

Table 13.2: Estimated budget of the materials for the templates and mould

Material	**Quantity**	**Price**	**Total price (€)**
Coil winder			
Plywood (100x75x12) mm	3	6.5 €/ 1Pcs (300x300x12) mm	6.5
Nails M5 100 mm	4	8 €/ 100Pcs.	0.32
Stud M10 150mm	1	6.5 €/ 4Pcs	1.625
Nuts and washers M10	5	2.42 €/ 100Pcs	0.121
Stator of the generator			
Plywood (600x600x13) mm	1	7 €/ 1Pcs	7
Board (600x600x19) mm	2	25 €/ 2Pcs	12.5
Bolts M6 35 mm	3	3 €/ 10Pcs	0.9
Screws	10	2.5 €/ 25Pcs	1
Rotor: magnet-positioning jig			
Plywood (300x300x6) mm	1	5 €/ 1Pcs	5
TOTAL			34.97

Table 13.3: Total estimated budget

Budget	**€**
Materials for the templates and mould	34.97
Materials for the manufacturing of the wind turbine	209.57
TOTAL	244.54

Chapter 14

Conclusions

During this project the process of design and manufacture of a small wind generation system for charging batteries has been developed. Although we have designed a specific wind turbine, we wanted to show the way of designing it, in order to allow someone to change the design according to its necessities.

To do so, we started analyzing the main characteristics of population and wind resource in order to acquire knowledge and to collect data. After that, it was been evaluated, giving a first idea to the designer of the layout requirements.

We studied one way of collecting data: anemometric analysis. Helped by some data already recorded in Africa, we started the first dimensioning and hypothesis about the measurements of the machine.

Once this thesis is completed, we can extract some conclusions in the execution of this project in relation to construction, cost and operation.

On the one hand, the simplicity of its manufacturing and on the other hand its easy and cheap acquisition of the materials in Africa used. Making it possible for the inhabitants in Africa with a few knowledge and facilities, to manufacture and to maintain their own wind turbine with the confidence of a good performance and lifetime.

Regarding to the economic cost of acquiring this wind turbine, one should mention that the cost here studied is only of the materials used and not of the labor hours.

We have talked about the different components in a wind turbine. There are improvements in all of these components, leaving these studies for future work, in case someone would like to continue with it.

Although we have manufactured a rotor with PVC pipes, in this project we have focused above all in the theoretical analysis of the design of the machine leaving the practical work for the course we did in Valence, where we manufactured and studied a whole wind turbine.

About the future work of the rotor, we have mentioned that an optimization loop should be done, to ensure that the blades designed are the best ones that can be manufactured from a PVC pipe.

Besides, we concluded that the rural electrification cannot be a laboratory, the robustness and reliability of the components, in other words the security, should always prevail over the new technologies.

Finally, we have to mention that during the realization of this project, not only we have acquire knowledge about all the subjects in relation to the engineering, but also we have learn how to use office automation programs such as Latex and another interesting software like FEMM or Autocad Inventor. Besides, we have to point out, we have learnt to use some different manufacturing equipment, such as milling, saw blade, welding machine

and amount of carpentry tools.

We want to highline that the elaboration of this project is rewarding for both, technical and personal aspects.

Bibliography

[1] Khalid Malik. Human development report 2013. *The rise of the south: human progress in a diverse world*, 2013.

[2] World Data Bank. *http://databank.worldbank.org.*

[3] *Human Development Index and its measurements.* *http* : *//es.slideshare.net/arslan$_b$zu/human − development − index.*

[4] United Nations. Department of Economic. *The Millennium Development Goals Report 2014.* United Nations Publications, 2014.

[5] IEA (International Energy Agency). *World Energy Outlook 2011.* OECD/IEA Paris, 2011.

[6] *http://www.fondationensemble.org/projet/sunnymoney-microsolar-project/.*

[7] *http://www.ruralelec.org.*

[8] Subhes C Bhattacharyya. *Energy Economics.* Springer, 2011.

[9] Nganga Marc Wohlert Matt Woods Nairobi, Kenya: Joseph. *Friends of the earth*, 2012.

[10] Lauha Fried. Global wind statistics 2014. *Report, Global Wind Energy Council (GWEC), Brussels, Belgium*, 2015.

[11] Alli D Mukasa, Emelly Mutambatsere, Yannis Arvanitis, and Thouraya Triki. *Development of Wind Energy in Africa.* African Development Bank, 2013.

[12] Thewindpower.net.

[13] Bruno Domenech Léga, Laia Ferrer Martí, and Rafael Pastor. Metodología para el diseño de sistemas de electrificación autónomos para comunidades rurales. Master's thesis, Universitat Politècnica de Catalunya, 2013.

[14] International Energy Agency. Energy in sub-saharian africa today. *World Energy Outlook 2014 Factsheet*, 2014.

[15] Gyan Ganga Institute of Technology and Sciences. Solar power - 1kw system energy generation study and cost calculation. *International Journal of Electrical and Electronics Engineering (IJEEE)*, 2014.

[16] IRENA (International Renewable Energy Agency). *irena.org.*

[17] *Course of Tecnología Energética. Eólica.* Universidad Pública de Navarra, 2014.

[18] *Frecuently Asqued Questions (FAQ) of Ropatec Vertical Energy.* http://www.ropatec.it/content/FAQ/19/en.

[19] Datosclima. *http://datosclima.es/Vientostad.php.*

[20] *Course of Energias Renovables.* Univeridad del Pais Vasco, 2014.

[21] Dennis G Shepherd. Historical development of the windmill. 1990.

[22] Senvion SE (Wind Energy Solutions). *http://www.senvion.com/.*

[23] William Kamkwamba, Bryan Mealer, and Elizabeth Zunon. *The boy who harnessed the wind.* Dial Books for Young Readers, 2012.

[24] Joaquin Navasquillo Hervas. *http://www.uv.es/navasqui/.*

[25] Build Your Own 10 Foot Diameter Wind Turbine. *http://www.otherpower.com/.* Otherpower.

[26] Hugh Piggott. *http://scoraigwind.co.uk/.*

[27] Hugh Piggott and Réseau Tripalium. *Construire Une Éolienne. Plans de construction d'éoliennes à axe horizontal.* Hugh Piggott and Réseau Tripalium, 2014.

[28] Hugh Piggott. *A Wind Turbine Recipe Book: The Axial Flux Windmill Plans.* Scoraig wind, 2008.

[29] Porf. dr. Mark Runacres. *Courses of Wind Energy.* Vrije Universiteit Brussel, 2014.

[30] James F Manwell, Jon G McGowan, and Anthony L Rogers. *Wind energy explained: theory, design and application.* John Wiley & Sons, 2010.

[31] *Gurit's own Wind Energy Composite Materials Handbook.* Gurit, 2015.

[32] $http://www.yourgreendream.com/diy_pvc_blades.php.$

[33] Paloma Zahonero Carrasco. Generador de flujo axial de imanes permanentes. Master's thesis, Universidad Pontificia Comillas, 2011.

[34] Asko Parviainen. *Design of axial-flux permanent-magnet low-speed machines and performance comparison between radial-flux and axial-flux machines.* PhD thesis, Lappeenranta University of Technology, 2005.

[35] Rodrigo Pérez Ramírez. Aplicación de aerogeneradores de baja potencia para la electrificación rural de viviendas indígenas de méxico. Master's thesis, Universidad de Zaragoza, 2005-2006.

[36] Pablo Paz Sagüés. Estudio y desarrollo de mejoras en el micro aerogenerador it-pe-100 para electrificación rural. Master's thesis, Universidad Publica de Navarra, 2009.

[37] Steve Constantinides and Dale Gulick. Ndfeb for high temperature motor applications. In *SMMA Fall Technical Conference.* Arnold, Magnetic Technologies, 2004.

[38] *http://www.motorpasion.com/industria/el-mapamundi-de-los-coches-mas-vendidos-por-pais.*

[39] INTI Córdoba. *Generalidades sobre imanes permanentes y su caracterización*. Instituto Nacional de Tecnología Industrial, October 2008.

[40] Charles Proteus Steinmetz. *Theory and calculation of electric circuits*, volume 5. McGraw-Hill, 1917.

[41] *www.femm.info*.

[42] David Wood. *Small Wind Turbines: Analysis, Design, and Application*. Springer-Verlag London, 2011.

[43] Lucian Mihet-Popa and Voicu Groza. *Modeling and Simulation of a 12 MW Active-Stall Constant-Speed Wind Farm*. INTECH Open Access Publisher, 2011.

[44] Mostafa Abarzadeh, Hossein Madadi Kojabadi, and Liuchen Chang. *Power Electronics in Small Scale Wind Turbine Systems*. INTECH Open Access Publisher, 2012.

[45] MG Kim and PH Dalhoff. Yaw systems for wind turbines overview of concepts, current challenges and design methods. *Journal of Physics: Conference Series*, 524(1):012086, 2014.

[46] Predrag Pejovic. *Three-Phase Diode Rectifiers with Low Harmonics. Current Injection Methods*. Springer, 2007.

[47] Michael Davis. *http://www.mdpub.com/555Controller/*.

[48] Richard Perez. Lead-acid battery state of charge vs. voltage. *Home power*, 36:66–69, 1993.

[49] $http://energybible.com/wind_energy/towers.html$.

[50] $http://www.kestrelwind.co.za/news_article.asp?ID = 175$.

[51] R Saidur, NA Rahim, MR Islam, and KH Solangi. Environmental impact of wind energy. *Renewable and Sustainable Energy Reviews*, 15(5):2423–2430, 2011.

[52] O Edenhofer, R Pichs-Madruga, Y Sokona, E Farahani, S Kadner, K Seyboth, et al. Ipcc, 2014: Climate change 2014: Mitigation of climate change. contribution of working group iii to the fifth assessment report of the intergovernmental panel on climate change. *Transport*, 2014.

Appendix A

Matlab codes

Contents

```
clear all
clc
%global foil

B=3;%INPUT %number of blades
lamdesign=6;%INPUT %TSR of design

V=6;%INPUT %free stream wind speed in m/s

%INPUT %Load the NACA 0012 profile
load NACA0012lift.txt;
liftdata=NACA0012lift;
load NACA0012drag.txt;
dragdata=NACA0012drag;
alphadata=NACA0012lift(:,1);
NI=find(liftdata(:,1)==0);
liftdata(1:NI-1,1)= liftdata(1:NI-1,1)-360; %Rectify the grades
dragdata(1:NI-1,1)= dragdata(1:NI-1,1)-360; %Rectify the grades

%Blade geometry
N=10; %INPUT
R=3;%INPUT Maximum radious
Rmin=0.1;%INPUT Minimun radious
nu=1.568e-5;%INPUT %kinematic viscosity of air at 300K

[c,r,dr,gamma,phi,x]=bladegeometry(lamdesign,V,nu,R,Rmin,N,B,liftdata,dragdata);
fprintf('Blade design\n');
fprintf('element: %4.2f [m] twist: %5.3f [-] chord: %5.3f [-]\n',[r, gamma,c]');

sol=B*c./(2*pi*r);%solidity

%initialise, first guess
a = 1 + ((4 * sin(phi).*sin(phi))./(sol * 1.* cos(phi) ));%axial induction factor
a = 1.0 ./a;
ap=zeros(N,1);%angular induction factor, set to zero for 1st guess
alpha=ap;%pre-allocate alpha

%iteration loop
maxIter=100;

lam=2:0.5:9;

%values initialization
m=length(lam);
Cp=zeros(m,1);
W=zeros(N,1);
F=W;
A=zeros(m,N);AP=zeros(m,N);PHImat=A;Amat=A;Apmat=A;Kmat=A;alphamat=A;


for i=1:m
for j=1:N
  %values initialization
  error_axial = 10; error_angular = 10;count=0;
  fprintf('\nIteration\n');
  % iterate
```

```
57  while ((abs(error_axial) > 0.000001 | abs(error_angular) > 0.000001)& count<maxIter)
58      count=count+1;
59      old_axial = a(j);
60      old_angular = ap(j);
61      phi(j)=(1-a(j))/((1+ap(j))*lam(i)*x(j));
62      phi(j)=atan(phi(j));
63      W(j)=V*(1-a(j))/sin(phi(j));
64
65
66      F(j)=(2/pi)*acos(exp(-((1-r(j)/R)*B*lam(i)*r(j)/R/(2*(1-a(j))))); %tip-loss factor function
67
68      alpha(j)= (phi(j)+gamma(j)/180*pi)-pi/2; %AOA in radians
69
70      [Cl,Cd,RE]=findClCd(nu,alpha(j),c(j),W(j),liftdata,dragdata);
71
72      k=Cl/Cd;
73
74      a(j)=4*F(j)*sin(phi(j))*tan(phi(j))/(sol(j)*Cl*(1+1/k*tan(phi(j))));
75      a(j)=1/(1+a(j));
76
77      ap(j)=sol(j)*Cl*(tan(phi(j))-1/k)/(4*F(j)*lam(i)*x(j)*sin(phi(j))*tan(phi(j)));
78      ap(j)=ap(j)*(1-a(j));
79
80       %Only to analyze: ------------------------------------------------
81       %REmat(i,j)=RE;
82      PHImat(i,j)=phi(j);
83      Amat(i,j)=a(j);
84      Apmat(i,j)=ap(j);
85      Kmat(i,j)=k;
86      alphamat(i,j)=alpha(j)*180/pi;
87       %-----------------------------------------------------------------
88      error_axial = a - old_axial;
89      error_angular = ap - old_angular;
90      fprintf('%g \b', count);
91       if count == maxIter
92          fprintf('\nWARNING: Iteration did not converge at j= %1.0f', j);
93       end
94
95   end %while
96 end
97 y=x.^3.*ap.*(1-a);
98 CP=8*lam(i)^2*trapz(x,y); % Calculate the CP for the lambda given.
99 Cp(i)=CP; %Cp in every different lambda values
100 A(i,:)=a;
101 AP(i,:)=ap;
102
103 end
104 [Cpmax,imax]=max(Cp); %find the max. Cp in all the lambda
105 lammax=lam(imax) %find the lambda where the Cpmax is.
106 Cpmax
107 rho=1.225;%rho=1.225 theoretical \ %rho=1.126 kg/m^3 in African conditions: Relative humidity: ↙
45\%, Temperature: 30ºC and Air pressure: 1010hPa
108 Power=Cpmax*(0.5*rho*pi*(R+0.07)^2*V^3) % Area= pi*(R+0.07)^2 to take into account the blade- ↙
hub assembling.
109
110 figure(1);
```

```
111 hold off;
112 clf
113 plot(lam,Cp);hold on
114 plot(lammax,Cpmax,'black*');hold on
115 axis ([ 4 10 0 0.6 ])
116 xlabel('\lambda')
117 ylabel('c_{p}')
118 fprintf('\n\rFinal values for induction factors:');
119 fprintf('element: %4.2f [m]  axial: %5.3f [-] angular: %5.3f [-] \n',[r,a,ap]');
120
121
122 %cp161 % Figure theoretical, use it to compare the results
```

```
function [c,r,dr,gamma,phi,x]=Nbladegeometry(lam,Vinf,nu,Rmax,Rmin,NS,Nb,liftdata,dragdata)

   omega=lam*Vinf/Rmax;
    %Division of the blade
   dr=(Rmax-Rmin)/NS;
    % Center of each division
   r=zeros(NS,1);
   r(1)=Rmin+dr/2;

    for i=2:NS
       r(i)=r(i-1)+dr ;
    end

   x=r/Rmax;

    %Iteration initializations
   RE1=300000;
   RE2=160000;

   while abs(RE1-RE2)>10

       %function to find Cl(alpha) and Cd(alpha) for each Re
       [liftdataRE,dragdataRE]=findliftdrag(RE1,liftdata,dragdata);

       CLCD=liftdataRE./dragdataRE;
       [CLCDmax idx] = max(CLCD);  %Find the index where the value of CL/CD is maximum
       %Find the alpha(in deg), Cl and Cd for the idx value
       alphadeg=liftdata(idx,1);
       Cl=liftdataRE(idx);
       %Cd=dragdataRE(idx);

       %Calculate the chord
       c=16*pi*Rmax./(9*Nb*lam^2*x*Cl);
       c=min(c, Rmax*0.15);  %avoid the inboard section become too wide (MARK)

       W=(Vinf^2+(omega*r).^2).^(1/2);
       RE=c.*W/nu;  %Calculate the Reynolds number

       RE2=RE1;
       RE1=mean(RE);  % ASSUMING!!!! RE numbers are similar in the whole blade, the number is ↙
approximated by its mean

   end

   alpha=alphadeg*pi/180;

    %Phi
   phi=atan(2./(3*lam*r/Rmax));

    %Gamma
   gamma=(pi/2-phi+alpha)/pi*180; %DEG


end
```

```
1 function [Cl,Cd,RE]=findClCd(nu,alpha,c,W,liftdata,dragdata)
2
3   RE=c.*W/nu; %Calculate the Reynolds number
4
5   %function to find Cl(alpha) and Cd(alpha) for the Re
6   [liftdataRE,dragdataRE]=findliftdrag(RE,liftdata,dragdata) ;
7
8   alphadeg=alpha*180/pi;
9   alphadegcolumn=liftdata(:,1);
10
11   %Evaluate liftdataRE at alpha using linear method.
12   Cl= interp1(alphadegcolumn,liftdataRE,alphadeg);
13   Cd= interp1(alphadegcolumn,dragdataRE,alphadeg);
14
15 end
```

```
function [liftdataRE,dragdataRE]=findliftdrag(RE1,liftdata,dragdata)
% Find the correct Reynolds columns in the NACA 0012 profile
 if 160000>RE1
     x=160000;
     y=360000;
     col1=2;
     col2=3;
 end

 if 160000<=RE1 & RE1<360000
     x=160000;
     y=360000;
     col1=2;
     col2=3;
  end

  if 360000<=RE1 & RE1<700000
     x=360000;
     y=700000;
     col1=3;
     col2=4;
  end

  if 700000<=RE1 & RE1<1000000
     x=700000;
     y=1000000;
     col1=4;
     col2=5;
  end

  if 1000000<=RE1 & RE1<2000000
     x=1000000;
     y=2000000 ;
     col1=5;
     col2=6;
  end

  if 2000000 <=RE1 & RE1<5000000
     x=2000000 ;
     y=5000000;
     col1=6;
     col2=7;
  end

  if RE1>=160000%Interpolate the data
 per=abs(RE1-x)/abs(y-x);
 liftdataRE=liftdata(:,col1)+per*(liftdata(:,col2)-liftdata(:,col1));
 dragdataRE=dragdata(:,col1)+per*(dragdata(:,col2)-dragdata(:,col1));
  else %Extrapolate the data
  per=abs(x-y)/abs(RE1-y);
  liftdataRE=(liftdata(:,col1)-per*(liftdata(:,col2)))/(1+per);
  dragdataRE=(dragdata(:,col1)-per*(dragdata(:,col2)))/(1+per);
  end
 end

```

```
%-----------------------------------------------------------------------
%AIRFOIL: NACA 0012
%DATA: Drag Coefficients
%-----------------------------------------------------------------------
%ORIGINAL SOURCE: Sheldahl, R. E. and Klimas, P. C., Aerodynamic
%Characteristics of Seven Airfoil Sections Through
%180 Degrees Angle of Attack for Use in Aerodynamic
%Analysis of Vertical Axis Wind Turbines, SAND80-2114,
%March 1981, Sandia National Laboratories, Albuquerque,
%New Mexico.
%
%NOTES: The data herein were synthesised from a combination of
%experimental results and computer calculations.
%
%The original report contains data for lower Reynolds numbers
%than contained herein, but there are some anomalies, in
%particular with CL at small angles of attack.
%
%Data extended to 360 degrees of attack and glaring anomalies
%corrected by L. Lazauskas. All deviations from the original
%are due to L. Lazauskas.
%
%Please refer to the original report for more details.
%
%-----------------------------------------------------------------------
%
%Drag Coefficient
%
%-------------------------------- REYNOLDS NUMBER ----------------------
%
%ALPHA    160000    360000    700000    1000000    2000000    5000000
%
%-----------------------------------------------------------------------
  185    0.0550    0.0550    0.0550    0.0550    0.0550    0.0550
  190    0.1400    0.1400    0.1400    0.1400    0.1400    0.1400
  195    0.2300    0.2300    0.2300    0.2300    0.2300    0.2300
  200    0.3200    0.3200    0.3200    0.3200    0.3200    0.3200
  205    0.4200    0.4200    0.4200    0.4200    0.4200    0.4200
  210    0.5750    0.5750    0.5750    0.5750    0.5750    0.5750
  215    0.7550    0.7550    0.7550    0.7550    0.7550    0.7550
  220    0.9250    0.9250    0.9250    0.9250    0.9250    0.9250
  225    1.0850    1.0850    1.0850    1.0850    1.0850    1.0850
  230    1.2250    1.2250    1.2250    1.2250    1.2250    1.2250
  235    1.3500    1.3500    1.3500    1.3500    1.3500    1.3500
  240    1.4650    1.4650    1.4650    1.4650    1.4650    1.4650
  245    1.5550    1.5550    1.5550    1.5550    1.5550    1.5550
  250    1.6350    1.6350    1.6350    1.6350    1.6350    1.6350
  255    1.7000    1.7000    1.7000    1.7000    1.7000    1.7000
  260    1.7500    1.7500    1.7500    1.7500    1.7500    1.7500
  265    1.7800    1.7800    1.7800    1.7800    1.7800    1.7800
  270    1.8000    1.8000    1.8000    1.8000    1.8000    1.8000
  275    1.8000    1.8000    1.8000    1.8000    1.8000    1.8000
  280    1.7800    1.7800    1.7800    1.7800    1.7800    1.7800
  285    1.7350    1.7350    1.7350    1.7350    1.7350    1.7350
  290    1.6650    1.6650    1.6650    1.6650    1.6650    1.6650
  295    1.5750    1.5750    1.5750    1.5750    1.5750    1.5750
```

```
%---------------------------------------------------------------------
%AIRFOIL: NACA 0012
%DATA: Lift Coefficients
%---------------------------------------------------------------------
%ORIGINAL SOURCE: Sheldahl, R. E. and Klimas, P. C., Aerodynamic
%Characteristics of Seven Airfoil Sections Through
%180 Degrees Angle of Attack for Use in Aerodynamic
%Analysis of Vertical Axis Wind Turbines, SAND80-2114,
%March 1981, Sandia National Laboratories, Albuquerque,
%New Mexico.
%NOTES: The data herein were synthesised from a combination of
%experimental results and computer calculations.
%The original report contains data for lower Reynolds numbers
%than contained herein, but there are some anomalies, in
%particular with CL at small angles of attack.
%Data extended to 360 degrees of attack and glaring anomalies
%corrected by L. Lazauskas. All deviations from the original
%are due to L. Lazauskas.
%Please refer to the original report for more details.
%---------------------------------------------------------------------
%Lift Coefficient
%--------------------------------- REYNOLDS NUMBER ----------------------
%ALPHA    160000    360000    700000    1000000    2000000    5000000
%---------------------------------------------------------------------
 185    0.6900    0.6900    0.6900    0.6900    0.6900    0.6900
 190    0.8500    0.8500    0.8500    0.8500    0.8500    0.8500
 195    0.6750    0.6750    0.6750    0.6750    0.6750    0.6750
 200    0.6600    0.6600    0.6600    0.6600    0.6600    0.6600
 205    0.7400    0.7400    0.7400    0.7400    0.7400    0.7400
 210    0.8500    0.8500    0.8500    0.8500    0.8500    0.8500
 215    0.9100    0.9100    0.9100    0.9100    0.9100    0.9100
 220    0.9450    0.9450    0.9450    0.9450    0.9450    0.9450
 225    0.9450    0.9450    0.9450    0.9450    0.9450    0.9450
 230    0.9100    0.9100    0.9100    0.9100    0.9100    0.9100
 235    0.8400    0.8400    0.8400    0.8400    0.8400    0.8400
 240    0.7350    0.7350    0.7350    0.7350    0.7350    0.7350
 245    0.6250    0.6250    0.6250    0.6250    0.6250    0.6250
 250    0.5100    0.5100    0.5100    0.5100    0.5100    0.5100
 255    0.3700    0.3700    0.3700    0.3700    0.3700    0.3700
 260    0.2200    0.2200    0.2200    0.2200    0.2200    0.2200
 265    0.0700    0.0700    0.0700    0.0700    0.0700    0.0700
 270   -0.0700   -0.0700   -0.0700   -0.0700   -0.0700   -0.0700
 275   -0.2200   -0.2200   -0.2200   -0.2200   -0.2200   -0.2200
 280   -0.3700   -0.3700   -0.3700   -0.3700   -0.3700   -0.3700
 285   -0.5150   -0.5150   -0.5150   -0.5150   -0.5150   -0.5150
 290   -0.6500   -0.6500   -0.6500   -0.6500   -0.6500   -0.6500
 295   -0.7650   -0.7650   -0.7650   -0.7650   -0.7650   -0.7650
 300   -0.8750   -0.8750   -0.8750   -0.8750   -0.8750   -0.8750
 305   -0.9650   -0.9650   -0.9650   -0.9650   -0.9650   -0.9650
 310   -1.0400   -1.0400   -1.0400   -1.0400   -1.0400   -1.0400
 315   -1.0850   -1.0850   -1.0850   -1.0850   -1.0850   -1.0850
 320   -1.0750   -1.0750   -1.0750   -1.0750   -1.0750   -1.0750
 325   -1.0200   -1.0200   -1.0200   -1.0200   -1.0200   -1.0200
 330   -0.9593   -0.9709   -0.9814   -0.9878   -1.0002   -0.9150
 333   -0.9230   -0.9412   -0.9583   -0.9683   -0.9882   -1.0680
 334   -0.9109   -0.9313   -0.9506   -0.9618   -0.9842   -1.0193
```

Appendix B

Autocad sheets

Contents

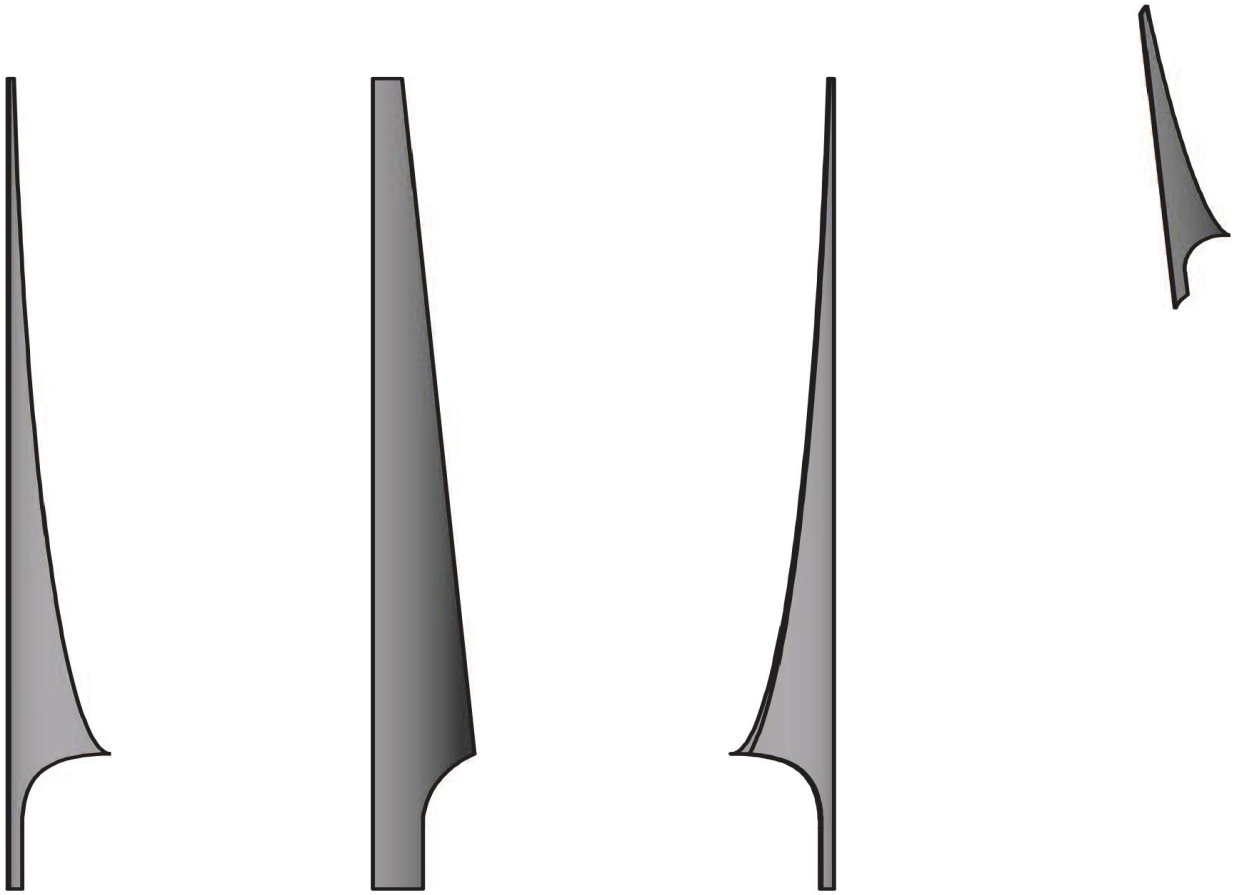

Left lateral view

Front view

Right lateral view

Top view

DRAWN	Nerea Arraiza Clemente Paula Íñiguez Chácharo	ESCALE 1:10	MASTER THESIS IN ELECTROMECHANICAL ENGINEERING. VUB
DATE	25/05/2015		
TITLE	Top lateral and front view of one blade of the rotor		Sheet 1 Signature
DESIGN AND MANUFACTURE OF A LOW COST WIND TURBINE FOR DEVELOPING COUNTRIES			

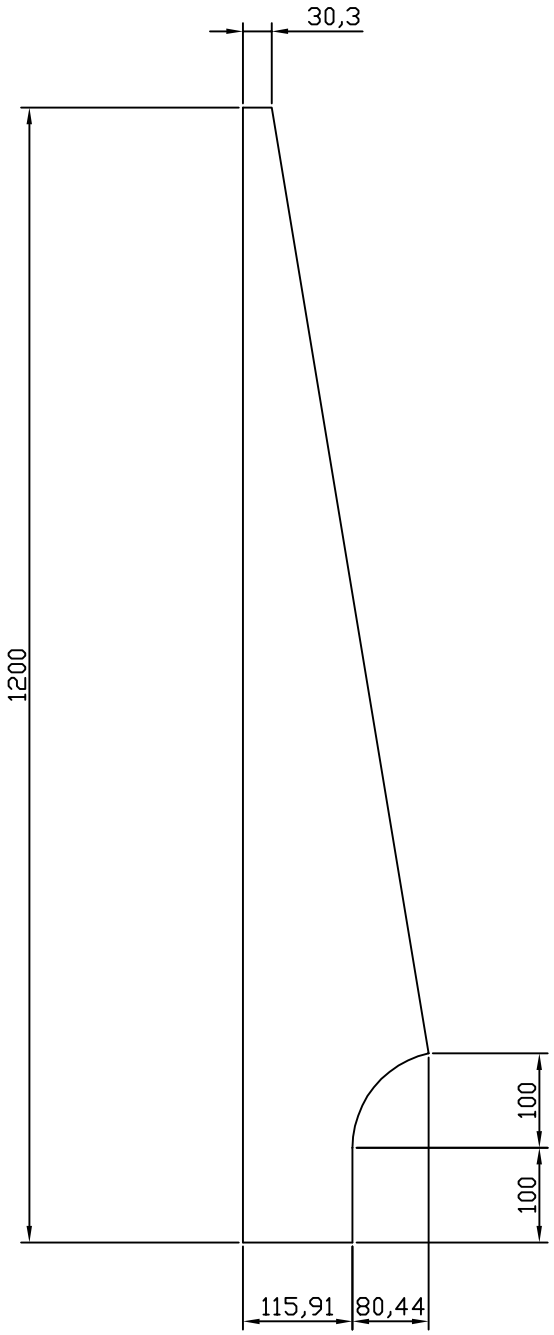

DRAWN	Nerea Arraiza Clemente Paula Íñiguez Chácharo	ESCALE 1:8	MASTER THESIS IN ELECTROMECHANICAL ENGINEERING. VUB
DATE	25/05/2015		
TITLE	Dimensions of the template of one blade of the rotor		Sheet 2
			Signature
DESIGN AND MANUFACTURE OF A LOW COST WIND TURBINE FOR DEVELOPING COUNTRIES			

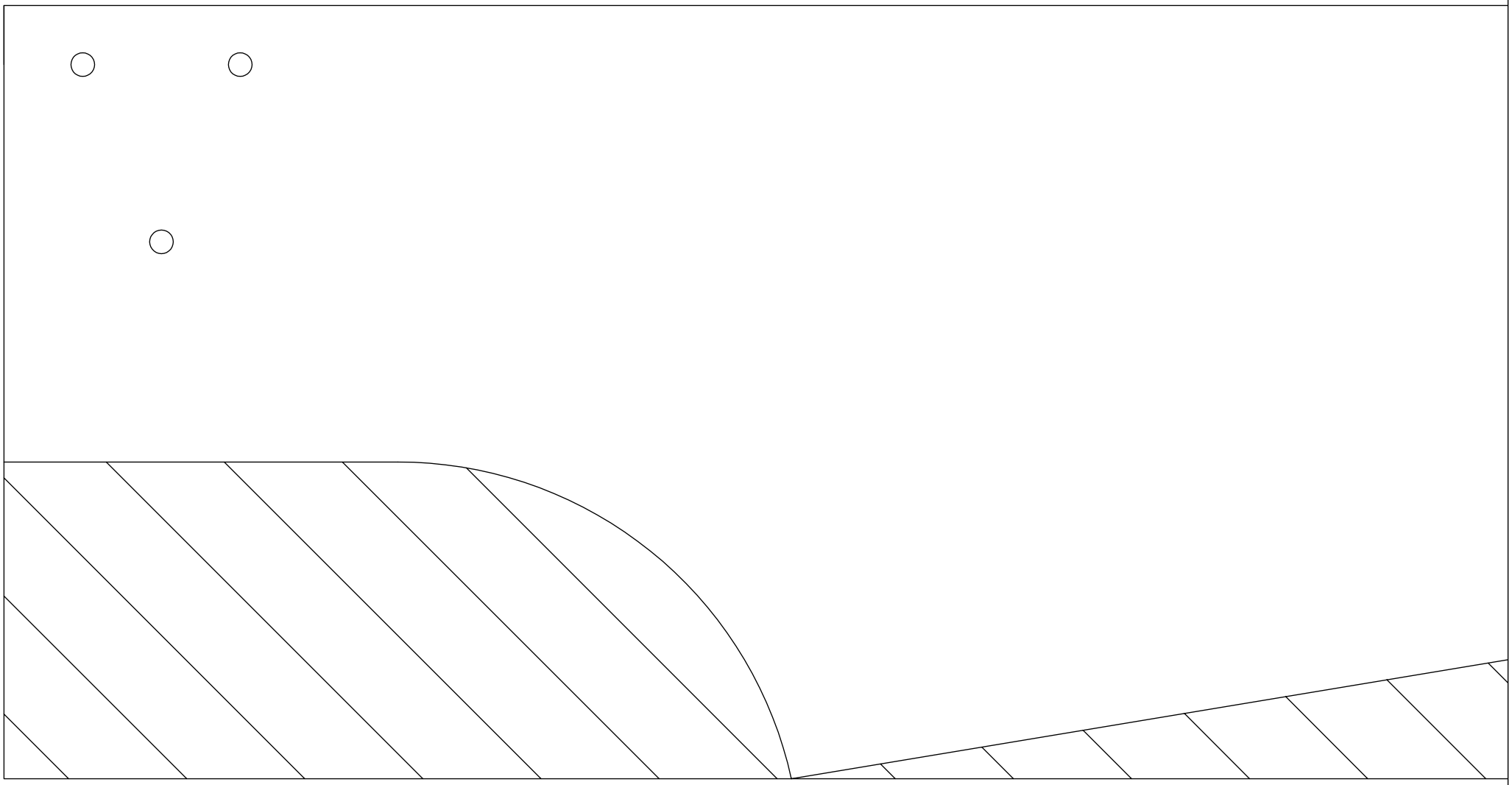

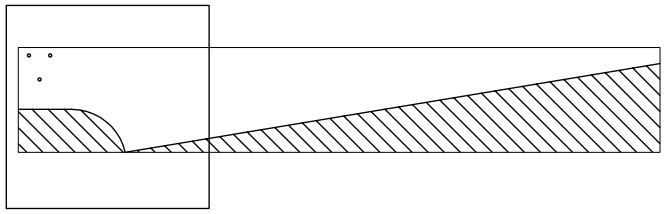

DRAWN	Nerea Arraiza Clemente Paula Íñiguez Chácharo	ESCALE 1:1	MASTER THESIS IN ELECTROMECHANICAL ENGINEERING. VUB
DATE	25/05/2015		
TITLE	Template of the manufacturing of the blades. Root	A3	Sheet 3
DESIGN AND MANUFACTURE OF A LOW COST WIND TURBINE FOR DEVELOPING COUNTRIES			Signatures

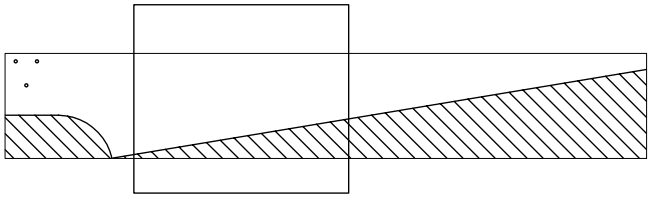

DRAWN	Nerea Arraiza Clemente Paula Íñiguez Chácharo	ESCALE 1:1	MASTER THESIS IN ELECTROMECHANICAL ENGINEERING. VUB
DATE	25/05/2015		
TITLE	Template of the manufacturing of the blades. Middle part 1	A3	Sheet 4
DESIGN AND MANUFACTURE OF A LOW COST WIND TURBINE FOR DEVELOPING COUNTRIES			Signatures

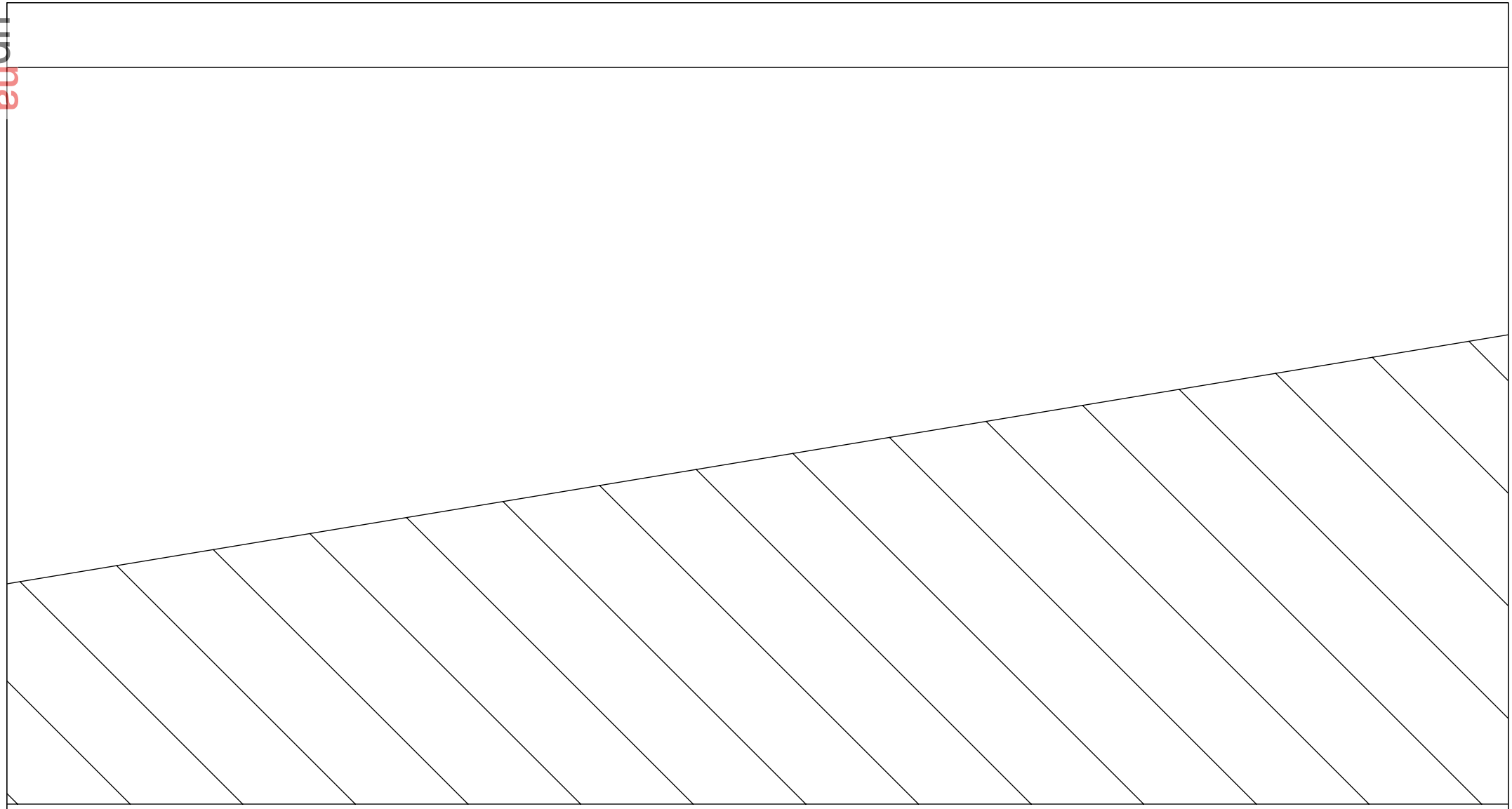

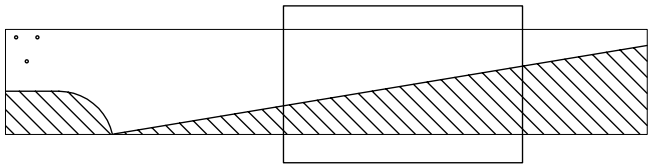

DRAWN	Nerea Arraiza Clemente Paula Íñiguez Chácharo	ESCALE 1:1	MASTER THESIS IN ELECTROMECHANICAL ENGINEERING. VUB
DATE	25/05/2015		
TITLE	Template of the manufacturing of the blades. Middle part 2	A3	Sheet 5
DESIGN AND MANUFACTURE OF A LOW COST WIND TURBINE FOR DEVELOPING COUNTRIES			Signatures

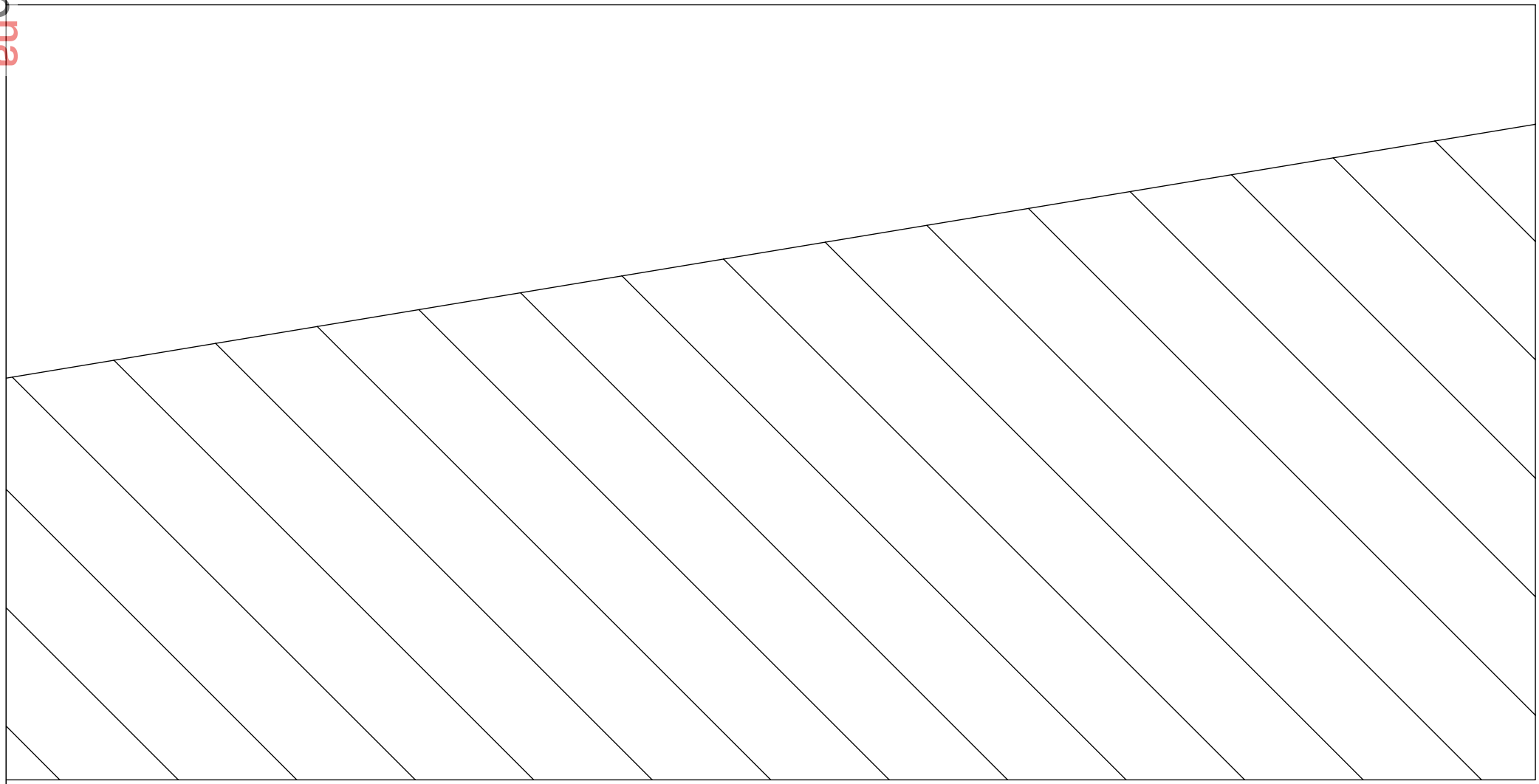

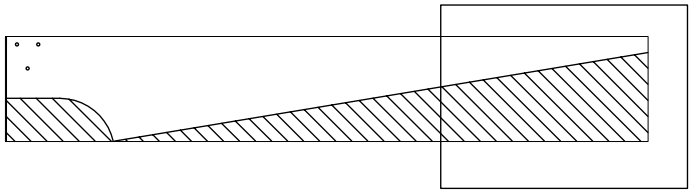

DRAWN	Nerea Arraiza Clemente Paula Íñiguez Chácharo	ESCALE 1:1	MASTER THESIS IN ELECTROMECHANICAL ENGINEERING. VUB
DATE	25/05/2015		
TITLE	Template of the manufacturing of the blades. Tip	A3	Sheet 6
			Signatures
DESIGN AND MANUFACTURE OF A LOW COST WIND TURBINE FOR DEVELOPING COUNTRIES			

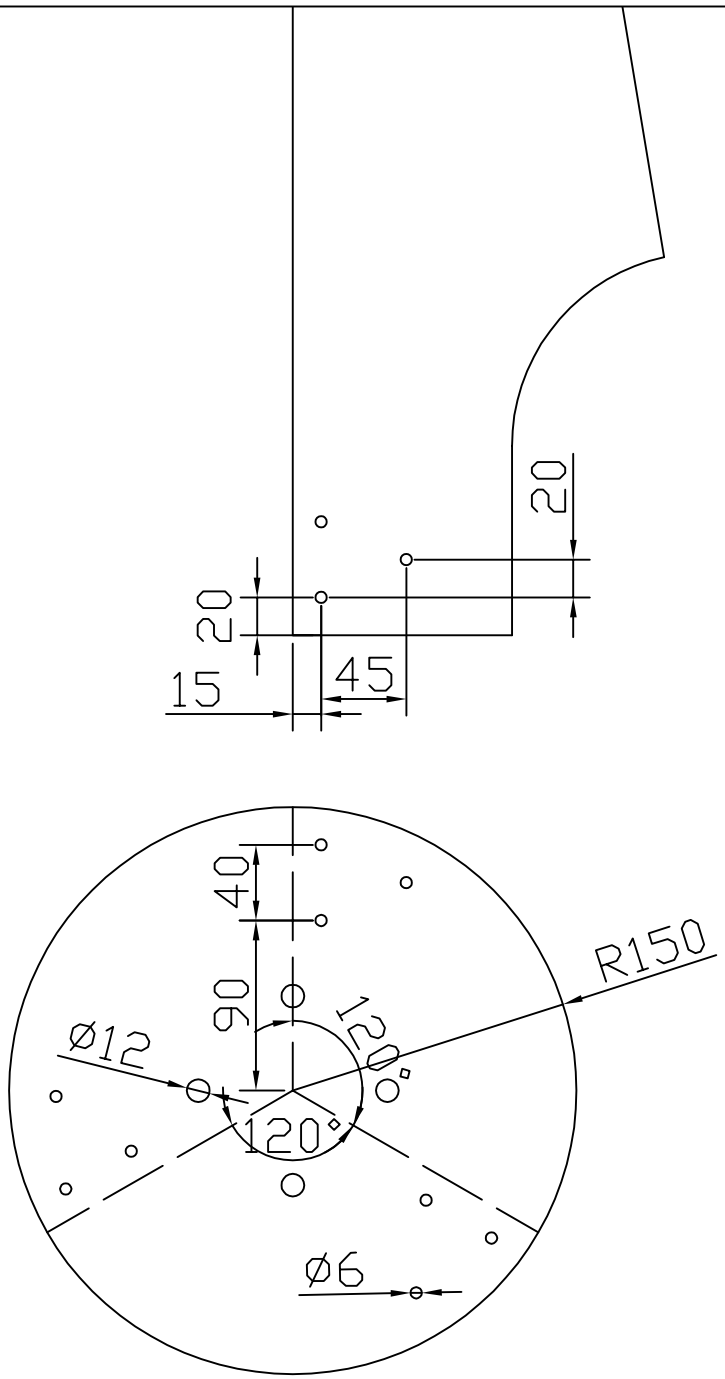

DRAWN	Nerea Arraiza Clemente Paula Íñiguez Chácharo	ESCALE 1:4	MASTER THESIS IN ELECTROMECHANICAL ENGINEERING. VUB
DATE	10/06/2015		
TITLE	Dimensions for the assembling blade – nacelle		Sheet 7
DESIGN AND MANUFACTURE OF A LOW COST WIND TURBINE FOR DEVELOPING COUNTRIES			Signature